

INFLUENCE OF GEOSYNTHETIC ENCASEMENT ON THE PERFORMANCE OF STONE COLUMN GROUPS IN CLAYEY SOIL

Ph.D. THESIS

by

SRIJAN



**DEPARTMENT OF CIVIL ENGINEERING
DELHI TECHNOLOGICAL UNIVERSITY
DELHI – 110042 (INDIA)
JUNE, 2024**

INFLUENCE OF GEOSYNTHETIC ENCASEMENT ON THE PERFORMANCE OF STONE COLUMN GROUPS IN CLAYEY SOIL

A THESIS

*Submitted in partial fulfilment of the
requirements for the award of the degree*

of

DOCTOR OF PHILOSOPHY

in

CIVIL ENGINEERING

by

SRIJAN

Under the supervision of

PROF. A. K. GUPTA



**DEPARTMENT OF CIVIL ENGINEERING
DELHI TECHNOLOGICAL UNIVERSITY
DELHI – 110042 (INDIA)
JUNE, 2024**

**©DELHI TECHNOLOGICAL UNIVERSITY, DELHI-2023
ALL RIGHTS RESERVED**



DELHI TECHNOLOGICAL UNIVERSITY DELHI

CANDIDATE'S DECLARATION

I hereby certify that the work which is being presented in the thesis entitled **“INFLUENCE OF GEOSYNTHETIC ENCASEMENT ON THE PERFORMANCE OF STONE COLUMN GROUPS IN CLAYEY SOIL”** in partial fulfilment of the requirements for the award of the Degree of Doctor of Philosophy and submitted in the Department of Civil Engineering of the Delhi Technological University, Delhi is an authentic record of my own work carried under the supervision of Prof. A. K. Gupta, Professor, Department of Civil Engineering, Delhi Technological University, Delhi, India.

The matter presented in this thesis has not been submitted by me for the award of any other degree or in any other Institution.

(Signature of the student)

Name: **SRIJAN**

Roll No: 2K17/PhD/CE/05

Programme: PhD

Department: Civil Engineering

Delhi Technological University

New Delhi, 110042

SUPERVISOR'S CERTIFICATE

It is certified that the work contained in the thesis titled **“INFLUENCE OF GEOSYNTHETIC ENCASMENT ON THE PERFORMANCE OF STONE COLUMN GROUPS IN CLAYEY SOIL”** by **“*Srijan*”** has been carried out under my supervision and that this work has not been submitted elsewhere for a degree

June, 2024

Prof. A.K. Gupta
Department of Civil Engineering
Delhi Technological University

ACKNOWLEDGEMENTS

I wish to convey my profound gratitude and heartfelt appreciation to the individuals who have been instrumental in supporting and assisting me in the successful completion of this thesis. It is with deep gratitude that I express my appreciation for their contributions, and I would like to dedicate the following words to acknowledge their invaluable assistance.

First and foremost, I extend my deepest gratitude, special thanks, and heartfelt appreciation to my supervisor, **Prof. A. K. Gupta**. His unwavering support throughout my PhD journey has been nothing short of remarkable. There were moments when I felt lost and demotivated, but his guidance and presence were my guiding lights. Professor Gupta's exceptional ability to motivate, lead, and pursue new frontiers in academia are qualities I deeply admire. Words cannot adequately express the depth of my gratitude for his support and cooperation.

I am equally appreciative of the support I received from the department head, Prof. K.C. Tiwari and DRC chairman, Prof. Vijay K. Minocha, during my doctoral journey. I hold him in high regard and will always be respectful of his contributions. I extend my sincere thanks to all the faculty members especially Prof. A. K. Sahu for providing me sensible guidance, faultless planning, helpful advice, and kind cooperation at various stages of my PhD journey.

Special gratitude goes to the members of the SRC, Prof. J. T. Shahu from the Department of Civil Engineering at IIT, Delhi and Prof. Ashwani Jain from the Department of Civil Engineering at NIT, Kurukshetra for their insightful and constructive feedback.

I am immensely grateful to the staff at the Geotechnical Engineering Laboratory and Computer-Aided Design Laboratory within the Department of Civil Engineering. I extend my sincere thanks to lab technician Mr. Shashikant and lab assistant, Mr. Atul, for their unwavering support during the experimental and simulation phases of my research.

My sincere appreciation extends to my senior and colleagues, Mrs. Istuti Singh, Mr. Nitin Lamba, Mr. Dinesh K. Reddy, Mr. Nikhil Singh and Dr Abhishek P. Paswan for their valuable suggestions and assistance whenever I sought their guidance.

I would like to extend my heartfelt appreciation to Dr. Balbir Pandey, my senior and dear friend. Your unwavering support during my PhD journey will forever remain etched in my memory. Your presence was akin to that of a supportive big brother, and I am immensely grateful for that.

I also want to express my gratitude to my friend, Mr. Gautam Narula, whose consistent support from my PhD days through to my thesis submission was instrumental in my success. His priceless review comments, suggestions, and discussions were crucial pillars in the successful submission of my thesis. I owe a great debt of gratitude for his unwavering assistance.

I extend my deepest gratitude to the pillars of my life, whose unwavering support has been my constant motivation throughout this doctoral journey. First and foremost, I express my heartfelt appreciation to my parents, **Shri ShreePrakash Purvey** and **Smt. Sarita Purvey** whose boundless love, sacrifices, and encouragement have shaped my academic path and instilled in me the values that drive my pursuit of knowledge. To my dear elder brother, **Mr. Saket**, whose camaraderie and guidance have been a source of strength and who have stood rock solid behind me through this journey, and to my sister-in-law, **Mrs. Rajani**, whose kindness and understanding have provided a comforting presence during challenging times, I am truly grateful. Special thanks are due to my two nieces, **Meher** and **Urvija**, whose infectious laughter and joy have been a source of inspiration, reminding me of the importance of balance in life. To my beloved wife, **Mrs. Aashima**, your unwavering belief in me, patience, and sacrifices have been the cornerstones of my success. Your constant support and understanding have made this journey not only possible but immensely meaningful. Last but certainly not least, my sincerest gratitude goes to my son, **Kiaan**. Your boundless enthusiasm, curiosity, and the joy you bring into our lives have been a daily reminder of the significance of the work I do and the legacy I hope to leave behind. Together, you have been my rock, my motivation, and my greatest cheerleaders. This achievement is as much yours as it is mine. Thank you for being the foundation upon which my academic dreams have flourished.

I am sincerely thankful and deeply grateful to all those who have supported and contributed to this significant milestone in my life.

(SRIJAN)

ABSTRACT

Geotechnical engineers have challenges in building due to the presence of soft soils in coastal areas, weak subsurface conditions, and poor fill soils. In order to overcome these challenges, there are several options for enhancing the quality of the soil. Granular stone columns are frequently employed to provide structural support in challenging site circumstances. Nevertheless, the inadequate lateral confinement provided by the poor soil around the stone columns results in their failure when the stone column material is compressed into the neighbouring soil. This weakens the overall strength of the technique being used and results in a reduced ability to handle heavy loads and settle properly. Therefore, the use of encasement for granular columns has been employed to address the aforementioned issue.

The current study examines a common soil condition frequently encountered by site and geotechnical engineers, which has a layer of weak, cohesive soil overlying a somewhat more rigid underlying soil layer. These soil profiles have been documented in the literature and are frequently observed in the Indian coastal region, as well as certain areas of the mainland and other countries. The literature extensively examines and documents the application of stone columns in soft cohesive soils to enhance load capacity. However, among the limited number of studies on strengthening cohesive soil using rammed stone columns, the results of this study will make a significant contribution to accurately understanding and confirming the load capacity and failure mode of ordinary end-bearing stone columns when installed in cohesive soil conditions. The current work contributes to the existing body of research by examining the impact of vertically and horizontally enclosing/reinforcing stone columns to reduce bulging failure experienced by ordinary end-bearing stone columns under compressive load in a cohesive soil medium.

In the current study, model testing for a single conventional stone column for diameter (D) = 50, 75 and 100mm was conducted. The load-settlement analysis and failure pattern were investigated. The analysis was further carried forward by using vertical as well as horizontal encasement for the stone column. For vertically encased stone column (VESC) four different variations of length of reinforcement (L_r) was used ($L_r=L$, $L_r=0.75L$, $L_r=0.5L$ and $L_r=0.25L$). For horizontally reinforced stone column (HRSC), three variations were employed where in first case horizontal discs were employed at 100mm spacing throughout the length of the column. Secondly, discs were provided only for the top half of the column i.e., from column head to the centre of the column and last it was reinforced only for the

bottom half of the column i.e., from column's centre to its end. All the above experiments in the single stone column were done for three different diameters of stone column i.e., $D=50\text{mm}$, 75mm and 100mm to understand the effect of area replacement ratio. Also, two different types of geotextiles (G1 and G2) were used for each of the experiments explained earlier to understand the effect of stiffness of geotextile material. The tests were also conducted for the stone columns in the group arranged in a triangular and square pattern for varying S/D ratio of 2, 3 and 4. The group analysis was also conducted for three different diameters of the column i.e., 50, 75 and 100mm. Both vertical encasement and horizontal reinforcement by a disc were used to study the encasement effect similar to that done in the analysis of a single stone column. The length of encasement (L_r) was used as $L_r=L$ for VESC and when horizontal discs were employed at 100mm spacing throughout the length of the column for HRSC tests. Also, only G1 type geotextile was used as an encasement material for both VESC and HRSC group analysis. Figure 3.6 represents the variation of both vertical and horizontal reinforcement used for the single stone column analysis. Table 3.4 and 3.5 shows the outline of the various experiments performed for single stone column and stone column in groups respectively.

Also, one of the industrial wastes i.e., steel slag is used as the column filler material which can act as a sustainable material and will also address the current environmental concern as the utilisation of steel slag for stabilisation of soil can be an eco-friendly and economical extraction method for getting rid of solid waste. A numerical analysis was done to study the various behavioural characteristics of virgin soft clay bed, when it was installed with ordinary steel slag column (OSSC) and also with encased steel slag column (ESSC). A comparison between was made among all for studying various parameters such as settlement, stress concentration ratio and excess pore water pressure.

The model testing findings showed that the load carrying capability was higher when geotextile reinforcement was used compared to conventional columns. Vertical reinforcement provides greater load capacity and reduced settlement compared to horizontal encasement. The shown failure mechanism shows that reinforced stone columns are more resistant to bulging than unreinforced stone columns. The VESC for full-length encasement with G2 type of geotextile for a 100 mm stone column diameter was most desirable among the various tests conducted on single stone column. For group analysis, with increasing S/D ratio, load bearing capacity decreases for both triangular and square arrangement. Model testing was also validated by the help of numerical investigations. In comparison to Ordinary Steel Slag Column (OSSC), the settling of soft clay at conclusion of embankment building phase has

been high of selected configuration and model specifications. By encasing column in a sufficiently stiff geosynthetics material, further settlement decrease can be seen. Underneath the embankment, where soft clay produces the maximum excess pore water pressure (PWP_{excess}), the amount of PWP_{excess} diminishes as the embankment slopes.

TABLE OF CONTENTS

	Page No
CANDIDATE’S DECLARATION	iv
SUPERVISOR’S CERTIFICATE	v
ACKNOWLEDGMENT	vi
ABSTRACT	viii
LIST OF TABLES	xv
LIST OF FIGURES	xvi
LIST OF SYMBOLS	xxii
ABBREVIATIONS	xxiv
CHAPTER 1	
INTRODUCTION	1
1.1 General	1
1.2 Motivation	4
1.3 Need of the study	6
1.4 Scope and Objectives of this study	7
1.5 Methodology	8
1.6 Structure of the thesis	9
CHAPTER 2	
LITERATURE REVIEW	11
2.1 General	11
2.2 Soft Soils	11
2.2.1 Soft soil properties	12
2.2.2 Problems of soft soil	12
2.2.3 Soft soil remediation	12
2.3 Stone Columns	14
2.4 Stone Column Construction Methods	22
2.4.1 Displacement Method of Construction	22
2.4.2 Replacement Method of Construction	23
2.5 Failure Mechanism of the Stone Columns	24
2.5.1 Mechanism of Load Transfer of Stone Columns	24
2.5.2 Failure Modes of Stone Columns	24
2.6 Stone Column Design	26
2.6.1 Ordinary Stone Columns	26

2.6.1.1	Enhancement of bearing capacity investigation on ordinary stone columns	26
2.6.1.2	Studies on the reduction of settlement in ordinary stone columns	31
2.6.1.3	Limitations of Ordinary Stone Columns	39
2.6.2	Geosynthetic Encased Stone Column	40
2.6.2.1	Bearing Capacity Enhancement of Geosynthetic Encased Stone Column	40
2.6.2.2	Geogrid Encased Stone Column Settlement Reduction Studies	43
CHAPTER 3		
METHODOLOGY		52
3.1	General	52
3.2	Materials Used	52
3.2.1	Clay	52
3.2.2	Stone Aggregates	54
3.2.3	Encasement Materials	55
3.3	Equipments & Apparatus	56
3.3.1	Tank	56
3.3.2	Loading and Measurement System	57
3.3.3	Iron Plate for Testing	57
3.3.4	Pipes for construction of Stone Column	57
3.3.5	Compaction Tools	58
3.4	Modelling Considerations	58
3.5	Clay Bed Preparation	58
3.6	Stone Columns Construction for Unreinforced Columns	59
3.6.1	Single Stone Column	59
3.6.2	Group of Stone Columns	60
3.7	Stone Columns Construction for Vertically Encased Stone Columns	61
3.8	Stone Columns Construction for Horizontally Reinforced Stone Columns	61
3.9	Test Procedure	62
3.10	Details of Experimental Program	63
3.11	Numerical Modelling	65
3.11.1	General	65
3.11.2	Plaxis 3d	66
3.11.3	Material Properties	67

3.11.4	Model Generation/ Geometry Modelling Process	70
3.11.5	Mesh Generation	72
3.11.6	Staged Construction and Calculations	73
3.12	Summary	74
CHAPTER 4		
RESULTS AND DISCUSSIONS OF EXPERIMENTAL AND NUMERICAL INVESTIGATIONS		75
4.1	General	75
4.2	Experimental Results: Findings from Model Tests for Single Stone Column	75
4.2.1	Analysis of the load-settlement behaviour of a clay bed	76
4.2.2	Clay bed reinforced with ordinary stone column- Single Stone Column	76
4.2.3	Clay bed reinforced with encased stone column- Single Stone Column	77
4.2.3.1	Vertically Encased Stone Column (VESC)	77
4.2.3.2	Horizontally Reinforced Stone Columns (HRSC)	78
4.2.4	Comparison between VESC and HRSC	78
4.3	Numerical Results: Single Stone Column	79
4.3.1	Validation	79
4.3.2	Analysis of the load-settlement behaviour of a clay bed	79
4.3.3	Clay bed reinforced with ordinary stone column- Single Stone	80
4.3.4	Clay bed reinforced with encased stone column- Single Stone	80
4.3.4.1	Vertically Encased Stone Column (VESC)	80
4.3.4.2	Horizontally Reinforced Stone Column (HRSC)	81
4.4	Comparative Analysis of Experimental and Numerical Outcomes of tests performed on Single Stone Column	81
4.5	Experimental Results – Group of Stone Columns	81
4.5.1	Clay bed reinforced with ordinary stone column- Group of stone columns	81
4.5.2	Clay bed reinforced with encased stone column- Stone Columns in Group	82
4.5.2.1	Vertically Encased Stone Column (VESC)	82
4.5.2.2	Horizontally Reinforced Stone Columns (HRSC)	83
4.6	Numerical Results – Group of Stone Columns	83
4.6.1	Clay bed reinforced with ordinary stone column- Group of stone column	83

4.6.2 Reinforcing clay bed with encased stone column- Group of Stone Columns	84
4.6.2.1 Vertically Encased Stone Column (VESC)	84
4.6.2.2 Horizontally Reinforced Stone Columns (HRSC)	85
CHAPTER 5	
SUSTAINABLE MATERIAL AS A COLUMN FILLER AS AN ALTERNATIVE TO CONVENTIOBAL AGGREGATE	86
5.1 General	86
5.2 Numerical Analysis	86
5.2.1 Problem Statement	
5.2.2 Geometry	87
5.2.3 Material Properties and Meshing	87
5.2.4 Model Sequence	87
5.3 Numerical Results and Discussions	88
5.3.1 Displacement Analysis	88
5.3.2 Stress Investigation	88
5.3.3 Stress Concentration Ratio	89
CHAPTER 6	
CONCLUSIONS	90
6.1 General	90
6.2 Conclusions	90
6.3 Novelty of the work	90
6.4 Area of Future Research	91
REFERENCES	93
LIST OF PUBLICATIONS	103

LIST OF TABLES

Table No.	Table Caption	Page
3.1	Properties of clay used in the present study	53
3.2	Stone column properties used in the present study	54
3.3	Attributes of Geosynthetics	55
3.4	Outline of the various tests performed on single stone column	64
3.5	Outline of the various tests performed on stone columns in group	65
3.6	Properties of soil and aggregate used for PLAXIS modelling	69
3.7	Predefined value of r_e (element distribution)	79
4.1	Comparison of stone column load capabilities measured	119

LIST OF FIGURES

Figure No.	Figure Caption	Page No.
2.1	Stress variation in soft clay as a function of distance from the column (Choobasti, 2011)	15
2.2	Schematic Illustration of GESC Modelling Specifications	18
2.3	Granular pile construction using an easy auger boring technique	23
2.4 (a)	Unit cells that are not deformed laterally (Han, 2015)	24
2.4 (b)	Unit cells that are deformed laterally (Han, 2015)	24
2.5	Failure mechanisms for a stone column in cohesive soil that is not homogeneous	25
2.6	Load-Settlement curve (Hughes and Withers, 1974)	27
2.7	Consolidometer examination of a solitary stone column (Hughes and Withers, 1974)	27
2.8	Chart for Improvement Factor (Priebe, 1976)	32
2.9	Unit cell model (Han and Ye, 2002)	34
2.10	The response frame's schematic diagram (Kolekar and Dasaka, 2014)	36
2.11	Unit cell cross section (Deb and Shiyamalaa, 2015)	37
2.12	Calculated rate of consolidation compared with various methods (Deb and Shiyamalaa, 2015)	37
2.13	S.R.R. vs. Bearing pressure for various compactive effort (Chardrawanshi, 2018)	39
2.14	Model test set up (Hasan and Samadhiya, 2016)	43
2.15	Geosynthetic encased column – Unit cell model (Raithel and Kempfert, 2000)	44
3.1	Particle size distribution of clay	53
3.2	Particle size distribution of aggregate	55
3.3	Model test tank	56
3.4	Line sketch of loading frame	56
3.5	Test setup showing various components	57
3.6	Pipes used for making stone column	58
3.7	Single column to be made up with stones having $d = 75\text{mm}$	60
3.8	Typical arrangement of triangular and square pattern of stone column in groups for $d=50\text{mm}$ and $s/d=3$	61
3.9	Schematic of (a) OSC (b) VESCs with various L_r (c)HRSCs with various geosynthetics arrangements	64
3.10	Real soil behaviour by Mohr - Coulomb model	67
3.11	E_0 , E_{50} and E_{ur} of a soil sample from triaxial test results	68

3.12	Model setup of soft clay	71
3.13	Model setup of an ordinary stone column for a reference case of $D=50\text{mm}$	71
3.14	Model setup of VESC with $L_r=L$ for a reference case of $D=50\text{mm}$	72
3.15	Model setup of VESC with $L_r=0.75L$ for a reference case of $D=50\text{mm}$	72
3.16	Model setup of VESC with $L_r=0.5L$ for a reference case of $D=50\text{mm}$	72
3.17	Model setup of VESC with $L_r=0.25L$ for a reference case of $D=50\text{mm}$	73
3.18	Model setup of HRSC with $L_r=L$ for a reference case of $D=50\text{mm}$	73
3.19	Model setup of HRSC with $L_r=0.5L$ from column's head to its centre for a reference case of $D=50\text{mm}$	73
3.20	Model setup of HRSC with $L_r=0.5L$ from column's centre to its foot for a reference case of $D=50\text{mm}$	74
3.21	Model setup of ordinary stone column arranged in a triangular pattern for $S/D=2$ for a reference case of $D=50\text{mm}$	74
3.22	Model setup of ordinary stone column arranged in a triangular pattern for $S/D=3$ for a reference case of $D=50\text{mm}$	75
3.23	Model setup of ordinary stone column arranged in a triangular pattern for $S/D=4$ for a reference case of $D=50\text{mm}$	75
3.24	Model setup of ordinary stone column arranged in a square pattern for $S/D=2$ for a reference case of $D=50\text{mm}$	75
3.25	Model setup of ordinary stone column arranged in a square pattern for $S/D=3$ for a reference case of $D=50\text{mm}$	76
3.26	Model setup of ordinary stone column arranged in a square pattern for $S/D=4$ for a reference case of $D=50\text{mm}$	76
3.27	Model setup of VESC with $L_r=L$ arranged in a triangular pattern with $S/D=2$ for a reference case of $D=50\text{mm}$	76
3.28	Model setup of VESC with $L_r=L$ arranged in a triangular pattern with $S/D=3$ for a reference case of $D=50\text{mm}$	77
3.29	Model setup of VESC with $L_r=L$ arranged in a triangular pattern with $S/D=4$ for a reference case of $D=50\text{mm}$	77
3.30	Model setup of VESC with $L_r=L$ arranged in a square pattern with $S/D=2$ for a reference case of $D=50\text{mm}$	77
3.31	Model setup of VESC with $L_r=L$ arranged in a square pattern with $S/D=3$ for a reference case of $D=50\text{mm}$	78
3.32	Model setup of VESC with $L_r=L$ arranged in a square pattern with $S/D=4$ for a reference case of $D=50\text{mm}$	78
3.33	10 - noded tetrahedral 3D soil element	79
4.1	Load-Settlement variation of clay bed without any reinforcement	84
4.2	Load-Settlement variation of clay bed reinforced with ordinary stone column with different area replacement ratio	84

4.3	Load-settlement variation of the vertically reinforced stone column with varying reinforcement lengths for D=50mm and G1 type geotextile	86
4.4	Load-settlement variation of the vertically reinforced stone column with varying reinforcement lengths for D=75mm and G1 type geotextile	86
4.5	Load-settlement variation of the vertically reinforced stone column with varying reinforcement lengths for D=100mm and G1 type geotextile	87
4.6	Load-settlement variation of the vertically encased stone column with varying reinforcement lengths for D=50mm and G2 type geotextile	88
4.7	Load-settlement variation of the vertically encased stone column with varying reinforcement lengths for D=75mm and G2 type geotextile	88
4.8	Load-settlement variation of the vertically encased stone column with varying reinforcement lengths for D=100mm and G2 type geotextile.	89
4.9	Comparison of load-settlement variation of unreinforced, OSC and VESC (for various Lr) for D=50mm with G1 and G2 type geotextile	89
4.10	Comparison of load-settlement variation of unreinforced, OSC and VESC (for various Lr) for D=75mm with G1 and G2 type geotextile	90
4.11	Comparison of load-settlement variation of unreinforced, OSC and VESC (for various Lr) for D=100mm with G1 and G2 type geotextile	90
4.12	Load ratio- Settlement variation of VESC for various Lr on single stone column for D=50mm	91
4.13	Load ratio- Settlement variation of VESC for various Lr on single stone column for D=75mm	92
4.14	Load ratio- Settlement variation of VESC for various Lr on single stone column for D=100mm	92
4.15	Load-settlement variation of the horizontally reinforced stone column with varying reinforcement lengths for D=50mm and G1 type geotextile	93
4.16	Load-settlement variation of the horizontally reinforced stone column with varying reinforcement lengths for D=75mm and G1 type geotextile	94
4.17	Load-settlement variation of the horizontally reinforced stone column with varying reinforcement lengths for D=100mm and G1 type geotextile	94
4.18	Load-settlement variation of the horizontally reinforced stone column with varying reinforcement lengths for D=50mm and G2 type geotextile	95

4.19	Load-settlement variation of the horizontally reinforced stone column with varying reinforcement lengths for D=75mm and G2 type geotextile	96
4.20	Load-settlement variation of the horizontally reinforced stone column with varying reinforcement lengths for D=100mm and G2 type geotextile	96
4.21	Comparison of load-settlement variation of unreinforced, OSC and HRSC (for various Lr) for D=50mm with G1 and G2 type geotextile	97
4.22	Comparison of load-settlement variation of unreinforced, OSC and HRSC (for various Lr) for D=75mm with G1 and G2 type geotextile	97
4.23	Comparison of load-settlement variation of unreinforced, OSC and HRSC (for various Lr) for D=100mm with G1 and G2 type geotextile	98
4.24	Load ratio- Settlement variation of HRSC for various Lr on single stone column for D=50mm	99
4.25	Load ratio- Settlement variation of HRSC for various Lr on single stone column for D=75mm	99
4.26	Load ratio- Settlement variation of HRSC for various Lr on single stone column for D=100mm	100
4.27	Comparison of Load-Settlement behaviour between VESC and HRSC for Lr = L on single stone column of D=50mm.	101
4.28	Comparison of Load-Settlement behaviour between VESC and HRSC for Lr = L on single stone column of D=75mm	101
4.29	Comparison of Load-Settlement behaviour between VESC and HRSC for Lr = L on single stone column of D=100mm	102
4.30	Comparison of Load Ratio-Settlement behaviour between VESC and HRSC for Lr = L on single stone column of D=50mm	102
4.31	Comparison of Load Ratio-Settlement behaviour between VESC and HRSC for Lr = L on single stone column of D=75mm.	103
4.32	Comparison of Load Ratio-Settlement behaviour between VESC and HRSC for Lr = L on single stone column of D=100mm	103
4.33	Multiple failure mechanisms for a column with a 100 mm diameter: (a) OSC, (b) VESC (i) Lr = L (ii) Lr = 0.75 L (iii) Lr = 0.5 L (iv) Lr = 0.25 L, (c) HRSC (i) Equal interval throughout the depth (ii) Top half—0.5 L from head (iii) Bottom half—from centre to bottom	105
4.34	Comparison of vertical load intensity settlement behaviour of end bearing column	106
4.35	Load-Settlement variation of clay bed without any reinforcement	107
4.36	Load-Settlement variation of clay bed reinforced with ordinary stone column with different diameters	108

4.37	Load-settlement variation of the vertically reinforced stone column with varying reinforcement lengths for D=50mm - NA	109
4.38	Load-settlement variation of the vertically reinforced stone column with varying reinforcement lengths for D=75mm - NA	109
4.39	Load-settlement variation of the vertically reinforced stone column with varying reinforcement lengths for D=100mm - NA	110
4.40	Load-settlement variation of the horizontally reinforced stone column with varying reinforcement lengths for D=50mm - NA	111
4.41	Load-settlement variation of the horizontally reinforced stone column with varying reinforcement lengths for D=75mm - NA	111
4.42	Load-settlement variation of the horizontally reinforced stone column with varying reinforcement lengths for D=100mm - NA	112
4.43	Various failure modes by numerical analysis for 100 mm diameter column (a) OSC (b) VESC (c) HRSC	114
4.44	Comparison of Experimental and Numerical results for VESC for D=50mm	116
4.45	Comparison of Experimental and Numerical results for VESC for D=75mm	116
4.46	Comparison of Experimental and Numerical results for VESC for D=100mm	117
4.47	Comparison of Experimental and Numerical results for HRSC for D=50mm	117
4.48	Comparison of Experimental and Numerical results for HRSC for D=75mm	118
4.49	Comparison of Experimental and Numerical results for HRSC for D=100mm	118
4.50	Load-settlement behaviour of stone column arranged in triangular and square pattern for S/D=2, 3 and 4 for D=50mm	121
4.51	Load-settlement behaviour of stone column arranged in triangular and square pattern for S/D=2, 3 and 4 for D=75mm	121
4.52	Load-settlement behaviour of stone column arranged in triangular and square pattern for S/D=2, 3 and 4 for D=100mm.	122
4.53	Load-settlement behaviour of VESC arranged in triangular and square pattern for S/D=2, 3 and 4 for D=50mm	123
4.54	Load-settlement behaviour of VESC arranged in triangular and square pattern for S/D=2, 3 and 4 for D=75mm	123
4.55	Load-settlement behaviour of VESC arranged in triangular and square pattern for S/D=2, 3 and 4 for D=100mm	124
4.56	Load-settlement behaviour of HRSC arranged in triangular and square pattern for S/D=2, 3 and 4 for D=50mm	125
4.57	Load-settlement behaviour of HRSC arranged in triangular and square pattern for S/D=2, 3 and 4 for D=75mm	125
4.58	Load-settlement behaviour of HRSC arranged in triangular and square pattern for S/D=2, 3 and 4 for D=100mm.	126
4.59	Load-settlement behaviour of OSC arranged in triangular and square pattern for S/D=2, 3 and 4 for D=50mm- Numerical Analysis	127

4.60	Load-settlement behaviour of OSC arranged in triangular and square pattern for $S/D=2, 3$ and 4 for $D=75\text{mm}$ - Numerical Analysis	127
4.61	Load-settlement behaviour of OSC arranged in triangular and square pattern for $S/D=2, 3$ and 4 for $D=100\text{mm}$ - Numerical Analysis	128
4.62	Load-settlement behaviour of VESC arranged in triangular and square pattern for $S/D=2, 3$ and 4 for $D=50\text{mm}$ - Numerical Analysis	129
4.63	Load-settlement behaviour of VESC arranged in triangular and square pattern for $S/D=2, 3$ and 4 for $D=75\text{mm}$ - Numerical Analysis	129
4.64	Load-settlement behaviour of VESC arranged in triangular and square pattern for $S/D=2, 3$ and 4 for $D=100\text{mm}$ - Numerical Analysis	130
4.65	Load-settlement behaviour of HRSC arranged in triangular and square pattern for $S/D=2, 3$ and 4 for $D=50\text{mm}$ - Numerical Analysis	131
4.66	Load-settlement behaviour of HRSC arranged in triangular and square pattern for $S/D=2, 3$ and 4 for $D=75\text{mm}$ - Numerical Analysis	131
4.67	Load-settlement behaviour of HRSC arranged in triangular and square pattern for $S/D=2, 3$ and 4 for $D=100\text{mm}$ - Numerical Analysis	132
5.1	3D cut representation of the encased stone columns supporting embankment sitting on soft clay	134
5.2	Details displaying cross section & plan of the embankment lying on soft clay improves with ESSC	134
5.3	Generated Mesh for (a) Virgin Soil without any reinforcement (b) OSSC (c) ESSC	136
5.4	Time-Displacement graph at the head of (a) 1 st column (b) 7 th column (c) 1 st and 7 th column combined	138
5.5	Generation of Excess PWP in final stage of building phase for virgin soil, OSSC and ESSC	139
5.6	Flow of developed excess pore pressure at final stage of the embankment building (60 days) for (a) virgin soil (b) OSSC (c) ESSC	140
5.7	Influence of OSSC and ESSC on stress concentration	141
5.8	Developed plastic points at final construction stage (a) Unreinforced (b) OSSC (c) ESSC.	142
5.9	Comparison of variation of principal effective stress below the embankment for the unreinforced case, OSSC and ESSC	143

LIST OF SYMBOLS

A_r	area replacement ratio
c	cohesion
C_c	coefficient of curvature
C_s	swelling index
C_c	compressibility index
C_u	undrained shear strength
C_u	coefficient of uniformity
d	average diameter of the aggregate
D	diameter of the stone column
EA	axial stiffness
E_s	soil's elastic modulus
E_c	column elastic modulus
E_{50}	secant modulus at 50% strength
E_0	tangent modulus
E_{ur}	unload-reload modulus
GA	in-plane shear stiffness
h	thickness of the soil layer
I_f	settlement improvement factor
K_0	earth pressure at rest
K_{ps}	coefficient of passive earth pressure of the stone column.
l_e	target element dimension
L	length of the column
L_r	length of the reinforcement
m_v	soil's volumetric compressibility coefficient
N	standard penetration test value
n	stress concentration ratio
N_c	terzaghi's bearing capacity factor
q_{ult}	ultimate bearing capacity
R	settlement reduction ratio

r_e	relative element size factor
S	spacing between the columns
S_{cl}	settlement of the columns
S_{sl}	settlement of the soil
S_u	untreated settlement in the foundation
u_o	initial excess pore-pressure
γ	bulk unit weight
γ_{sat}	saturated unit weight
σ_c	stress over the column
σ_s	stress over the soil
σ_{rL}	limiting radial stress
ϕ'	frictional angle of stone column aggregates
σ_{ro}'	initial radial effective stress around the column
σ_{vo}	average initial effective vertical stress
μ	poisson's ratio
$\Delta\sigma_z$	pressure due to surcharge
$\sigma'_{v,0}$	initial vertical effective stress
$\sigma'_{h,0}$	initial horizontal effective stress
ψ	dilatancy angle

ABBREVIATIONS

BCR	bearing capacity ratio
BEM	boundary element method
COV	coefficient of variation
DEM	discrete element method
ESCR	effective vertical stress on the surrounding soft clay
ESSC	encased steel slag column
FDM	finite difference method
FEM	finite element method
HRSC	horizontally reinforced stone columns
LDCOL	lateral deformation of column
LL	liquid limit
LR	load ratio
MC	mohr-coulomb
OSC	ordinary stone columns
OSSC	ordinary steel slag column
PL	plastic limit
PTA	paraxylene terephthalic acid
PWP _{excess}	excess pore water pressure
RSM	response surface methodology
SCR	stress concentration ratio
SG	specific gravity
SIF	settlement improvement factor
SL	shrinkage limit
SPSS	statistical package for the social sciences
SPT	standard penetration test
SS	soft soil
SRR	settlement reduction ratio
VESC	vertically enclosed stone columns

CHAPTER 1

INTRODUCTION

1.1 GENERAL

The country is experiencing tremendous growth in civil infrastructure due to the increase in population, urbanisation, and economy. The availability of suitable locations for construction is diminishing steadily. This requires the enhancement and refinement of marginal locations that would have otherwise been deemed unsuitable for construction. The soils that are deemed poor and difficult for construction purpose includes soft clay, loose sand, silt, expansive soil, frozen soil, collapsible soil, organic soil, loess etc. The primary challenges faced in these soils are associated with shear strength, compressibility, volume change, creep deformation, and permeability (Han, 2015).

Ground enhancement is defined as a technique employed to enhance the characteristics of soil, namely its behaviour in terms of strength, compressibility, and permeability. Numerous ground enhancement strategies have been extensively utilised and proven efficient in improving the quality of soft deposits. For the purpose of improving the stability of loose sandy soils, such as silty or clayey sands, as well as soils with low undrained shear strength, the stone column is a method that is frequently utilised. This procedure involves the creation of boreholes in the pliable soil at specific locations. The space is filled with granular particles of varying sizes. The composite earth serves as a flexible and semi-rigid foundation for embankments, liquid storage tanks, and other construction projects. Reducing settlement, increasing bearing capacity, and improving stiffness are all outcomes of using stone columns. The soil's drainage improves, leading to a faster consolidation process.

The utilisation of the stone columns was initially introduced in an European country, France around 1830. Since the late 1950s, they have been widely utilised in Europe for the purpose of site enhancement (Barksdale and Bachus, 1983). In India, the vibro-flot technique was used to erect stone columns for the first time in 1961 in Ennore, Madras, as documented by Basarkar et al. in 2009. Subsequently, the approach has been extensively employed at many areas throughout the country.

Datye and Madhav (1988) have documented the case studies of foundations utilising stone columns in India. The performance of foundations for various applications, including stone columns for area treatment, pipe pedestals, small and large groups of isolated footings,

and bridge abutments, was discussed. The various cases discussed encompass various projects, such as the footings for pipe rack work at IFFCO, Kandla in 1972, the treatment of foundations for the abutments of Belapur and Kasheli Bridge in 1975, the enhancement of soil for lagoon embankment and foundations for a sewage treatment plant near Bhandup, Bombay in 1982, the ground treatment for a pipeline at Sion-Koliwada, Bombay, and the hazardous storage liquid tanks at Manglore Chemical and Fertilisers, Manglore, as well as at IFFCO, Kandla.

Both the displacement method and the replacement approach are viable options for accomplishing the construction of the stone column. The displacement method involves using a closed casing pipe to displace the surrounding dirt and create a hollow in the ground. Following this, stones are used to fill the hole that was created by the casing. The replacement method involves excavating the earth to create a cavity or hole of the specified depth, which is then filled with stones. In the case of cohesive soils, the replacement approach is suitable, whereas the displacement method is suitable for both unsaturated cohesive and cohesionless soils (Han, 2015).

The stone column functions as a composite substructure that transfers the impending load to the neighbouring soil. The tributary area of the soil that surrounds each stone column constitutes a regular hexagon around the column. This hexagon can be approximated to a certain extent by an equivalent circular area that has the same overall area as the hexagon. The comparable circle encompasses both the tributary soil and a single stone column, with a diameter that effectively encompasses them. This is commonly known as a unit cell. When doing an analysis of the functioning of the column group, the utilisation of the unit cell concept proves to be particularly beneficial. Based on this information, it may be inferred that, with the exception of the boundaries of the loaded region, conducting a test on a single stone column in soft clay can provide insights into the behaviour of a group of columns (Balaam et al., 1978).

According to Barksdale and Bachus (1983), the usual design loads for stone columns range from 20 to 50 tonnes. Following the building of a stone column, a composite structure has been created within the soft ground, exhibiting reduced compressibility and increased shear strength compared to the surrounding soft soils. The pliable earth serves as a containment for the column material. The column and the soil around it move downward simultaneously due to the tension exerted by the superstructure, as a consequence of which

the column experiences stress concentration. The rigidity of the column material causes the stress concentration. The column experiences greater stress compared to the surrounding soil because of the disparity in modulus between the column material and the neighbouring soil. The stress concentration ratio (SCR) is a measure of the ratio between the stress over the column and the stress on the adjoining soil. It is commonly used to illustrate how the load is transferred between columns and soft soils. Barksdale and Bachus (1983) indicate a stress concentration ratio of 1–5, and IS 15284 (Part I) gives a ratio of 2.5–5.

The failure mechanism of a single stone column, when subjected to load over its area, is greatly influenced by the length of the column. In general, the stone column will fail in the bulging condition if the length of the column is greater than four times the column's diameter, which is referred to as the critical length. On the other hand, if the length of the column is less than the critical length, it may fail in the general shear failure or punching shear failure (IS15284 Part 1).

The strength of conventional stone columns is derived from two factors: the friction between the granular materials that make up the column, and the constraint offered by the encompassing loose soil. When compared to the native soil that was present initially, the loaded ground exhibits the characteristics of increased bearing capacity and decreased settling. However, its performance may still fall short of expectations due to the following factors (Murugesan and Rajagopal, 2009):

- (i) The adjacent loose soil has the potential to infiltrate the stone columns, leading to a decrease in their frictional qualities.
- (ii) The stones can slide laterally into the soft adjacent soil thereby may not have a major impact compared to if they were in their original, undisturbed state.

In order to address this issue, an alternate approach has been explored including the use of a geogrid-encased tube to reinforce rammed stone columns. This method has been found to enhance the strength and compressibility property of the stone columns. Several trials have been conducted in a limited number of projects (Deshpande and Vyas, 1996; Richard and Yogesh, 2005; Raithel et al., 2006) to implement the placement of a geogrid casing, followed by the charging of stones into it. Despite the deviation from the conventional vibro-technique, the resulting columns exhibit consistent diameter throughout, and the inclusion of a geogrid provides the required lateral confinement. Several research have been conducted on laboratory model stone columns with encasement (Sivakumar et al., 2004; Bauer and Nabil,

1996). These studies have observed an enhancement in bearing capacity, mostly utilising sand in conjunction with stone particles which helps to explain the scaled-down effect. The inclusion of an encasement serves to enhance the structural integrity and rigidity of stone column. Additionally, it serves to mitigate the developed lateral compression of stones during installation, particularly in soils with low bearing capacity. Without sacrificing the column's drainage capacity or the frictional properties of the stones used, this allows for faster installation processes. Despite the numerous advantages of encased stone columns, this particular approach is not extensively employed in comparison to stone columns. This is mostly due to a poor understanding of how encased stone columns respond to applied loads. Hence, it is believed that conducting a comprehensive investigation on encased type stone columns is imperative to elucidate the mechanism by which the encasement enhances the strength of the column and identify the aspects that impact its behaviour. To determine how encasement affects the strength of a bed stabilised by stone columns, it is necessary to compare encased stone columns with those without encasement. This analysis should be performed under comparable testing conditions to facilitate the quantification of the aforementioned effect. Consequently, the study's scope and objectives have been developed.

1.2 MOTIVATION

The rapid urbanisation and industrialization of society have resulted in a diminishing supply of construction sites that possess the necessary soil qualities. Consequently, field engineers have limitations in their selection of sites characterised by weak strata and complex behaviour, mostly because of the existence of problematic soil layers exhibiting diverse technical qualities. Abandoned sites frequently consist of soft clay exhibiting notably high compressibility, low shear strength, and substantial settlement, or weak cohesionless type soil with inadequate bearing capability. These sites are susceptible to landslides, liquefaction, or areas filled with materials that raise concerns regarding global and local stability. Consequently, in order to guarantee the structural soundness and practicality of a building project, it is necessary to conduct comprehensive site preparation prior to commencing any construction activities. However, while considering the various approaches available for ground improvement/modification, it is important to carefully choose and implement an appropriate solution that aligns with both economic feasibility and design specifications.

In recent years, a commonly utilised restorative technique involves the implementation of using granular aggregate within a weak soil layer in the shape of cylindrical columns. This

process is achieved using either vibration compaction or rammed compaction. The efficacy of reinforcing the soil using stone columns, a technique involving the insertion of granular material columns into loose sandy, alluvial silty-clays, sandy silts, and soft cohesive soils, has been seen to be satisfactory (Ketkar and Telang, 1994; Kumar et al., 2002). As a result of its development in 1970, the use of stone columns has been utilised to improve, modify, repair, and rehabilitate the foundations and underlying soil of a wide variety of structures. These constructions include high-rise buildings, industrial plants, towers, and petroleum storage tanks.

JBF Petrochemical Industries Ltd has put out a proposal to establish a novel paraxylene terephthalic acid (PTA) facility in Mangalore, India, with a projected annual production capacity of 1.25 million metric tonnes. The plant primarily consisted of storage tanks, process plants, substations, and various ancillary buildings. Keller was contracted to undertake the design and implementation of ground improvement measures for three paraxylene tanks and two fire water storage tanks, which had respective diameters of 64m and 35m. In addition to the three paraxylene tanks and two fire water storage units, civil works for tank pads were also necessary. The characteristics of the subsoil that were observed at the location included layers of sand that varied in thickness among themselves, ranging from soft to solid, followed by highly compacted silty sand or weathered rock. The primary objective of the project was to enhance the load-bearing capability of the tank pad foundation while simultaneously minimising both overall settlement and differential settlement. Keller devised a ground improvement methodology by employing bottom feed vibro stone columns to augment the soil's bearing capacity while simultaneously mitigating both differential and total settlement. The scope of tank pad construction encompassed several key components, namely the installation of a stone blanket, HDPE membrane, sand pad, stone ring beam, and bitumen works.

Likewise, Cochin International Airport Ltd. (CIAL) has put out a proposal to enhance the aprons in close proximity to the current apron area, along with the corresponding airfield infrastructure. Keller was contracted by the primary construction company to carry out ground enhancement operations with vibro stone columns in order to facilitate the construction of new aircraft parking bays. The location exhibited complex geological characteristics, including the presence of highly compressible plastic clay. Additionally, the apron area, spanning roughly 41,000 m², was situated on loosely filled soil layers. The presence of a subterranean nallah also poses a potential hazard in terms of unequal

settlement. The execution of tasks at an operational airport necessitated meticulous coordination and strategic organisation of all rig movements. Given the geotechnical difficulties that need to be addressed, we have put forth a refined foundation approach utilising vibro stone columns. The proposed solution successfully addressed the issues related to bearing capacity and settling, while also implementing efficient drainage pathways to facilitate quick consolidation. In addition to reducing expenses for the client, this also resulted in significant time savings. The treatment area was expanded beyond the footprint of the apron in order to provide a confinement effect for the outside rows and to permit a seamless transition between the soils that were treated and those that were left untreated. The project was successfully delivered within the designated timeframe through the utilisation of four rigs.

Soil and foundation experts have also undertaken commendable projects that employ the stone column enhancement approach. The project encompasses the establishment of a temple situated in Rohtak, Haryana, with granular piles with a 12m diameter and rammed type stone columns measuring 500mm of diameter. Following a similar pattern, the restoration of around 1000 pillars of the Kalyana Mandapa, which is situated in Hanuma Konda, Warangal, involved the utilisation of rammed stone columns measuring 400 mm in diameter, together with granular piles of 7 m in length. Similarly, the construction of the picture tube facility at Karzan, Vadodara used the use of gravel piles with a diameter ranging from 300 to 400 mm. The fire water tank that is located in the LPG Bottling Plant in Madanpur Khadar, which is owned and operated by the Indian Oil Corporation Ltd. has been supported by a foundation utilising a group of gravel columns measuring 3×22 m. Recently, the construction committee that is in charge of the foundation construction of the well-known Ram Temple in Ayodhya has proposed the utilisation of vibro-stone columns as a means of providing support for the raft foundation. Therefore, it is evident that the implementation of the stone column as a construction method has been extensively carried out across different superstructures and soil conditions, serving as a feasible approach to enhance the stability of poor ground conditions.

1.3 NEED OF THE STUDY

Soft clays are geological formations of relatively recent origin that can be observed in many regions across the globe. These deposits are also observed in several locations throughout India. The region of Thane creek in Mumbai is characterised by a substantial

deposition of highly flexible clay, with a thickness ranging from 15 to 20 metres. In the city of Cochin, there exists a substantial layer of marine-derived clay measuring over 20 metres in thickness. This clay, characterised by its soft consistency, poses challenges for any construction of even modest structures like a two-storey building. Additionally, this layer is found beneath a surface fill ranging from 2 to 3 metres in depth. The Vishakapatnam port area is characterised by the presence of a substantial layer of highly compressible clay, with a considerable thickness of around 100 metres, extending offshore. Likewise, inside the coastal region of Chennai, there exists a layer of extremely soft clay whose thickness can vary from a few metres to over 20 metres. This clay layer is situated beneath a depleted crust, measuring approximately 2 to 3 metres in thickness, and presents significant challenges in terms of foundation stability. Typically, the predominant components found in these deposits consist of fine-grained soils that have clay fractions ranging from moderate to high. The clay portions exhibit a higher degree of plasticity, characterised by low strength and great compressibility. The inherent moisture content frequently approaches or exceeds its liquid limit. As a result of these circumstances, occurrences of foundation failures in soft clay are relatively frequent. The application of surface loading, such as embankments or shallow foundations, inevitably leads to significant settlements that must be accounted for in the design process. Additionally, these settlements often require ongoing maintenance of engineered structures. Weak soils present numerous engineering challenges, making it necessary to enhance the ground to ensure its suitability for civil engineering projects and to mitigate potential future damage.

Therefore, it is a regular occurrence for site engineers to encounter loose soft soil overlaying a hard stratum composed of thick sand or stiff clay. Given the abundance of reported studies on the enhancement of cohesive soil through the implementation of stone columns, it is imperative to conduct a thorough investigation into the reinforcing effects on cohesive soil.

1.4 SCOPE AND OBJECTIVES OF THIS STUDY

In order to study the possibility of increasing the load carrying capacity of soft soil through the use of ordinary stone columns (OSC), vertically enclosed stone columns (VESC), and horizontally reinforced stone columns (HRSC), the primary purpose of this thesis is to investigate the possibility of doing so. Additionally, the present study aims for the purpose of investigating the influence of various parameters by conducting laboratory tests on scaled

models. In addition, numerical analyses were performed in order to verify the findings of the experiment.

Hence, the primary aims of this study are as follows:

- To investigate the impact that the area replacement ratio has on the settlement behaviour of conventional and enclosed stone columns.
- To investigate the impact that vertical and horizontal encasement have on the performance of a single stone column.
- To investigate the impact of different lengths of encasement on the performance of stone columns.
- To investigate the performance of stone columns in groups (square and triangular pattern) with varying spacing(S)/diameter(D) ratio.
- To investigate the impact of using steel slag as a sustainable material as column filler in soft clay bed which is reinforced with encased stone columns in group.

1.5. METHODOLOGY

In order for the research to be successful in achieving its objectives, laboratory experiments were conducted using a setup that was specifically created for this particular study. A solitary stone column, either with or without encasement, is constructed inside a soft clay bed autonomously. It is then subjected to load testing utilising a circular rigid plate as a model footing. The experiment involved varying various factors, including the diameter of the columns, the length of the encasement, the stiffness of the encasing material, various arrangement of stone columns in group, and spacing(S)/diameter(D) ratio. This study examines the effects of the aforementioned parameters on enhancing the load-bearing ability of encased stone columns when compared to conventional stone columns. The similar study was done when the stone columns were arranged in groups.

The model tests were simulated numerically using the PLAXIS finite element algorithm, and the resultant results were afterwards validated with the experimental findings. The Soft soil model and Mohr-Coulomb model are utilised to depict the characteristics of soft type clay and the stone column material, respectively. The models of stone column encased by a encasement material are also examined using the Geogrid material model in PLAXIS software. This model is used to simulate the behaviour of the encasing material, in addition to the material models used to represent the clayey soil and stone column. A comprehensive

investigation is conducted to examine the impact of various parameters discussed above experimentally and numerically.

1.6. STRUCTURE OF THE THESIS

The thesis is structured into six distinct chapters, with each chapter being briefly summarised in the following sections.

In the introductory section of Chapter 1, a concise explanation is provided on the importance of ground improvement, the specific constraints associated with the use of stone column approach, and the requirement for encasing the conventional stone column. Additionally, the motivation, need and objectives of the present study are also presented.

Chapter 2 provides a detailed overview of previous research details pertaining to the behaviour and functioning of ordinary stone columns and geosynthetics encased stone columns, comprising analytical, experimental, and numerical investigations.

Chapter 3 provides a comprehensive account of the experimental inquiries conducted on stone columns and enclosed stone columns. The fundamental characteristics of the materials employed in the experiments are provided, alongside the facilities that have been constructed for the purpose of conducting model testing. The details regarding the PLAXIS 3D used for simulating experimental investigations has also been explained in current chapter.

The findings of the experimental tests that were conducted on conventional stone columns, vertically encased stone columns (VESC), and horizontally reinforced stone columns (HRSC) are presented in Chapter 4 of the research paper. In order to determine the load-settlement behaviour, a number of parameters, including the diameter of the column, the length of the reinforcement, and the stiffness of the geotextiles, were evaluated and adjusted. Another aspect of the stone columns that was investigated was their failure mechanism. The investigation was carried out on a single stone column as well as stone columns that were grouped together. The spacing (S)/diameter (D) ratio of 2,3, and 4 was used for stone columns in a triangular and square pattern.

The experimental results were validated by numerical modeling using PLAXIS 3D for all the variation of experimental tests whose results have been presented in this chapter. In addition to that, a comparison between the numerical results and the experimental ones has been provided.

Chapter 5 provides the results of a parametric investigation that was carried out to explore the effect of employing a sustainable material, specifically steel slag, as a column filler in soft soil bed reinforced with enclosed stone column with the PLAXIS finite element code. This chapter presents an overview of the findings that were gained from the inquiry. Various behaviours such as settlement, stress concentration ratio, excess pore water pressure, and lateral deformation of columns were studied.

In Chapter 6, significant findings that have been derived from a combination of experimental and numerical investigations on the stabilisation of soft soil bed beds using ordinary stone columns and encased stone columns are presented. This chapter also highlights potential areas for future research.

CHAPTER 2

LITERATURE REVIEW

2.1 GENERAL

The background knowledge about the soft soils and ground improvement strategies has been provided in this chapter. As discussed in the previous chapter, the stone column technique offers an easy, quick, and affordable solution for ground improvement. It is widely used for constructing embankments, liquid storage tanks, and offshore structures, and it reduces the likelihood of liquefaction in soils. Therefore, brief case studies of some of the success stories are presented. Furthermore, in extremely soft soils, settling of the composite ground may still be a problem even after regular stone columns are built. For this reason, it has been suggested in the literature that using geosynthetics to encapsulate the granular material will increase the columns' effectiveness. As a result, a research review has been done on the design, construction, and performance of both regular and encased stone columns.

2.2 SOFT SOILS

Because soft soils have a low shear strength and high degree of compressibility, building civil engineering structures on or in these types of soils can cause structural problems during and after the project's completion. Geologically young, typically fine-grained, consolidated, under-consolidated, or light-over-consolidated soils; weathered clays in upper crust; and quick clay deposits, which stabilise on their own but have not undergone appreciably delayed or secondary consolidation since formation, can all exhibit characteristics of soft soils. This group may include loose sand, soft clays, and fine silts. These soils were created by recurrent surface wetting and desiccation near rivers, lakes, and the sea. These places are where the soils first formed. Soft soils comprise the marine and river delta deposits that encompass the Gulf of Kutch, river delta regions, the beaches of the Gulf of Cambay, and the Eastern and Western coastal belts of India as a whole. This group includes the following soil types (apart from SP): MI, MH, CI, CH, MI-MH or CI-CH, MI –CI, MH –CH.

The following standards have been proposed by the German Geotechnical Society to characterise soft soil for construction purposes.

- a. Consistency that is very soft to soft, having a consistency index (I_c) < 0.75
- b. Nearly or at full saturation
- c. The undrained shear strength, $C_u \leq 40 \text{ kN/m}^2$
- d. Low to medium plastic property

- e. Inclined to flow
- f. Thixotropic property
- g. Very sensitive to vibrations

2.2.1 Soft soil properties

The following are the basic characteristics of soft soils, which account for their great compressibility and low shear strength:

- a. More than 50% of the soil particles passing through 75 μ .
- b. They can be found in the zone of organic and inorganic clays and silts, with low to moderate plasticity.
- c. Lower shear strength of a value lower than 25kPa (Madhav and Miura, 1994, Priebe, 1995, Muir-Wood et al., 2000, Alexiew et al. 2005, Wehr 2006, Gniel and Bouazza 2009, Mohanty and Samanta 2015, Fattah et al. 2014, Dutta et al. 2016, Mehrannia 2018).
- d. According to Ranjan and Rao (2000), these deposits have low SPT (Standard Penetration Test) "N" values, usually less than 8 for cohesive deposits that are medium to extremely soft and less than 10 for cohesionless soils.
- e. In general, the activity serves as a gauge for a clayey soil's compressibility as well as its swelling and shrinking properties. A clay with an activity value greater than 1.25 is considered active.
- f. High level of organic matter, which promotes compressibility.

2.2.2 Problems of soft soil

- a. Soft soils may experience bearing failure. This can happen when the applied pressure exceeds their ultimate bearing capacity, or when loads are inclined.
- b. There may be significant overall and differential settlement in the soft soils. This occurs because such soils have a high degree of compressibility, allowing for the observation of significant total and differential settlement even with modestly increased applied pressure.
- c. Because minerals like montmorillonite have an affinity to absorb significant volumes of water upon saturation, soft soils may exhibit shrinkage fissures or ground heave.

2.2.3 Soft soil remediation

The following solutions can be used to address the soft soil issue (Hausmann, 1990):

- a. Alter the construction site indefinitely.
- b. Similarly, planning the superstructures.

- c. Take out any damaged soils and replace them with robust materials.
- d. Development of the soil's characteristics and the surrounding terrain using the appropriate methods.

Various ground improvement techniques are:

1. Replacement
2. Drainage and consolidation
3. Chemical stabilisation
4. Thermal and biological treatment
5. Reinforcement

We go over each of the aforementioned methods in brief below:

1. Replacement- Both of shallow and deep depth have been employed with the replacement procedure. Above the groundwater table and at shallow depths (up to 3 m), some qualitative material replaces the problematic soil. The earth becomes more robust and compacted as a result. There are five ways to replace deep foundations: using stone columns, sand compaction columns, rammed aggregate columns, vibroconcrete columns, and geosynthetic encased columns. Hard, stiff material replaces loose, mushy soil in the earth during deep replacement. All columns have a treatment depth of 5 to 10 m, with the exception of sand columns, which have a depth of 5 to 15 m. Stone columns, on the other hand, may have a depth of 30 m (Han, 2015). Deep replacement work lowers the likelihood for settlement and liquefaction while increasing bearing capacity and stability and speeding up consolidation.
2. Drainage – On soft soils, a top layer of permeable materials, nonwoven geotextile, or geomaterials may be used to boost load carrying capacity and hasten consolidation settlement.

Consolidation - To strengthen them and lessen settlement, soft soils with saturated inorganic clays and even silts may be temporarily subjected to vacuum pressure or surcharge.
3. Chemical stabilisation – Soft soil deposits that are either shallow or deep may receive the treatment. Unsaturated clay and silts can be blended with a mixture of lime, cement, or fly ash at shallow depths (up to 0.3 metres). Grouting and deep mixing, in which cement-based fluids are poured into the ground under tremendous pressure, have produced the deep stabilisation. For grouting and deep mixing, the treatment depths are 30 m and 70 m, respectively.

4. Thermal and biological treatment – It is possible for the earth's temperature to drop below freezing and for less heat to escape from below the surface, solidifying the soil. As a result, there is less earth movement and less water flow. This works well with saturated clay and sand when the ground requires temporary improvement, like during soil excavation.

Biological treatment involves the use of plants and their roots, or the modification of soil properties through bio-mediated geochemical processes. These processes include the formation of minerals, the generation of gases, the construction of biofilms, and the production of biopolymers. Both cohesive and non-cohesive materials can be used with it, yet the method is not well-established.

5. Reinforcement – There are two components to this kind of treatment: fills reinforcement and in-situ reinforcing. The goal of the reinforcing treatment is to make the ground more stable. For both temporary and permanent slopes of soil and rocks, steel bars with grout mix have been provided, while ground anchors, soil nails, and micropiles are classified as in-situ reinforcement. For tensile resistance and other uses, high strength geosynthetics have been placed at slopes, embankments, earth walls, foundations, and roadways with fill reinforcement. This treatment lessens settlement and improves stability and bearing capacity.

Geotechnical experts are familiar with these corrective actions; nevertheless, they have drawbacks and aren't usually practical for use in field settings. Stone columns serve several crucial geotechnical purposes, including drainage, reinforcement, and densification. It is the most creative method for enhancing a range of deficient soils, including trash fills, ash ponds, soft clays, and loose sands.

2.3 STONE COLUMNS

The compressed hard rock chunks arranged vertically into the strata beneath the surface are known as stone columns. Using ground improvement techniques (replacement, displacement, or other methods), it is a sub-structural part that is created in situ. It transfers the superstructure's load to geo-material above, below, and through the confines of the surrounding soil via compression, shear, or rotation.

The French military engineers were the first to employ Vibro methods in the 1800s, but these were quickly forgotten. Nevertheless, it was once more utilised in Germany in the 1930s to build a racetrack (McKelvey and Sivakumar, 2000). Since that time, the vibro stone column has emerged as one of the most important deep compaction methods utilised all over the

world. (Serridge, 2005) and one of the primary deep compaction techniques used worldwide (McCabe et al., 2009). It has evolved into a reasonably priced substitute for traditional piling techniques in constructions that are less susceptible to settlement (Weber et al., 2006). The following section discusses the variables that impact the strength of stone columns.

1. Stress variation around the boundaries of the stone column

The surrounding soil is subjected to compression and radial displacement as a result of the construction of stone columns. For the purpose of quantifying the stresses that occur along the periphery of stone columns, the soil earth pressure at rest (K_0) serves as the metric. For the reason that the installation of stone columns is followed by horizontal displacement and compression of the soil in the surrounding area, the K_0 value increases after the installation of the columns. Clay experiences radial displacement around the stone column's periphery, which helps with vibrocompaction until the material completely expands horizontally up to the column's radius. It is possible to quantify the changes in the values of stresses by calculating the ratio of the effective horizontal stresses to the vertical stresses (Chobbasti, 2011 and Rao, 1992). The outcome of 3D modelling tests suggests that the stress concentration at the interface between the earth and stone column varies significantly.

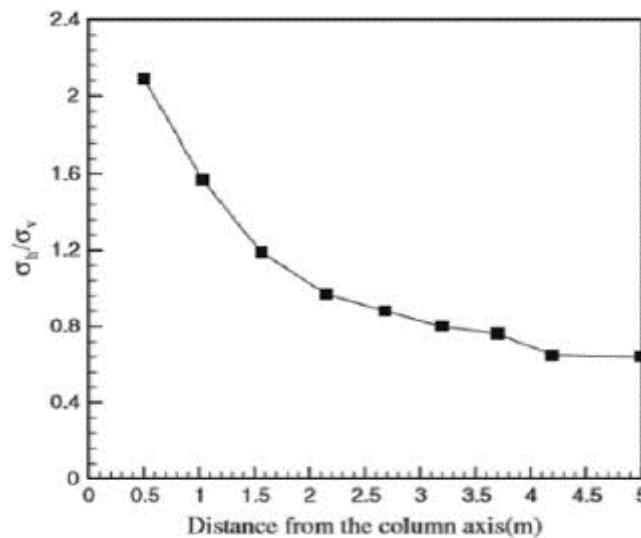


Figure 2.1. Stress variation in soft clay as a function of distance from the column (Choobasti, 2011)

Analysis is done on how well stone column technology works in the Perm, Russia region in terms of improving foundation stability and reducing subgrade deformation. To avoid

financial losses, the ideal pile depth is always taken inside the calculated foundation depth. When installing stone columns, the earth next to the borehole compresses; therefore, any deformation that may exist should be taken into account before the column shell is worked (Shenkman and Ponomaryov, 2016).

The column material begins to expand laterally as the structure's load increases, but the geosynthetic encasement and lateral soil pressure stop the fill material from moving in this direction. Plotting the effective vertical stress over time for both entirely and partially embedded Geosynthetic Encased Stone Columns (GESC) revealed that the GESC's effective stress was 1.25 times higher than that of stress attained by the Ordinary Stone Column (OSC). This variation in effective stress could be attributed to the extra lateral confinement that the geogrid encasement provides (Rajesh, 2017).

2. Confining Pressure

The magnitude of the confining pressure significantly influences the ability of stone columns to sustain applied loads. Because of the increased confining pressure, encasing the stone columns in geosynthetic material boosts their load bearing potential. Extensive triaxial and uniaxial testing on OSC and GESC reveal that the confining pressure of regular stone columns is restricted to 200 kPa, while the residual strength of geotextile-encased columns is approximately 800 kPa. Because of their increased confining pressure, GESCs can tolerate high loads even after failure or deformation (Chen et al., 2009).

There is a correlation between the ratio of the increase in axial stress of encased columns and that of conventional stone columns, which may be used to determine the augmentation of the strength of encased columns. Compared to the higher range, the improvement is more noticeable in the lower range of confining pressure (Miranda and Costa, 2016). The effect of encasing the stone columns can also be described by the fact that the strain rate for encased stone columns is lower than the strain rate for uncased stone columns, which is comparatively higher.

3. Settlement / Consolidation behavior

Since the primary benefits of stone columns are reduced settlement and enhanced consolidation rate, settlement is regarded as one of the most crucial characteristics when working with soil reinforced by stone columns. It is found that settlement decreases as the stone column's buried depth in the soil strata increases.

According to Black et al. (2011), there was a correlation between the area replacement ratio and the settlement characteristics of stone column group configurations. With an increase in the area replacement ratio, there is a corresponding increase in the settlement improvement

factor, but this is only the case up to an area replacement of 30-40%. Similar findings were found in Shahu and Reddy's (2011) investigation. The area replacement ratio (A_r), relative density, column length, and water content of the stone material are some of the foundation elements that affect the consolidation behaviour of the conventional stone column. Because a higher value of A_r results in a higher failure stress, there was a decrease in settlement for a given applied vertical load as A_r increased.

According to the Response Spectra Methodology, the amount that the stone columns settle depends on their diameter and depth. The first stage of construction shows an improvement in soil behaviour, which serves as preloading for the second stage and aids in enhancing the soil's stiffness and shear strength in that stage (Elsawy, 2013).

To analyse the performance of floating stone columns, especially when subjected to uniform loading, one can use the settlement improvement factor, which is the ratio of the ultimate settlement of soil with and without columns, and function β , which is the ratio of the length of the columns and the thickness of the soft soil (Ng and Tan, 2014). The most widely used semi-empirical technique, which was presented by Priebe (1995), served as the foundation for this investigation. The pore pressure dissipation similarly reduces as the value of β lowers. The flow of pore water from the surrounding soil to the column occurs radially.

The efficiency of stone columns is significantly impacted by the permeability of soft clays (Rajesh and Jain, 2015). The Yoo and Kim (2009) study, which produced a 6 m high embankment in three successive increments of 2 m each, served as the basis for the creation of the hypothetical GESC-treated embankment (Figure 2.2). The final settlement of the soft clay that had not been treated was nearly three times greater than the settlement of the soil that had been treated with stone columns. There was a reduction of 43% and 61% in the ultimate settlement of OSC and GESC in relation to soft clay, respectively.

When taking into account the cyclic loading caused by the transport load, it is noted that elastic deformations on the column and soil happen immediately following the application of load due to embankment, leading to the occurrence of undrained settlements (Basack et al., 2016). The deformation of the embankment on soft soil may be observed as it gradually bends due to the stiffness of the column-soil interaction (Indraratna et al., 2013). The amount of deformation in the stratum is affected differently by the imposed surcharge load before to, during, and after consolidation. For regular soil, OSC, and GESC, the dissipation of pore pressure takes 7000, 52, and 30 days on average, respectively. According to Rajesh (2017), the maximum immediate settlement of GESC is 21% less than that of OSC and 42% less than that of regular clay.

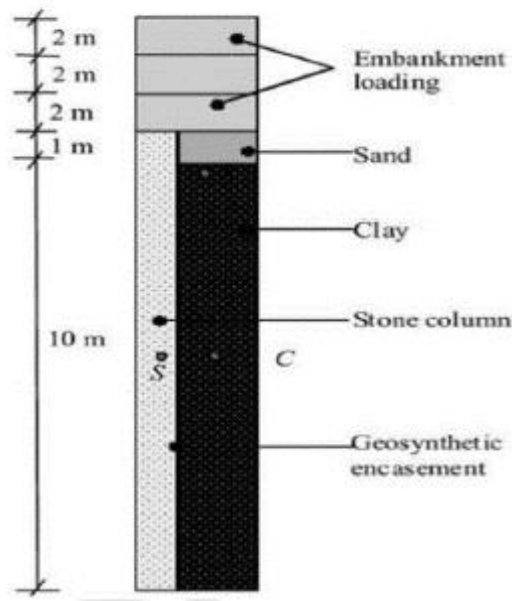


Figure 2.2. Schematic Illustration of GESC Modelling Specifications. (Rajesh, 2014)

The smear zone of the soil's permeability and compressibility have a significant effect on the time taken by the stone column to consolidate. Since the vertical path is comparatively longer than the horizontal path, the mathematical method to calculate the rate of consolidation is predicated on the idea that there is no flow in the soil in a vertical direction (Han and Ye, 2001). Permeability and compressibility have a circular influence region. The total load applied to the stone column is distributed between the disturbed and undisturbed zones.

The stone column, along with the adjacent soil, undergoes axial deformation during consolidation. Often, complex localised bands that challenge conventional analytical explanations accompany shear deformation in stone columns. In their finite element analysis, Singh et al. (2019) demonstrated that, even when coupled formulation is used, the shear band thickness inside the stone column reduces when the mesh is refined. It was also discovered that the overall temporal settlement profile of the column was unaffected by localization.

The load carried by undisturbed soil is greater than the load supported by disturbed soil when compressibility along the smear zone varies because of variations in volume compressibility. The compressibility of the zone of smear has a considerable impact on the degree of the consolidation of the stone column. According to Deb and Behera (2017), the smear zone actually has the least consolidation. If the diameter ratio is increased from two to

five times, or if the smear zone radius is increased from one to three times, the time needed for 90% consolidation can increase by as much as two to three times.

The soil-column system's settlement is found to increase hyperbolically with applied vertical tension, according to research using the Fast Lagrangian Finite-Difference method (Basack et al., 2017). The discrete element finite difference (DEM-FEM) model Indraratna et al. (2015), which is predicated on the assumptions that deformation occurring in columns and soil is axisymmetric and that pore water flows horizontally (Han and Ye, 2002), closely resembles the graph illustrating the relationship between lateral deformation and depth in a column. According to the Lateral Deformation of Column (LDCOL) program's findings, applied vertical stress causes a hyperbolic increase in the soil-column system's settlement.

The influence of the stone column's length and diameter on the settlement of soft soil was solved mathematically using Response Surface Methodology (RSM) software (Madun et al., 2018). For various combinations of the parameters, the response plots from the RSM provided the best link between the stone column's diameter and settlement. Singh et al. (2018) suggested a regularised solution for the incorrect shear localization results in the geomaterials analysis. The solution from finite element analysis becomes more or less reliant if the constitutive formulation has no internal length scale (Etsee and William, 1999; Needleman, 1988; Schreyer, 1996 and Wang et al., 1997). The regularisation technique is used to solve this issue. Stress-strain response and shear band thickness are impacted by mesh refinement. After the mesh is refined, an increase of 0.02 m is noted in the total settlement.

The type of material used to build stone columns has an impact on how quickly the surrounding subsoil settles and consolidates. Three different types of stone columns—pebble gravel, crushed pebble gravel, and quarry stones—were used to enhance the Slovakian test site. Laboratory studies revealed the original subsoil's characteristics (Abusharar and Han, 2011; Barksdale and Bachus, 1983). Pebble gravel took the longest to consolidate out of the three types of column materials and generated the most distortion. The stones with the shortest consolidation times are quarry stones. Because quarry stones have the quickest rate of consolidation and the least amount of settling out of the three types of gravel, they make the ideal choice for stone material (Stacho and Sulovska, 2017).

4. The surrounding soil's bearing capacity

Increasing the soil's carrying capacity is a crucial prerequisite for using stone columns to reinforce soft soils and make them appropriate for engineering uses. It has been discovered that stone columns significantly improve the soil's bearing capability by creating a composite

soil-column system that functions as a supporting stratum for the underlying structure (Jadid, 2013).

The bearing capacities of reinforced and unreinforced soil are compared using the bearing capacity ratio (BCR) factor. The size of the footing is one of the determining variables that affects the bearing capacity of stone columns (Choobbasti, 2011 and Nazaruddin, 2013). The roughness of footings has a little effect on the stability and deformation of stone columns; however, the difference in bearing capacity between smooth and rough footings is so small that it may be ignored in designs.

There is a significant increase in the bearing capacity of the stone column encased with geogrid. From the relation between $q_{\text{treated}}/q_{\text{untreated}}$ and undrained shear strength of end-bearing soil, it is found that there is no significant role of end-bearing soil in increasing the strength of ordinary stone columns because, in ordinary stone columns failure occurs by lateral bulging which is affected mainly by the surrounding soil, on the other hand, in encased stone columns, there is a punching failure which is mainly affected by the end bearing soil (Fattah and Majeed, 2012).

Fattah and Majeed (2012) employed the Statistical Package for the Social Sciences (SPSS) to create a regression equation based on prior experimental outcomes and experiments conducted. The connection for carrying capacity was calculated as a function of c_u : the soil's undrained shear strength, the L/D ratio, N_s : Number of stone columns, A_r , the area replacement ratio, and it was provided as:

$$q_u = 15.34 \times c_u^{0.401} \times A_s^{0.266} \times N_s^{0.084} \times (L/D)^{0.526} \quad (2.1)$$

In order to determine the stone columns' bearing capacity, Bowels (1996) and Bouassida et al. (1995) provided a number of additional formulae.

The relationship between bearing capacity and influencing parameters is also ascertained by the application of Design Expert software and Response Surface Methodology (RSM). For various combinations of the parameters, the response plots from the RSM provided an ideal relationship between the stone column's length, diameter, and load-bearing capacity. The best bearing capacity was found to be 3260.7 N for a desirability of 77% at 44 mm diameter and 10 cm length, according to the results of the ANOVA result interpretation approach (Madun et al., 2018).

5. Area Replacement Ratio (A_r)

The area of stone columns in relation to the surrounding soil area is known as the "area replacement ratio," or " A_r ." The diameter of the stone columns can be raised to raise the area replacement ratio.

Cimentada et al. (2011) examined two distinct stone column diameters: 8.47 cm and 6.35 cm. Calculations showed that the A_r was 11.11% and 6.25%, respectively. For the two values of the diameter, the Stress Concentration Ratio (SCR) ranged from 0.68 to 0.75. This resulted from a drop in the stiffness ratio between the surrounding soil and the stone column as pressure increases. The improvement in bearing capacity begins even at lower values of Length / Diameter (L/D) ratios as the value of " A_r " increases. This indicates that the area replacement ratio has a greater impact on increasing the stone column's bearing capacity than does the column's length (Fattah and Majeed, 2012).

According to Shahu and Reddy (2011), there is a correlation between an increase in A_r and an improvement in the stiffness of the floating column in the end-bearing column. In addition to A_r , additional elements that influence consolidation rate include the angle of internal friction, loading intensity, and post-installation pressure, with A_r having the most significant impact. Ng and Tan (2014) provided a design equation that demonstrates how the area replacement ratio, internal friction angle, load intensity, and ground pressure during postconstruction affect the settling of stone columns.

6. Depth of penetration or L/D ratio

The stone column's stiffness increases as the column's length to diameter (L/D) ratio rises. Moreover, increasing the buried depth of the column will boost the soil's final bearing capacity, while increasing the diameter will lessen the likelihood of the stone column bulging (Shahu and Reddy, 2011).

According to a study by Black et al. (2011), an increase in the L/D ratio significantly improves the stone column's settlement profile. The ideal L/D ratio for an average column is between 7 and 8. There is no difference in $q_{\text{treated}}/q_{\text{untreated}}$ after 8. However, for GESC's, the $q_{\text{treated}}/q_{\text{untreated}}$ continues to rise even when $L/D = 8$, indicating that there is no such limiting value for the L/D ratio in the case of reinforced stone columns (Fattah and Majeed, 2012).

Madun (2018) carried out a separate analysis for the regulation of the stone column's height and diameter to assess the effect on bearing capacity and settlement, respectively, using Design Expert software. The bearing capacity reached its maximum at 44 mm diameter and 10 cm length, or 3260.7 N, for a 77% desirability.

7. Stress Concentration Ratio

A key consideration in choosing the stone column design is the Stress Concentration Ratio (SCR). Its definition is the ratio of the tension that the surrounding earth and the stone

column carry to each other. The purpose of adding a stone column to any soft soil is to lessen the surrounding tension because the stone column will be responsible for carrying the majority of the load. Therefore, a higher stress concentration will result in a higher stone column efficiency ratio.

According to Elsayy (2013), SCR in encased stone columns rises as the weight increases, whereas it remains nearly constant in ordinary stone columns (OSC). While the value of the stress concentration ratio for the GESC increases gradually over the course of the consolidation period, the effective stress concentration ratio of an OSC increases gradually during consolidation for the first loading period and begins to decrease after saturation limits with a constant value (Rajesh, 2017). The GESC endured an effective stress that was 1.25 times higher than the OSC. Early on in the loading process, there is less concentration of stress. The stress produced in the column columns rises with increasing loads until it reaches a particular value and eventually stabilises over time. There is a higher stress concentration factor for low stress levels during the initial loading phase.

Rajesh and Jain (2015) investigated how permeability affected the stone columns' strength and functionality. It is discovered that the GESC's Effective Stress Concentration Ratio (ESCR) rises over the course of the consolidation phase. Permeability of the soil has a major impact on treated ground and postconstruction settlement of soft clays.

2.4 STONE COLUMN CONSTRUCTION METHODS

There are two ways to create a stone column: the displacement method and the non-displacement approach, also known as the replacement method. Whereas the replacement method backfills the borehole with granular material, the displacement approach pushes the soil laterally and backfills it with the material. IS 15284 (Part -1): 2003 has covered these techniques. Other well-known building methods include the rammed stone column (Datye and Nagaraju, 1981), the simple boring method (Ranjan and Rao, 1983), and the vibro-compaction method.

2.4.1 Displacement Method of Construction

When building stone columns, the soft soil is first treated by lowering the vibrator into the ground. This causes a void in the ground to be formed, which is subsequently filled in by stone aggregates. Aggregates are vibrated into a dense state while backfilling the cavity by inserting the vibrator again. The resulting column-soil composite lessens the ground's compressibility and settling. Additionally, it raises the soil's stiffness, shear strength, and bearing capacity (Charles and Watts, 1983). Where a bearing stratum is present, the best outcomes are typically obtained (Barksdale and Bachus, 1983).

2.4.2 Replacement Method of Construction

As illustrated in Figure 2.3, the replacement method of building a stone column involves creating a cavity, which is aided by digging under the influence of strong air or hydraulic pressure. As a result, the soft soil is removed and replaced with stone aggregates. The other steps are the same: to achieve a uniform density, the stone aggregates are backfilled gradually and compressed using a vibrator.

A straightforward technique was created by Rao (1982) and Ranjan and Rao (1983), which is especially helpful in developing nations. The borehole is made with a spiral auger and human labour. Once the borehole reached the appropriate depth, it is completely cleaned. The powdered substance is then layered in the borehole in intervals of 300–500 mm, with a layer of sand between 50 and 100 mm in between. To supply the compactive effort to the granular material layer, a power winch with a fall of 750 mm powers a cast iron hammer that weighs 125 kg and has a diameter smaller than the borehole. Sand fills in the spaces left by the granular materials during the hammer's compaction process, and then the charged material is moved laterally and downward until the surrounding soil is fully compacted. Figure 2.4 displays a schematic depiction of the procedure.

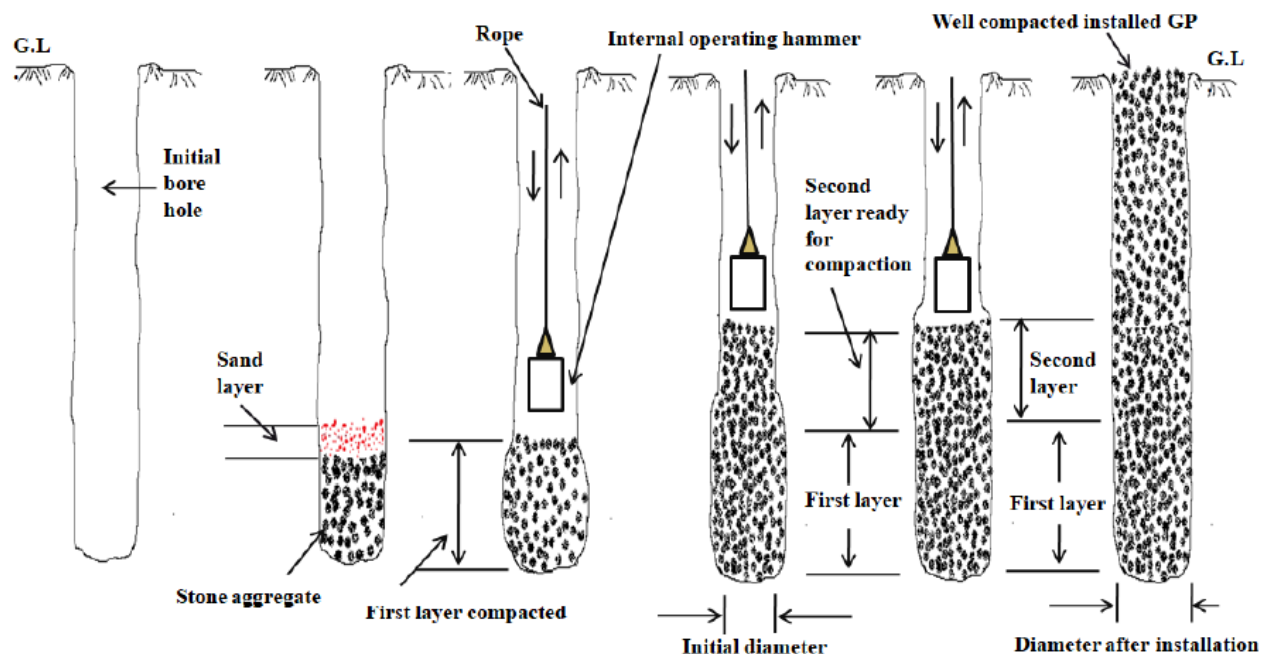


Figure 2.3. Granular pile construction using an easy auger boring technique (Rao, 1982)

2.5 FAILURE MECHANISM OF STONE COLUMNS

2.5.1 Mechanism of Load Transfer of Stone Columns

Equal strain and equal stress are the two optimal loading and displacement conditions in geotechnical analysis. Equal stress and strain conditions exist under flexible loading (such as tyre pressure) and rigid loading (such as rigid footing). Because of the variation in modulus among the columns and the nearby soil, the columns bear a greater stress than the soil under an equal strain condition (also known as equal settlement on the columns, S_{cl} , and the soil, S_{sl}) (Figure 2.4).

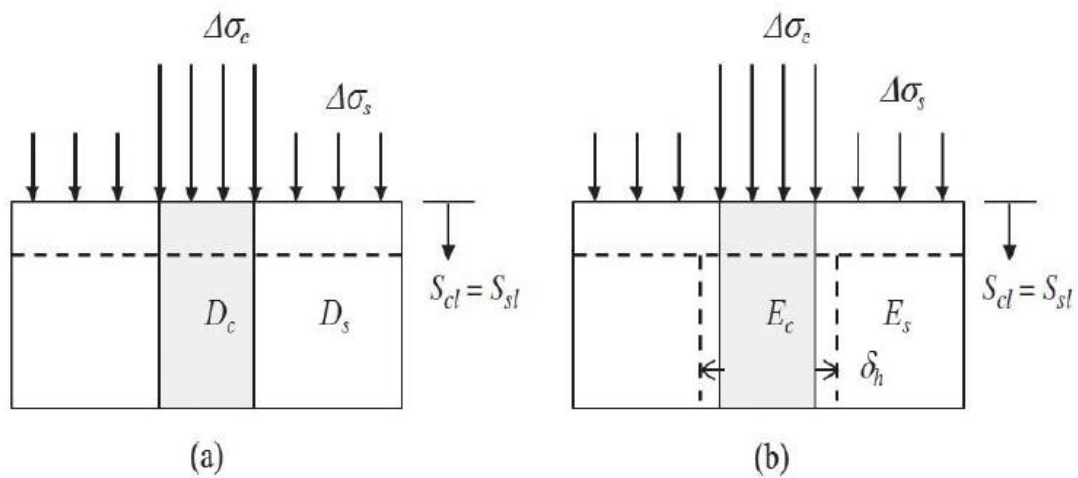


Figure 2.4. (a) Unit cells that are not deformed laterally (b) Unit cells that are deformed laterally (Han, 2015)

Stress concentration ratio (n), which is frequently used to characterise the transfer of load between columns and soft soils, is known as the ratio of the stress over the column (σ_c) to that over the soil (σ_s). In contrast, under an equal stress condition, the soil and columns have different settlements (i.e., $S_{sl} > S_{cl}$) but bear the equal stress (i.e., $n = 1$). The consequence is a difference in settlement between the soil and the columns.

Since equal vertical strain is more pronounced beneath embankments and footings than that of equal stress, it is typically assumed to simplify theoretical solution development and design (Castro and Sagaseta, 2009). This requirement suggests that the column's and the surrounding soil's settlement under rigid loading is equal (Han, 2015). Owing to its increased rigidity, the column bears a greater weight than the surrounding earth.

2.5.2 Failure Modes of Stone Columns

Generally, two different sorts of columns that are built, depending on their length and the resistance forces that are created within them (Barksdale and Bachus, 1983):

- End-bearing, or reaching the entire depth of a hard, sustaining stratum and
- Floating (partial depth), resisting pressures by side friction

According to Figure 2.5, the columns can be long or short depending on the value of slenderness ratio, that can be defined as the ratio of the diameter of the column to its length (McKelvey et al., 2004). The following type of failures could happen:

- Failure due to bulging: column has been restricted from upper to lower solid layer. The column material resists the impending load, increasing its lateral length. The surrounding material is now under stress instead of the bulged section, and equilibrium has been reached.
- Local shear failure can occur in short columns ($L/D < 6$) that are positioned above a bearing stratum. In these columns, L and D represents the length and diameter of the column, respectively (McKelvey et al., 2004).
- Both floating columns and end-bearing columns may fail in bulging, and short columns in a weak strata might fail in end bearing or punching prior to the bulging occurring inside the critical length (Hughes and Withers, 1974). When designing a short end bearing column, it is important to take into account the possibility of local bearing capacity failure occurring prior to bulging, particularly if the column is supported by weak strata. When the columns are not lowered to a suitable depth, there is a possibility of punching shear failure (Barksdale and Bachus, 1983).

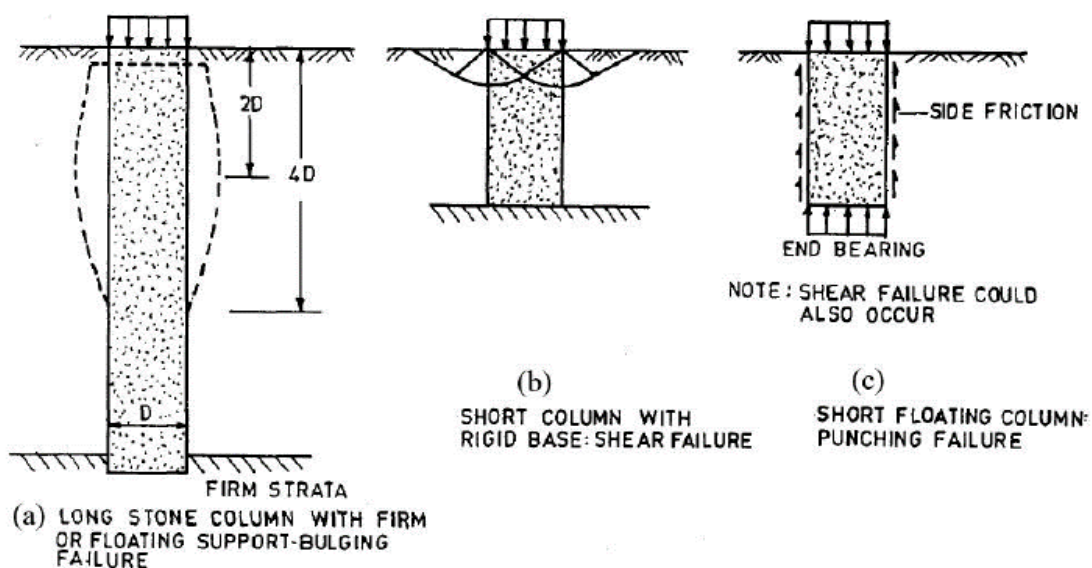


Figure 2.5. Failure mechanisms for a stone column in cohesive soil that is not homogeneous (IS 15284)

When wrapped in an appropriate geosynthetic material, an ordinary column can assist a stone column in many ways. For example, it can provide additional lateral confinement, act as a semirigid element to facilitate load transfer to deeper depths, prevent stones from being squeezed into surrounding soft clays, minimising stone loss, enable a higher degree of compaction than with conventional stone columns, promote vertical drainage by serving as an effective filter, preserve the frictional properties of the aggregates, and increase the stone column's shear resistance (Murugesan and Rajagopal, 2009).

2.6 DESIGN OF STONE COLUMNS

The two primary types of stone columns are conventional (without any encasement) and geosynthetics encased stone column. Based on the aforementioned two categories, bearing capacity and settling studies should be separated.

2.6.1 Ordinary Stone Columns

2.6.1.1 Enhancement of bearing capacity investigation on ordinary stone columns

Numerous researchers looked into the load carrying ability of the foundation which is being reinforced with the help of granular columns. Their findings showed a direct relationship between the frictional properties of the material which makes up the column and the lateral support (confinement) given by the nearby soil.

After conducting an experimental study on deformation surrounding a stone column placed in a bed of kaolin clay, **Hughes and Withers (1974)** came to the conclusion that the column bulges within a radius four times its diameter, as measured from the head of the column. Additionally, the nearby earth and the column share the applied vertical load. These findings served as the basis for further investigation and stone column design. The load-settlement curve that was acquired for their investigation is presented in the Figure 2.6 and the setup in Figure 2.7.

Hughes et al. (1975) postulated a state of failure in both the soil and the column, as well as a triaxial stress state within the column. As previously mentioned, Hughes and Withers' (1974) laboratory model experiments served as the foundation for the proposal of this theory. The total limiting radial stress that the neighbouring soil can generate to support the column is considered the confining stress (σ_{rL}) in this study. The maximum vertical stress that the column can endure (σ_v) is calculated by multiplying the confining stress by the coefficient of passive earth pressure (K_{ps}) of the granular column.

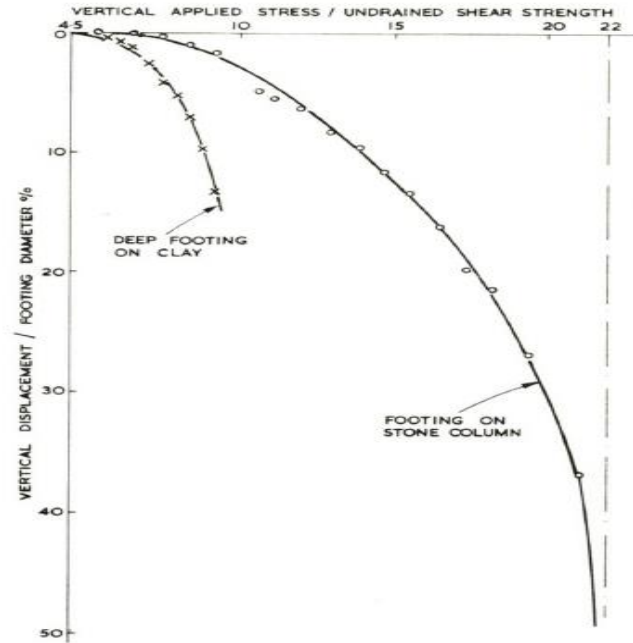


Figure 2.6. Load-Settlement curve (Hughes and Withers, 1974)

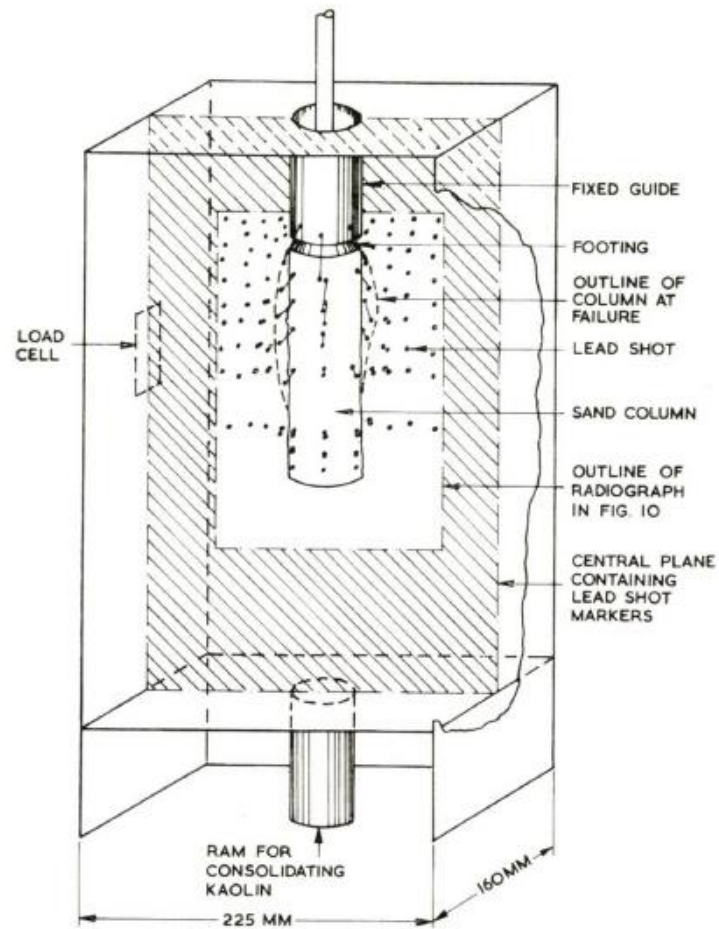


Figure 2.7. Consolidometer test on single stone column (Hughes and Withers, 1974)

$$\sigma_v = \sigma_{rL} \frac{(1 - \sin \phi')}{(1 + \sin \phi')} \quad (2.2)$$

$$K_{ps} = \frac{(1 - \sin \phi')}{(1 + \sin \phi')} \quad (2.3)$$

Where, σ_{rL} = Limiting radial stress,
 ϕ' = Frictional angle of stone column aggregates,
 K_{ps} = Coefficient of passive earth pressure of the soil.

$$\sigma_{rL} = 4c_u + \sigma_{ro'} + u_o \quad (2.4)$$

where, $\sigma_{ro'}$ = Initial radial effective stress around the column,
 σ_{rL} = Total limiting radial stress of the column,
 u_o = Initial excess pore-pressure,
 c_u = Undrained shear strength of soil.

For the analysis of a solitary stone column present in a saturated soft clay stratum under the undrained conditions, **Brauns (1978)** suggested a convenient method to calculate the confining stress of the neighbouring soil.

$$\sigma_r = \left(\Delta\sigma_s + \frac{\Delta c_u}{\sin 2\Psi} \right) \left(1 + \frac{\tan \Psi_p}{\tan \Psi} \right) \quad (2.5)$$

where, σ_r = Lateral confinement from the neighbouring soil,
 Ψ_p = Column passive failure plane angle,
 Ψ = Angle of surrounding soil failure plane,
 c_u = The surrounding soil's undrained shear strength.

According to equation (2.5), the confining stress varies with the soil failure plane's angle. Finally, the confining stress can be determined by taking the derivative of the previous equation with respect to the failure plane angle and setting it equal to zero. The granular column's coefficient of passive earth pressure (K_p) multiplied by the confining stress gives the ultimate vertical stress that the column is capable of withstanding (σ_c).

$$\sigma_c = K_p \times \sigma_r \quad (2.6)$$

where, σ_c = Ultimate vertical stress,
 K_p = Coefficient of passive earth pressure of the stone column.

According to **Barksdale (1987)**, the column and the neighbouring soil mobilise their strength at an equal strain level, or the equal strain scenario. As a result, the composite foundation's ultimate bearing capacity (q_{ult}) can be stated as follows:

$$q_{ult} = q_{ult, c} A_s + q_{ult, s} (1 - A_c) \quad (2.7)$$

Additionally, he recommended estimating the surrounding soil's ultimate bearing capacity ($q_{ult, s}$) using $5c_u$. Equation (2.7) can therefore be reduced to:

$$q_{ult} = 5c_u (3A_s + 1) \quad (2.8)$$

IS Code Method (IS 15284 Part 1: 2003)

(1) Capacity Determined by Column Bulging

$$\sigma_v = \sigma_{rl} \cdot K_{pcol} \quad (2.9)$$

where, σ_v = Limiting axial stress generated in the column when it gets closer to shear failure because of bulging,

σ_{rl} = Limiting radial stress

$$\sigma_{rl} = \sigma_{ro} + 4c_u \quad (2.10)$$

K_{pcol} = Column's passive earth pressure coefficient

$$\sigma_v = (\sigma_{ro} + 4c_u) K_{pcol} \quad (2.11)$$

σ_{ro} = Initial effective radial stress

c_u = Undisturbed undrained shear strength of the clay around the column.

$$\sigma_{ro} = K_o \sigma_{vo} \quad (2.12)$$

K_o = For clay soils, the mean lateral earth pressure coefficient has a value of 0.6, or alternatively, it can be calculated using the formula $K_o = 1 - \sin\phi_s$, where ϕ_s is the effective angle of soil's internal friction.

σ_{vo} is the average initial effective vertical stress, calculated by taking the column's diameter ($\gamma 2D$) twice as the average bulging depth.

γ = The soil's effective unit weight in the influence zone,

D = Diameter of the column.

$$K_o = 1 - \sin\phi \quad (2.13)$$

$$K_{pcol} = \tan^2 (45^\circ + \phi/2) \quad (2.14)$$

Safe load on column alone,

$$Q_1 = (\sigma_v \cdot \frac{\pi}{4} D^2) / 2 \quad (2.15)$$

where, 2 is the factor of safety.

(2) Surcharge Effect

$$\Delta \sigma_{ro} = q_{safe} (1 + 2 K_o) / 3 \quad (2.16)$$

q_{safe} = Soil safe bearing pressure with a 2.5 safety factor

$$q_{safe} = C_u N_c / 2.5$$

C_u = Undrained shear strength,

N_c = Terzaghi bearing capacity factor.

For a safety factor value of 2, increase in the safe load due to surcharge,

$$Q_2 = K_{pcol} \cdot \Delta \sigma_{ro} \cdot A_s / 2 \quad (2.17)$$

(3) Intervening soil support

$$\text{For a column, area of the intervening soil, } A_g = 0.866 S^2 - \frac{\pi}{4} \cdot D^2 \quad (2.18)$$

$$\text{Safe load supported by the intervening soil, } Q_3 = A_g \cdot Q_{safe} \quad (2.19)$$

(4) Total safe load on every column and the surrounding soil

$$Q = Q_1 + Q_2 + Q_3 \quad (2.20)$$

Ambily and Gandhi (2007) varied the factors, like the distance that exist between the columns, the soft clay's shear strength, and the loading situation, to investigate the behaviour of single as well as group of end-bearing stone columns. Two different loading arrangements have been used in the investigation: (i) only the stone column's area has been loaded (for the stone column's load carrying capability), and (ii) the full unit cell has been loaded (for the stiffness of the enhanced ground). Stone columns measuring 100 mm in diameter and 450 mm in height were selected for both individual and group analysis. Test tanks with diameters ranging from 210 to 420 mm for single stone columns and a sizable tank having a diameter of 835 mm for a group of seven columns have been taken in order to maintain the spacing requirements. For the model testing, soft clay having the undrained shear strengths of 7, 14, and 30 kPa was utilised. Using the replacement approach, stone aggregates with sizes varying from 2 to 10 mm were utilised to construct the stone columns. The stone column has been built with a light compacting method to prevent bulging during installation. Axial stress applied to the loading ranged from 100 to 150 kPa until the settling exceeded 10 mm. It was noticed that the bulging occurred at a depth that was half the diameter of the stone column when only the column region was loaded. There was no bulging seen throughout the loading of the entire area. The FEM analysis was performed for parametric research and to compare

the experimental results using the PLAXIS programme (15-noded triangular elements with boundary condition). The relative relationship among the axial stress and settlement for various undrained shear strengths has been observed to be similar for single column loading at constant s/d ratio. Up to s/d ratio = 3, the column's limiting axial stress reduces; after that, the reduction in axial stress is minimal. The confining action from the unit cell boundary prevents the failure for the entire area loading. The relationship between axial stress and settlement was found to be almost linear for varying soil shear strength and s/d ratios. The stiffness improvement factor, that is dependent on the s/d ratio and independent of the surrounding clay's shear strength, is the ratio of treated ground's stiffness to untreated ground's stiffness. There was no discernible improvement in stiffness for s/d ratio more than 3. The behavior of a group of stone columns was found to be comparable with that of a single stone column for s/d ratios ranging from 0 to 3. This demonstrates that a single stone column with a unit cell idea is capable of simulating the field behavior of an inside column when a large number of columns are loaded simultaneously. FEM analysis has been used to determine the stress concentration ratio using s/d ratio (1.5 to 4) for both individual and group columns. Stress concentration is found to be equivalent in the two scenarios, supporting the validity of the unit cell concept. Furthermore, it is observed that the stress concentration on the stone column would increase when shear strength of the soft soil falls.

2.6.1.2 Studies on the reduction of settlement in ordinary stone columns

Many techniques for forecasting the settlements of feeble subsurface deposits reinforced by stone columns have been put forth over the past thirty years. A summary of the key techniques is provided below.

The stone column was recognised by **Priebe (1976)** as rigid-plastic, incompressible, and end-bearing. It was demonstrated that in these circumstances, the stress concentration ratio, n ($=q_p/q_s$), falls with a factor of $1/\alpha$ (α being the earthquake design reduction factor). Using the unit cell concept, he devised the fundamental improvement factor approach as illustrated in Figure 2.8, taking into account the soil's Poisson's ratio (μ), frictional angle of the column material (ϕ), and the area replacement ratio (A_r). The elastic soil contained in the unit-cell underwent an oedometric settlement, yielding the subsequent expression.

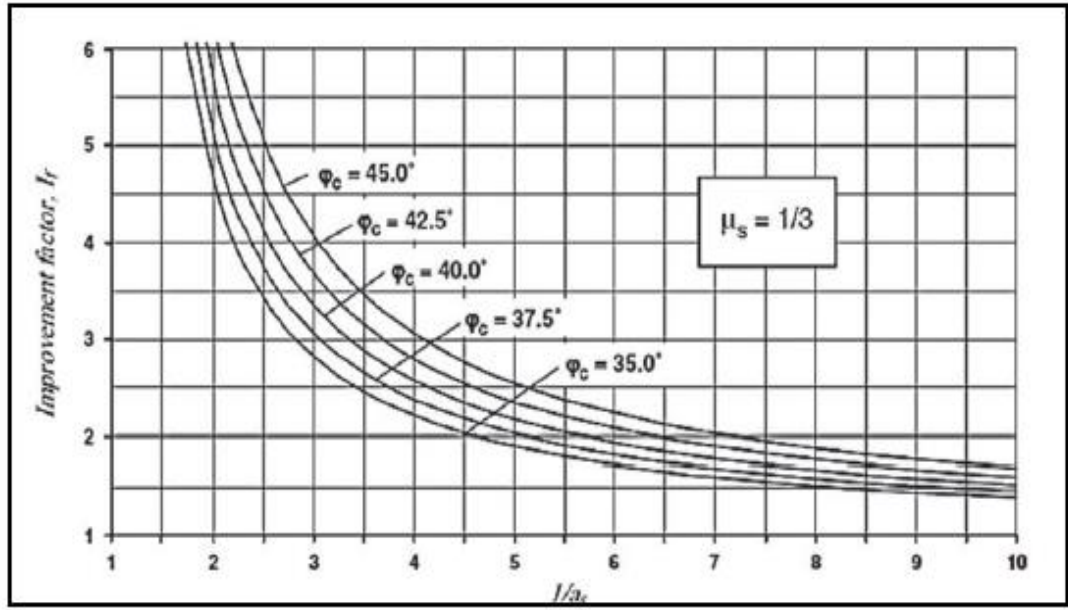


Figure 2.8. Chart for Improvement Factor (Priebe, 1976)

Following the previous figure's improvement factor (I_f) computation, the decreased settlement can be computed using the formula below:

$$S' = \frac{S_u}{I_f} \quad (2.21)$$

$$I_f = 1 + A_r \left[\frac{0.5 + f(\mu, A_r)}{(K_a)_s f(\mu, A_r)} \right] \quad (2.22)$$

$$f(\mu, A_r) = \left[\frac{1 - \mu^2}{1 - \mu - 2\mu^2} \right] \left[\frac{(1 - 2\mu) + (1 - A_r)}{1 - 2\mu + A_r} \right] \quad (2.23)$$

$$K_a = \tan^2(45 - \phi/2) \quad (2.24)$$

Where, S' = The introduction of granular columns results in lesser settlement,

S_u = Untreated settlement in the foundation

Under the influence of larger loading area, S_u can be obtained as:

$$S_u = m_v \cdot \Delta\sigma_z \cdot h \quad (2.25)$$

Where, m_v = Soil's volumetric compressibility coefficient,

h = Thickness of the soil layer,

$\Delta\sigma_z$ = Pressure due to surcharge.

Based on the unit-cell idea, **Aboshi et al. (1979)** analysed a case where the vertical displacement in the column and soil was equal and the total vertical load applied at the top equaled the load on the column and the soil. Moreover, it was presumed that the column's entire length experiences the same level of vertical stress.

The replacement factor (A_r) and stress concentration ratio (n) have been linked to the settlement reduction ratio (R). The total settlement (S_t) is determined as:

$$S_t = m_v (\mu_c \cdot \sigma) H \quad (2.26)$$

Where, m_v = Soil's volumetric compressibility coefficient,
 σ = Unit normal stress,
 H = the height of stone column.

The settlement reduction ratio, R was given by

$$R = \mu_c = \frac{1}{1 + (n-1)A_r} \quad (2.27)$$

IS Code Method (IS 15284 Part1:2003)

Consolidation settlement of the treated composite soil S_t , is given as:

$$S_c = m_v \sigma_z h \quad (2.28)$$

$$\sigma_z = \sigma / \{1 (n - 1) a_s\} \quad (2.29)$$

Where, m_v = Coefficient of volume compressibility,
 σ_z = Vertical stress in the neighbouring ground,
 h = Thickness of the treated soil,
 σ = Applied stress,
 n = Stress concentration factor / ratio,
 a_s = Area replacement ratio.

A theoretical method for calculating the consolidation rate of foundations reinforced by granular column that takes the well resistance and smear zone into account was presented by **Han and Ye in 2002**. Han and Ye (2001) introduced a streamlined approach to ascertain the consolidation rate of reinforced stone column foundations in a previous paper. The area of disturbed soil surrounding a column caused by stone material seeping into the soil during construction is known as the smear zone. The decrease in the column material's permeability brought on by nearby soil seeping into the stones is known as the well resistance. The unit cell components depicted in Figure 2.9 are utilised in the theoretical solution to determine the consolidation rate of foundations reinforced by granular column.

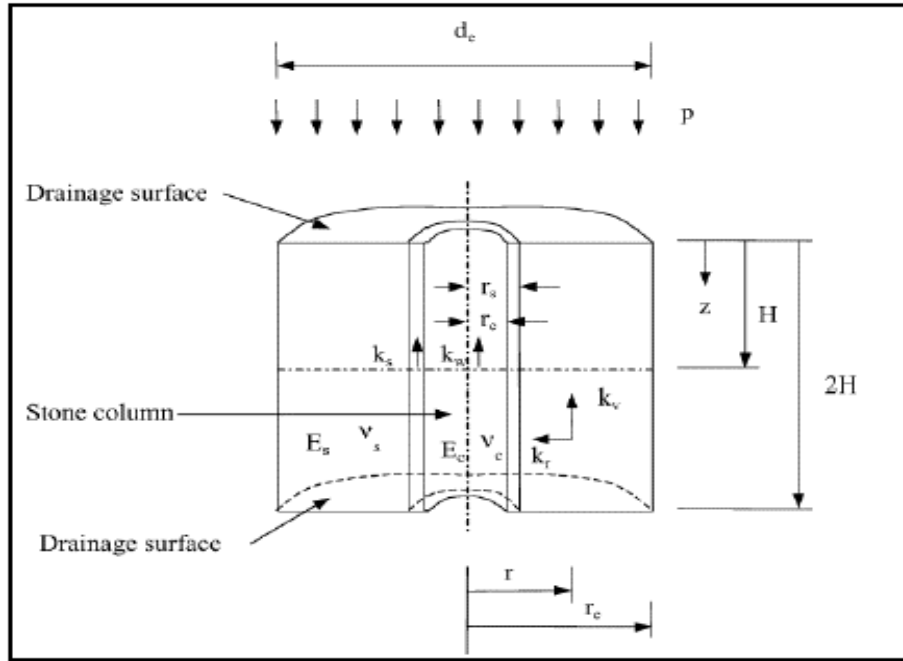


Figure 2.9. Unit cell model (Han and Ye, 2002)

The equivalent diameter (d_e), soil's elastic modulus (E_s), and column elastic modulus (E_c) make up the unit cell. The permeability of the soil is described by the smearing zone (k_s), stone column (k_w) (or k_c), and radial and vertical directions (k_r and k_v). The unit cell's equivalent radius is r_e , the undisturbed soil zone's radius is r_s , the stone column's radius is r_c , and the smeared zone's radius is r_s . The symbols "H" and "z" stand for the thickness of the soil strata and the depth of pore pressure, respectively.

A parametric analysis has been conducted on six variables that impact the consolidation rate. The variables are - Diameter ratio of the smeared zone to that of the column = d_e/d_c (N), permeability of granular column (k_c), stress concentration ratio = σ_c / σ_s (n_s), diameter ratio of smeared zone to the drain well = d_s / d_c (S), permeability of soil in smear zone (k_s) and thickness of the soil layer undergoing drainage (H). The effect of each factor has been discussed below.

- (i) The drainage path is shortened and the diameter ratio "N" is decreased when a stone column's diameter increases. This is the reason why the rate of consolidation is accelerating.
- (ii) When tiny particles from soil slurry are deposited onto the stone column region during installation, the stone columns permeability " k_c " decreases. The ratio of

permeability, k_r/k_c , rises as a result of this permeability decrease, slowing the rate of consolidation.

- (iii) Because the column experiences more stress than that of the nearby soil, the stress concentration ratio " n_s " rises, accelerating the pace of consolidation in a radial direction.
- (iv) Because the permeability of the zone of smear is thought to be lower than that of the undisturbed soil, the area of smear zone " S " has an impact on the consolidation rate. Reducing the smeared zone area could hasten the consolidation process.
- (v) The permeability of the soil in the zone of smear is decreased when soft soil is smeared because it alters the soil's structure and destroys the fine layers of horizontal drainage. The smearing-induced decrease in soil permeability, or " k_s ," substantially decreases the process of consolidation.
- (vi) The mean rate of consolidation decreases as the drainage path " H " increases and pore water dissipation could take longer.

In order to generate big clay bed samples by consolidation, **Kolekar and Dasaka (2014)** presented a gravity loading methodology using lever arm technology, which does away with the necessity of placing massive dead weights on the clay (Figure 2.10). The slurry state of the clay beds is prepared. There are two test series administered: A and B. Each series consists of seven tests. The purpose of these experiments is to prepare consolidated clay beds, which are then exposed to consolidation pressures of 18, 36, and kPa, respectively. It is noticed that the coefficients of variation (COV) of the shear strength measured and the recorded water content of consolidated clay bed are considerably lesser than 10%, which is deemed acceptable.

Deb and Shiyamalaa (2015) put up a mathematical model that takes particle migration-induced blockage into account when estimating the consolidation rate of soil enhanced by stone columns. There are some fine particles that have been liberated from the soil as well as some impure water in the soil's pores. These fluid-containing particles ooze out of the fluid along with it. The degree of particles concentration in the seepage water determines the quantity of clogging that occurs and the resulting decrease in the stone column's permeability. Clogging, thus, slows down the rate at which the stone column-improved ground consolidates. Only single stone column and its area of influence are taken into account in their study. As a result, as seen in Figure 2.11, the unit cell which is cylindrical and having a

circular ring containing soil covering the stone column. The unit cell in this investigation is separated into four zones: the soil zone, the zone of smear, the clogged zone, and the unclogged zone.

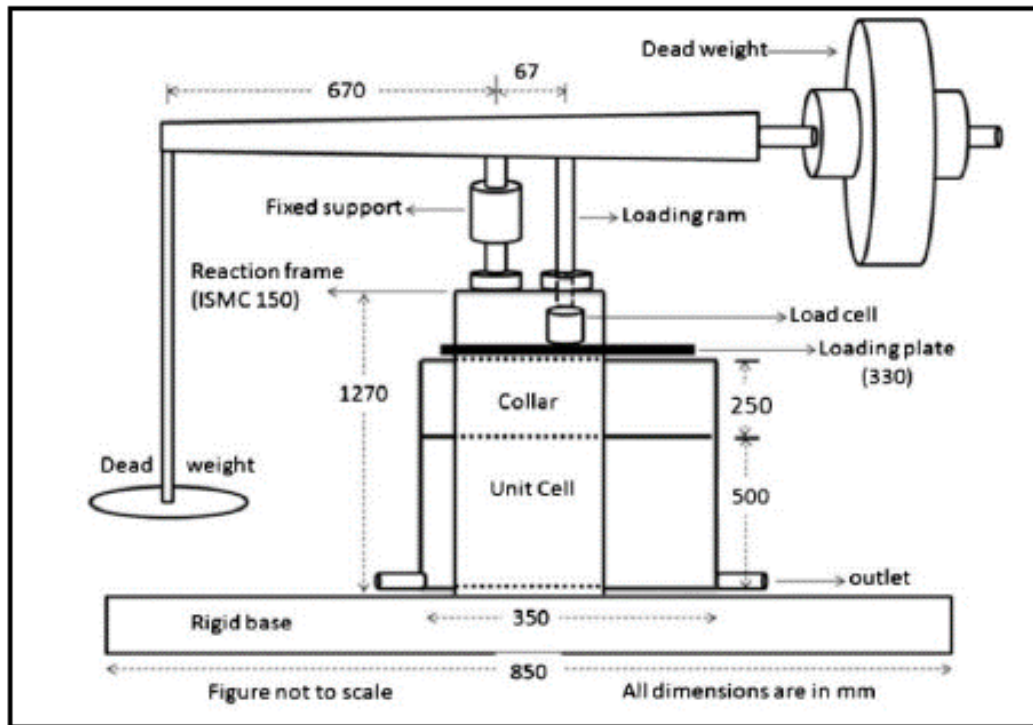


Figure 2.10. The response frame's schematic diagram (Kolekar and Dasaka, 2014)

As seen in Figure 2.12, the outcomes are related with the various available models considering the rate of consolidation for stone column–improved ground, both with and without clogging. Additionally, the impact of several parameters which are varied in the constructed model on the consolidation rate are examined. It has been noted that when clogging increases, so do the diameter ratio and stress concentration ratio.

The laboratory investigation on the settling of clay which is reinforced with sandy columns under continuous pressure was performed by **Rangeard et al. (2016)**. The investigation examined the impact of the building method for sand columns and the compaction force used during their installation on the hydromechanical behaviour of the soil/column system. Sand with particles ranging from 1 to 1.25 mm was utilised as the column material for the construction of stone columns, while the soil utilised was industrial kaolin, which was categorised as CH. The wet kaolin bed was subjected to continuous pressure for a specific amount of time to prepare the soft soil bed.

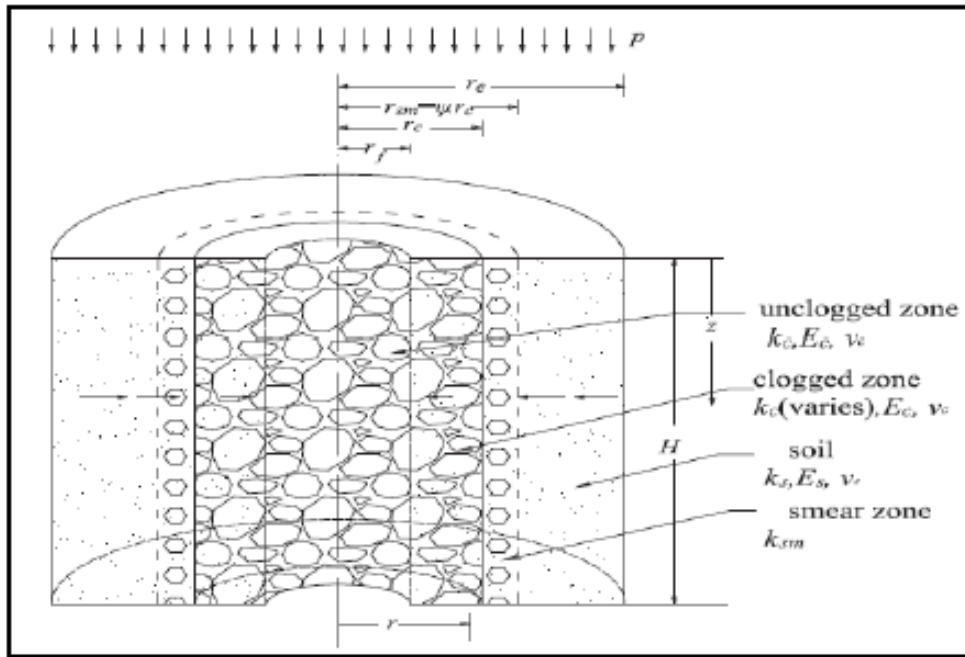


Figure 2.11. Unit cell cross section (Deb and Shiyamalaa, 2015)

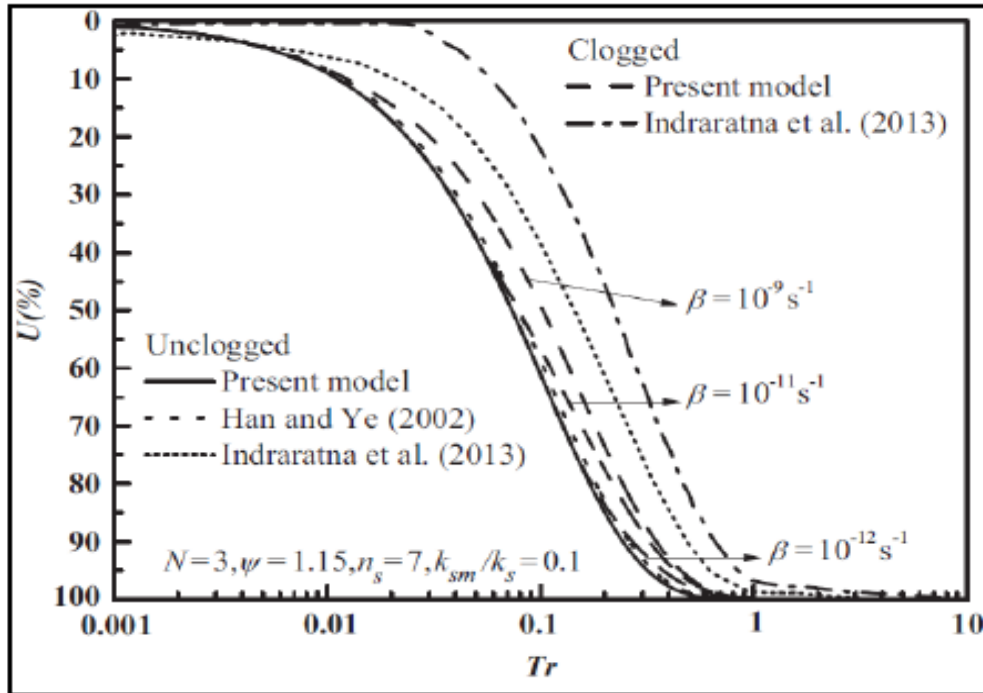


Figure 2.12. Calculated rate of consolidation compared with various methods (Deb and Shiyamalaa, 2015)

Subsequently, the sand columns were put in place by displacement or replacement, with or without compaction. The terms "NR-NC" (no displacement of clay soil and no sand

compaction of the sand), "NR- WC" (no displacement and with sand compaction), and "WR- WC" (with displacement and with sand compaction) refer to the different approaches to bed preparation. The range of the area replacement ratio was maintained at 1–6%. The following are the study's main conclusions:

- (i) It was seen that the clay soil near the column had locally densified. It was discovered that the densified kaolin zone surrounding the column had the same area as the column's radius. As a result, the clay's permeability decreases and its coefficient of consolidation rises near the column. This, however, has no effect on the fast drainage that occurs when the sand column is being installed.
- (ii) The effect of reinforcing on improved soil settling is represented by the term "settlement reduction rate," or " T_r ." $T_r = [(\Delta h_{ur} - \Delta h_r) / \Delta h_r] \times 100$ is the equation for the settlement reduction rate, where h_{ur} denotes the settlement without reinforcement and h_r is the settling of the reinforcement specimen.
- (iii) It is observed that in all three approaches, T_r rises with column diameter. The building method determines the settlement reduction for the same diameter. The WR-WC construction method, which involves moving the earth and compacting the column material, is the most efficient. It was found that the NR-WC method outperformed the NR-NC method.
- (iv) It should be recorded that the time it takes for settlement to start is essentially constant, regardless of the method used for column installation and column diameter.

Chardrawanshi (2018) investigated the settling behaviour of extremely soft soil with an undrained shear strength of 2.5 to 7.5 kPa when subjected to sustained loads of 100, 150, and 200 kPa for at least thirty hours. The method to ascertain the settling of extremely soft soil with undrained shear strength less than 7 kPa is not provided by IS 15284 (part 1): 2003. Using a specified area replacement ratio in the field, he created design charts (Figures 2.13) that assist in determining the intended SRR (settlement reduction ratio). Stone columns provide a shorter radial drainage path in addition to the vertical path, which speeds up the composite foundation's consolidation process due to the high permeability of the column material. Because of their greater stiffness relative to the surrounding soil, the stone columns can bear more stress than the surrounding soil. This lowers the vertical stress carried by the surrounding soil and speeds up the consolidation process.

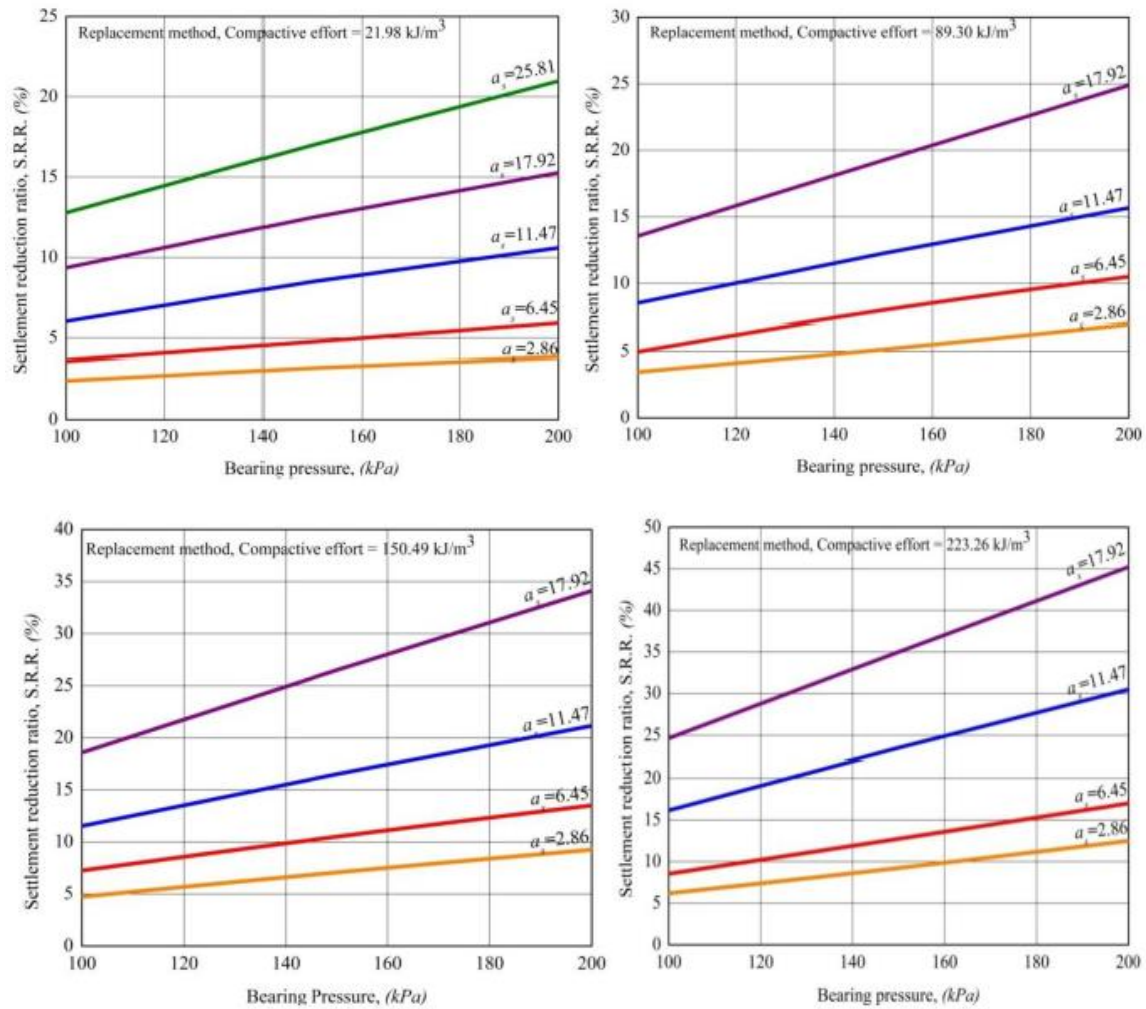


Figure 2.13. S.R.R. vs. Bearing pressure for various compactive effort (Chardrawanshi, 2018)

2.6.1.3 Limitations of Ordinary Stone Columns

Under some conditions, using stone columns is subject to a number of limitations, such as:

- (i) A soil that has an organic content, such as one that has a peat layer thicker than the diameter of a column, may shrink over time due to moisture content ten times its weight, leading to excessive settlements from the long-term dissipation of excess pore water pressure (Waltham, 2009).
- (ii) According to Priebe (2005), it is not permitted to utilise stone columns in soils that have an undrained shear strength (c_u) value of less than 15 kPa since these types of soils may not provide enough strength for the installation process.
- (iii) In order to prevent unforeseen long-term failures under such conditions, the long-term settlements should be taken into consideration in the design. Loose fills and

clay fills produce additional settlements, which are not beneficial in the long run (McCabe et al., 2009).

2.6.2 Geosynthetic Encased Stone Column

The stone column serves a variety of purposes, including densification, drainage, reinforcement, and replacement. Generally speaking, soil or geomaterials are strong in shear and compression but weak in tension. Tensile resistance for geomaterials can be provided by geosynthetics like geotextiles and geogrids. In order to maintain the integrity and functionality of two incompatible materials and keep them from mixing, geosynthetics are utilised as a separator between them. Because there is less "smear zone" between the column material and the soft soils due to this function, the stone column is improved (Han and Ye, 2002). The standard ranges for geosynthetic encasement's tensile stiffness and ultimate hoop tensile strength are 1500–6000 kN/m and 100–400 kN/m, respectively. While geosynthetic-encased stone columns are highly appropriate for soft soils with shear strengths between 5 and 15 kPa, regular stone columns—those without the encasement—are best suited for soils with undrained shear strengths more than 15 kPa (Han, 2015). Encased stone columns typically reach depths of 5 to 10 metres. According to Castro et al. (2013), the stress concentration ratio for a geosynthetic-encased column might reach 8.5. Bursting the geosynthetic reinforcement is one conceivable way for a geosynthetic stone column to fail. According to Alexiew and Thomson (2013), the area replacement ratio for the design of an enclosed stone column is between 0.1 and 0.2.

2.6.2.1 Bearing Capacity Enhancement of Geosynthetic Encased Stone Column

The load settlement behaviour of stone columns with and without geogrid encasement was studied by Malarvizhi and Ilamparuthi (2004) using a range of parameters, including the l/d ratio and the type of geogrid material. Granite stone chips were utilised as column material, and marine clay served as soft soil. Three distinct geogrid nets with varying aperture sizes and tensile strengths were used in the investigation. The findings indicate that whether a stone column is end-bearing or floating, its load carrying capacity rises with increasing encasement length. The rigidity of the encasing material increases the final load carrying capacity. In relation to the soft soil bed, it is discovered that the final load carrying capacity of an encased column increases by three times, while that of a conventional stone column increases by roughly two times. When compared to regular stone columns, it was discovered that covered stone columns were better suited for reducing settling.

Murugesan and Rajagopal (2006) used a thorough parametric study with finite element analysis to examine the qualitative and quantitative improvement in the stone column's load

capacity by encasing. The analyses revealed that, in comparison to ordinary stone columns, the encased stone columns have substantially higher load carrying capacities and experience less compression and lateral bulging. The findings have demonstrated that with encasement, the lateral confining forces that form in the stone columns are greater. It is discovered that encasing the top part of the stone column up to twice its diameter is sufficient to increase its load carrying capacity. Compared to regular stone columns, the load carrying capability of enclosed columns rises as the stiffness of the encasement increases.

Murugesan and Rajagopal (2010) conducted a thorough parametric investigation utilising the finite element analysis to closely examine the qualitative and quantitative improvement in the stone column's load capacity by encasement. The analyses revealed that, in comparison to ordinary stone columns, the encased stone columns have significantly higher load carrying capacities and experience fewer compressions and lateral bulging. The findings have demonstrated that with encasement, the lateral confining forces that form in the stone columns are greater. In comparison to regular stone columns, the load carrying capability of enclosed columns improves as the stiffness of the encasement increases. He computed the bearing capacity of an enclosed granular column taking into account the extra confinement offered by the geosynthetic encasement, assuming a bulging length of four times the column diameter as follows:

$$q_{ult,c} = (\sigma_{r0} + 4c_u + \sigma_{r,g})K_p \quad (2.30)$$

Where, σ_{r0} = The initial radial stress of the surrounding soil;

K_p = The coefficient of passive earth pressure of the granular material.

The extra confinement that the geosynthetic ($\sigma_{r,g}$) provides is directly proportional to the encasement's hoop tensile strength (T_g), which may be computed as follows:

$$\sigma_{r,g} = 2T_g/d_c \quad (2.31)$$

The hoop strain (ϵ_g) and stiffness modulus (J) of the geosynthetic can be used to compute the geosynthetic hoop tensile strength as follows:

$$T_g = J \cdot \epsilon_g \quad (2.32)$$

$$\epsilon_g = \frac{1 - \sqrt{1 - \epsilon_a}}{\sqrt{1 - \epsilon_a}} \quad (2.33)$$

where ϵ_a = the compressive strain of the column vertically (vertical compression divided by the bulging length).

In order to investigate the load settlement behaviour of soft expansive black cotton soil with a CH of 50 kPa UCS, **Kumar and Jain (2013)** adopted the granular pile approach. The granular material for the columns was sand. End bearing piles with diameters of 50, 65, and 80 mm were built in cylindrical tanks using the replacement method, maintaining s/d ratios of 3.3, 3.2, and 3.5, respectively. By installing a footing on test beds with regular granular piles and granular piles wrapped in geogrid, the load settlement behaviour of the granular piles was investigated. According to the test results, the enclosed granular pile and regular granular pile could support loads around 300% and 470% higher, respectively, than the unreinforced clay base. Additionally, encased granular piles may support loads ranging from 25% to 50% higher than regular granular piles.

In a model tank with a diameter of 200 mm and a height of 525 mm, **Hasan and Samadhiya (2016)** carried out a short-term laboratory load-settlement research using a floating granular pile that was 375 mm long and 75 mm in diameter. The pile was placed in a clay substrate with an undrained shear strength of 5 kPa (Figure 2.13). The replacement approach was used to install the granular pile. The direction of reinforcement, i.e., vertically enclosed pile, horizontally reinforced pile, and combined vertical and horizontal reinforced pile, was one of the study's variable characteristics. For vertical reinforcement, geotextile was utilised, and for horizontal reinforcement, circular geogrid strips. Another study variable was the horizontal reinforcement's spacing. The test findings were compared to untreated soft soil beds and regular granular pile reinforced beds. A plate the same size as the granular pile's diameter applied the weight. The findings indicate that the maximum load intensity for the treated to untreated clay bed was 195% for the conventional granular pile, 440 for the vertical encased pile, and 396 for the horizontal strips reinforced pile (strip spacing of 50 mm, c/c). In comparison to untreated soil, the ultimate load intensity for combined vertically encased and horizontally reinforced granular pile at 25, 50, and 75 mm spacing was 485, 432, and 428%, respectively. Based on these findings, it can be inferred that the granular pile's load carrying capacity is increased by both vertical and horizontal reinforcement; however, the effect of horizontal reinforcement spacing on the combined vertically encased and horizontally reinforced floating granular pile's load carrying capacity is minimal.

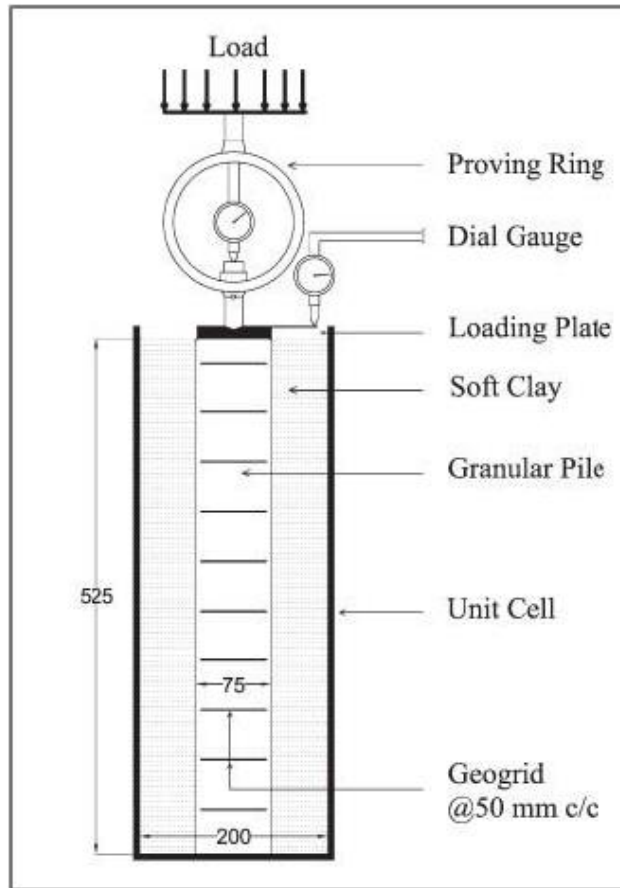


Figure 2.14. Model test set up (Hasan and Samadhiya, 2016)

2.6.2.2 Geogrid Encased Stone Column Settlement Reduction Studies

The following assumptions form the basis of Raithel and Kempfert's (2000) approach for calculating the settlement of a granular column-reinforced foundation covered in geosynthetic encasement.

- (i) Because the loading size is far more than the soft soil's thickness, the added stress imparted does not decrease with depth.
- (ii) There is equal settling on the soft soil and the top of the column.
- (iii) There isn't any settlement below the column's toe.
- (iv) There is active earth pressure on the column.
- (v) The soil is in an at-rest state prior to loading. The earth pressure coefficient of the soil for an excavation installation method is $K_{o,s} = 1 - \sin \phi_s$ (ϕ_s = soil friction angle). A higher ground pressure coefficient, $K_{o,s}$, should be utilised when installing using a displacement approach.
- (vi) The behaviour of the geosynthetic encasement is linearly elastic.

(vii) Granular columns have constant volumes because they are incompressible.

(viii) The design is based on a drained condition

The unit cell idea (Figure 2.14) serves as the basis for the Raithel and Kempfert (2000) technique of calculating the settlement of a granular column-reinforced foundation enclosed in geosynthetic.

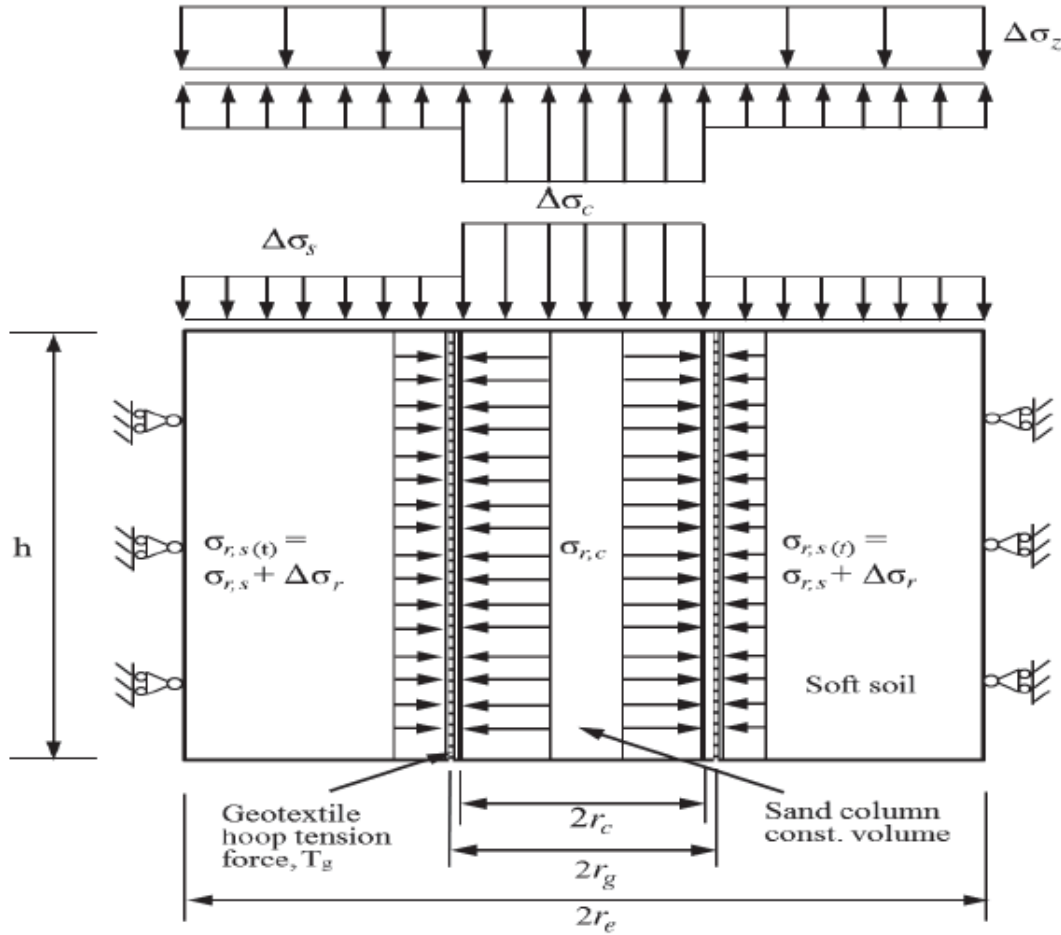


Figure 2.15. Geosynthetic encased column – Unit cell model (Raithel and Kempfert, 2000).

The overburden stresses on the soil and column as well as the additional stresses on them as follows contribute to the radial stresses in the soil and column:

$$\sigma_{r,c} = \Delta \sigma_c \cdot K_{a,c} + \sigma_{z0,c} \cdot K_{a,c} \quad (2.34)$$

$$= (1/a_s \Delta \sigma_z - (1 - a_s) / a_s \Delta \sigma_s) K_{a,c} + \sigma_{z0,c} K_{a,c} \quad (2.35)$$

$$\sigma_{r,s} = \Delta \sigma_s K_{0,s} + \sigma_{z0,s} K_{0,s} \quad (2.36)$$

Where, $\sigma_{z0,c}$ = Overburden stress of the column,
 $\sigma_{z0,s}$ = Overburden stress of the soil,
 $\Delta\sigma_c$ = Additional vertical stress in the column,
 $\Delta\sigma_s$ = Additional vertical stress in the soil,
 $K_{a,c}$ = Active earth pressure coefficient in the column,
 $K_{0,s}$ = At-rest earth pressure coefficient in the soil, ($K_{0,s}$, should be used if a displacement installation method is used).

Using the FEM programme PLAXIS, **Malarvizhi and Ilamparuthi (2007)** examined the behaviour of a stone column covered in geogrid in a soft soil bed. The parametric study's findings are as follows:

- (i) The hoop force is activated over the top 1D depth of a column encased in geogrid, and as the pressure is applied, it is activated along the column's length while also growing in magnitude. The highest value of the hoop stress was discovered by the investigators at the column's 1D depth.
- (ii) The stress concentration on the column is increased by the encasement. This lessens the load on the clay and slows down the composite soil's settling.
- (iii) The stress concentration factor rises and the settlement decreases as the encasement's stiffness increases. Nevertheless, the contribution to settlement reduction ratio was determined to be negligible when the stiffness increased above 2000 kN/m.
- (iv) The shearing resistance of the material in the column has an impact on the settlement reduction ratio (SRR). The efficiency of the stone column material increases with compacted column material.

A set of small-scale model tests were carried out by **Gniel and Bouazza (2009)** in order to study the behaviour of encased stone columns. Compared to geotextile, the geogrid was the preferred geosynthetic material since it is more resilient and rigid and can be compressed to the necessary density in the column material. The investigation of the settlement decrease of solitary and group columns with respect to non-encased columns and untreated soft soil bed involved the consideration of both partial and full encasement of geogrid. The applied loads have prepared the consolidated soft soil beds (clay with LL=62, PI=32, G=2.64, γ_{sat} =16.2kN/m³, moisture content = 63%, compression index = 0.80, Cu=5kPa) to obtain homogenous soil that represents natural soil deposits. Since the replacement method is seen

to be the most easily replicable technique for installing columns in soft soils, it was employed to install stone columns. The column material was sand with particle sizes ranging from 11 to 4 mm, $G=2.80$, compacted saturated unit weight = 20.2 kN/m^3 , and $\rho=350$. The strain has been reduced by 30, 40, and 50% at encasement percentages of 25, 50, and 75% of column length, respectively. On the other hand, there was an almost 80% reduction in vertical strain in fully-encased columns. For the non-encased and fully encased columns, the stress concentration ratio values were found to be 2 and 10, respectively. The confinement of geogrid, which boosts stiffness and regulates the column's radial strain, is cited as the cause. It was determined that the failure of isolated columns occurred due to radial expansion beneath the encasement level and that the vertical strain of both solitary and group columns steadily decreased with increasing encased length. The length of the encasement increased the column capacity for isolated columns, while the strain at failure stayed relatively constant. There was a noticeable improvement in capacity for the fully-encased column. Profound bulging of the radial column was noted immediately under the encasement's base. This bulging was seen for group columns that were partially enclosed throughout the nonencased portion. The bulging was limited to a length of around two column diameters for isolated columns that were partially encased.

Deb et al. (2011) investigated how improved soft clay was affected by using geogrid as basal reinforcement beneath the footing on stone columns. The footing was positioned beneath a sand cushion, which encased the geogrid. By altering variables like the sand pad's thickness, the geogrid sand bed's thickness, and the geogrid layer's diameter, the load-settlement properties of the produced clay bed were investigated. The pebbles utilised to create the stone columns ranged in size from 2 to 6 mm, while the soft clay utilised was CL with a UCS of 19 kPa. One millimetre thick biaxial geogrid was employed. The geogrid's diameter was adjusted between 200 and 500 mm. The ideal thickness for an unreinforced and geogrid-reinforced sand bed is determined by multiplying the footing's diameter by 0.5 and 0.3, respectively, based on the findings of a short-term load test. The ideal diameter of the reinforcement is three times the footing diameter at the optimal thickness of the geogrid-reinforced sand bed.

A thorough experimental and numerical study of the consolidation and deformation behaviour of stone columns was conducted by **Castro et al. (2013)**. They carried out small-scale laboratory experiments with a scale factor of 1:10 and contrasted the outcomes with those of the finite element method's numerical analysis. The model parameters were set in a

way that was comparable to the small-scale experimental experiments. It was discovered that the stress concentration factor of the columns is significantly influenced by the friction and dilatancy angles. The column's settling is influenced by the soil-stress transmission mechanism and rises with an accelerated rate of consolidation. The comparative results also showed that the stiffness ratio has very little effect on the columns' decreased settlement. The analysis also showed that the dissipation of excess pore water pressure is significantly impacted by the changing of stress concentration factor over time.

Hanna et al. (2013) studied the behaviour of a single or a group of stone columns during failure by presenting a numerical model and performing parametric analysis. The parametric studies showed that the load ratio increases hyperbolically as D/B increases. This increase was significant up to a value of D/B less than 0.6 and it becomes nearly constant when $D/B=1$, that is, when the total of all the stone column diameters in the stone column group equals the foundation width. The findings also showed that, for a given D/B , the load ratio rises when the Poisson's ratio of sand decreases and the Poisson's ratio of clay decreases. It was observed that the modulus ratio and the angle of the stones' shearing resistance increased with the load carrying capability. Additionally, it was deduced that shear failure happened when stone columns replaced 10–35% of the area, but bulging failure happened when the area replacement ratio was less than 10%.

According to **Najjar et al. (2013)**, the columns broke when they were loaded from the top, with the bulging happening between 0.5 and 3 times the column's diameter. Column load carrying ability increased under distributed loads with a notable decrease in bulging. Columns broke down due to shearing, bending, or bulging. Whereas shorter columns punched and penetrated into the soft soil, longer columns deformed in the top portion of the column length; for the encased columns, the bulging decreased significantly; additionally, the bulging of encased columns reduced at the top and transmitted to the lower portion of the column length. The bulging of columns was greater in soft clays than in stiffer clays. It was also discovered that the stiffness and strength of the composite system improved as the area replacement ratio rose. For a certain area replacement ratio, an increase in the length to diameter ratio resulted in an increase in the columns' ultimate stress and stiffness. Additionally, it was found that efficient load transfer was facilitated by columns whose lengths varied between five and eight times their diameter. Additionally, it was determined that, up to a particular loading level, the stress concentration factor grew; after that, it declined. Covering the columns with geotextiles or geogrids lowered pore pressure while increasing the composite ground's stiffness and load-bearing capability. It was also mentioned

that the load carrying capacity and column stiffness increased with an increase in encasement stiffness. Additionally, columns with smaller diameters showed a greater improvement in efficiency than columns with larger diameters. The study also showed that specimens in a loosely packed state gain strength more than ones in a densely packed state. Additionally, it was discovered that the lateral earth pressures surrounding the columns were greatly impacted by the column spacing. The investigation also found that, when it came to group loading, the matrix soil was more important than the installation technique, kind of column, and composition.

Castro et al. (2014) investigated the decrease in composite ground settlement following the installation of stone columns through numerical calculations. It has been discovered that when modest loads are applied and columns are positioned widely apart, poor column installation leads to an increase in ground settlement, particularly in overconsolidated clay. By rotating the soil fabric from cross anisotropy to vertical and back to horizontal once the embankment is loaded, soil anisotropy increases the radial stresses. This decreases settlement as the stiffness increases with an increase in the radial stresses. The study also found that the presence of extra pore water pressure reduces the effective stress, which leads to greater settlements, and that the settlement increases with increases in soil plastic stresses because of a drop in the overconsolidation ratio.

In order to investigate the effects of applying vacuum through enclosed columns and gauge how much vacuum application affects soft clay's strength, **Kumar et al. (2014)** carried out model experiments. Test results showed that the amount of vacuum pressure applied had an effect on the clay soil's undrained shear strength. The application of vacuum pressure also significantly improved the columns' stiffness and ability to support loads. Furthermore, it was observed that the stone columns with vacuum pre-loading had a greater capacity to support loads than the columns with surcharge loading. Additionally, the results demonstrated that a pre-loaded column had a much larger load carrying capacity than a column that was not pre-loaded when vacuum consolidation was present. It thus verified that the enclosed columns offered an effective route for applying vacuum pressure.

In their study, **Ng and Tan (2014)** employed the unit cell concept in two-dimensional finite element analyses to investigate the consolidation properties and settlement behaviour of floating stone columns under spread loading. They found that the consolidation property of the improved ground decreased as the depth ratio decreased, and that the settlement observed increased as the depth ratio decreased. Additionally, at a particular value of depth ratio, it was observed that the floating columns showed similar settling to end-bearing columns. This led

to the required consolidation at an acceptable long-term ground settlement. Additionally, the analyses revealed that the area replacement ratio, the ground pressure after installation, the intensity of loading, and the friction angle of the stone column aggregates all had a substantial impact on the settling of floating columns. Since the column constraint modulus is dependent on the passive resistance of the surrounding soil, the effect of the modular ratio was determined to be negligible.

Using laboratory testing and numerical analysis, **Hasan and Samadhiya (2016)** conducted a comparative study of the behaviour of granular pile reinforced with geosynthetic. The short-term loading situation was taken into consideration when using the unit cell approach. The loading might be applied to the full cylindrical tank area or just the granular column region. A variety of columns were built for the model trials, including unreinforced, vertically enclosed, reinforced with horizontal strips, and combination vertically and horizontally reinforced granular columns. It was stated that the construction of granular columns—either reinforced or unreinforced—increased the ground's capacity to support weight. In addition to outperforming unreinforced end-bearing granular piles, the reinforced floating columns also performed better due to less bulging; for unreinforced and vertically encased columns, bulging occurred over a depth of approximately 1.0 to 1.6 times the column diameter, whereas for horizontally reinforced and combined reinforced granular columns, bulging occurred over a depth of approximately 1.0 to 1.6 times the column diameter. The results showed that longer columns and a clay bed with a higher undrained shear strength contributed to improved column performance. The ultimate load bearing capacity of an unreinforced column remained constant, while that of a reinforced column declined with increasing column diameter. While the combined reinforced columns remained independent of the influence of spacing, the floating columns demonstrated higher load bearing capacity with decreased geogrid strip spacing.

A numerical method to assess the behaviour of soft soil reinforced with stone columns was reported by **Basack et al. (2017)**. The study used unit-cell settings and placed special emphasis on the columns' lateral deformation. It was found that the amount of time that had passed before columns bulged and that the zone where the bulging occurred was close to the ground's surface. The difference in the restraint coefficients had a significant impact on the deformation of the columns; the lateral stress on the columns varied linearly with column depth, but the time-dependent vertical stress on the columns increased as column depth increased, up to a designated maximum stress value. An increase in the radial distance from the column resulted in an increase in the vertical stress acting on the soft surrounding soil.

Bulging decreased in magnitude but grew in depth when the soft soil's initial undrained cohesiveness strength increased. The amount of the bulging increased as the bulging depth decreased for a decrease in column diameter. Additionally, when column spacing grew, both the ultimate load-carrying capacity and the bulging magnitude increased. Furthermore, columns' bulging got deeper and their bulging decreased as the stress concentration ratio rose.

Studies on reinforced and unreinforced sand beds on vertical stone columns were carried out by **Debnath and Dey (2017)**. It was stated that the weight carrying capability multiplied several times over with the installation of stone columns. The growth for enclosed columns was much greater. The maximum bulging depth was raised and the amount of bulging was drastically reduced when a geogrid reinforced sand bed was built on encased columns. Additionally, it was determined that the best length for encased columns with a geogrid-reinforced sand substrate produced the greatest increase in load carrying capability. This length was six times the column diameter. The study also found that three times the column diameter is the ideal encasement length.

Miranda et al. (2017) examined the impact of geotextile encasement on the properties of soft clay reinforced with geotextile-encased columns using small-scale laboratory experiments. Encased columns were found to be able to withstand a vertical load that was about 1.7 times greater than that of regular columns. Therefore, when comparing the stress concentration factor for the enhanced ground to that of the regular columns, it was nearly two to four times greater. When compared to untreated ground, the results indicated a decrease in settlement when the ground was reinforced with both regular and enclosed stone columns.

In order to study the behaviour of fully and partially penetrated geosynthetic encased stone columns (GESC) under time-dependent stress conditions, **Rajesh (2017)** carried out a numerical analysis. The results of the investigation demonstrated that covering the stone columns with a geosynthetic aided in reducing the amount of time needed for excess pore water to dissipate and the columns' lateral distortion or bulging due to increased column stiffness, both of which decreased settlement. When comparing an encased column to a regular stone column, the effective stress concentration ratio—that is, the ratio of the effective vertical stress on the column to the effective vertical stress on the surrounding soft clay, or ESCR rose noticeably. Over the course of the consolidation period, the ESCR in encased columns increased consistently. However, following a significant amount of consolidation, the ESCR for a typical stone column first climbed before eventually declining. It is also found that there was a considerable increase in load transfer from the column to the surrounding soft soil as the stiffness of the geosynthetic increased. It was shown that the

ESCR decreased by a significant margin when the length of the partially penetrated columns was decreased.

Das and Deb (2018) investigated the time-dependent behaviour of improved ground under embankment stress circumstances using model experiments and numerical analysis on stone-column improved ground. The study showed that when the spacing to diameter ratio, embankment height, and modular ratio grew, so did the stress concentration ratio—that is, the ratio of stress on the stone column to that on the soft soil. Additionally, the stress concentration ratio rose over time and eventually stabilised. However, because of an arching effect that occurred over time and the embankment soil partially reclaimed its stress, the stress concentration ratio declined after reaching a peak value for greater ranges of spacing to diameter ratio, embankment height, and modular ratio. Furthermore, it was discovered that the maximum stress concentration ratio had no effect on the relative densities of the soft soil thickness and embankment material. The surface of the embankment showed negligible (almost zero) differential settling when the minimum height of the embankment was twice the column spacing. With an increase in embankment height and duration, the columns' lateral distortion increased; the greatest deformation was seen at a depth that was nearly 2.5 times the diameter of the stone columns. Over half of the time needed to create the entire lateral deformation, around 90% of the lateral deformation happened. No matter where the columns are located below the embankment, the pore water pressure around the stone column and surrounding soil was found to be similar under steady-state conditions. However, because of the water buildup in the unimproved ground, a larger pore water pressure occurred.

CHAPTER 3

METHODOLOGY

3.1 GENERAL

This chapter presents the examination of the behavior of stone columns in clayey soil. The analysis is conducted through laboratory testing on models of both conventional and geosynthetic encased stone columns placed in a soft type of soil. An examination has been conducted to study the effectiveness of a single column and also for groups of three and four columns arranged in triangular and square pattern. The investigation focused on the impact of different factors, including the stiffness of the geosynthetics and various parameters of the stone columns (like diameter, length, and spacing between the columns). Two distinct experimental series were conducted. The initial set of experiments consisted of individual stone columns that were reinforced in different arrangements. The subsequent set of experiments focused on investigating stone column in groups under various situations. Both unreinforced and reinforced type stone columns (horizontally and vertically) were investigated for both scenarios. The accuracy of the experimental results was validated by numerical modeling conducted with the aid of PLAXIS 3D software.

3.2 MATERIALS USED

This study employed three distinct materials, namely a sample of soil, aggregates required for the stone column, and a polymeric geotextile material for the purpose of encasement. The properties of the aforementioned components are outlined below:

3.2.1 Clay

After thorough literature investigation it was noticed that there has been vast presence of soft cohesive soil across the region. Also, there exist a weak cohesive soil up to a certain depth below the natural ground level. Therefore, in order to calculate the intended strategy to be used with careful subsurface soil analysis, it is necessary to assess the efficiency of stone columns in cohesive soil, i.e., clay, for predicting their capacity for carrying loads and settlement. Soil samples were collected and transported from the sites in Bhopal, Madhya Pradesh. The index properties of the fine soil are measured by performing the hydrometer test (IS: 2720 (Part 4)-1985), Specific gravity test (IS: 2720 (Part 3)-1980), Atterberg limit test (IS: 2720 (Part 5)-1985), and the light compaction test (IS: 2720 (Part VII)-1980). Figure 3.1 represents the particle size distribution of the sample. The soil parameters determined are displayed in Table 3.1.

Table 3.1 Properties of the clay used in the present study

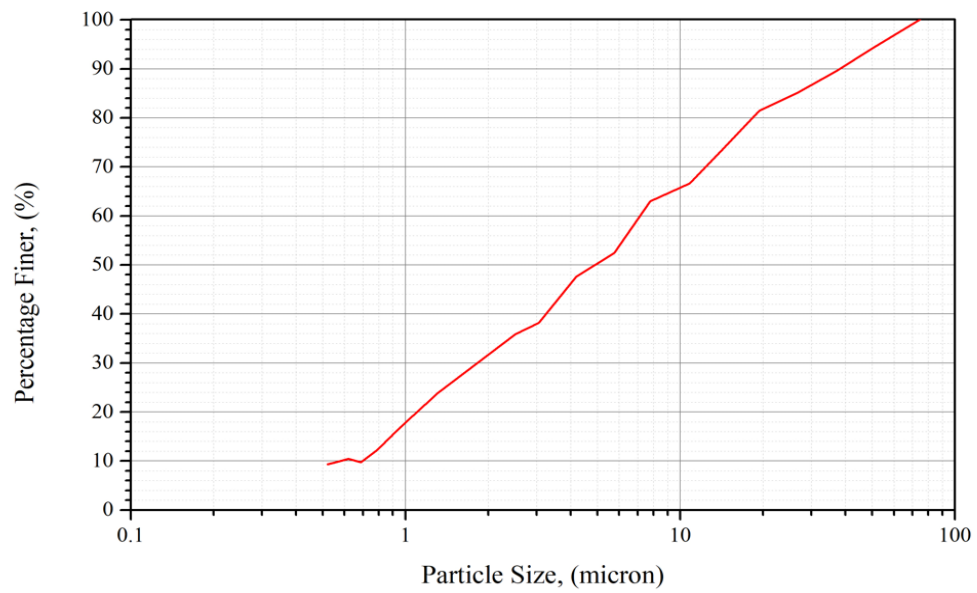


Figure 3.1. Particle size distribution of clay

3.2.2 Stone Aggregates

The size of the pebbles used in building stone columns was identified as a critical factor. The dimension of the particles (d) of the crushed aggregates/gravels utilised in real-time practice was kept between 25 and 50 mm for the building of columns with these stones, with diameters (D) of column varying from 0.6 to 1.0 m. As per Ali et al. (2011), crushed-type stones with sizes that ranges from 6 to 40 mm can be employed as aggregates, with a D/d ratio ranging from 12 to 40 can be used for prototypes. Thus, for the current investigation, D/d ratios of 4–50 and aggregate sizes ranging from 2 to 10 mm were utilized to create model stone columns having $D = 50\text{mm}$, 75mm , and 100 mm . The aggregates were tested for their particle size distribution, dry density, and also shear strength test using a direct shear test with a rate of shearing of 1.25 mm/min , for a normal stress of values 100 kPa , 150 kPa , 200 kPa , and 300 kPa . Stone material was classified as GP, according to USCS. The values of the coefficient of uniformity and coefficient of curvature were calculated as 2.14 and 1.10, respectively. Table 3.2 includes the aggregate qualities established through laboratory testing. Figure 3.2 represents the particle size distribution of aggregates used in the current study.

Table 3.2 Stone column properties used in the present study

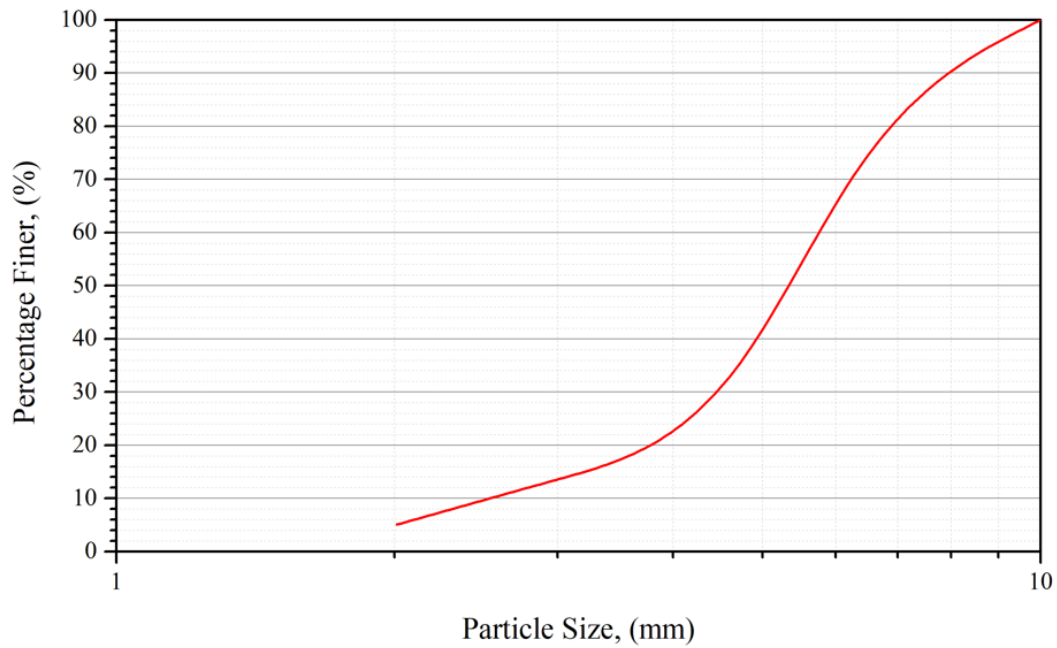


Figure 3.2. Particle size distribution of stone aggregate

3.2.3 Encasement Materials

Geosynthetics are a subset of polymeric reinforcement materials used in civil engineering. As to the ASTM, geosynthetic is a polymeric planar material that is essential to the civil engineering business and is utilised for soil, dirt, and geotechnical-related materials. Two varieties of polypropylene (non-woven type) geotextiles were considered as a strengthening substance in the proposed testing. Table 3.3 shows the value of the tensile strength of considered geosynthetics (provided by the manufacturer).

Table 3.3 Attributes of Geosynthetics

3.3 EQUIPMENTS & APPARATUS

3.3.1 Tank

A model tank was constructed, measuring 1500 mm in length, 900 mm in width, and 600 mm in height, to simulate the characteristics of a clay bed and stone columns. Figure 3.3 and Figure 3.4 illustrates the model tank and its corresponding dimensions. The wall thickness of the tank sides was sufficient to prevent any potential lateral distortion that may arise during the filling process. A thin coating of grease was used at the inner walls of the testing box to minimize friction between the clay and the wall of the tank.



Figure 3.3. Model test tank

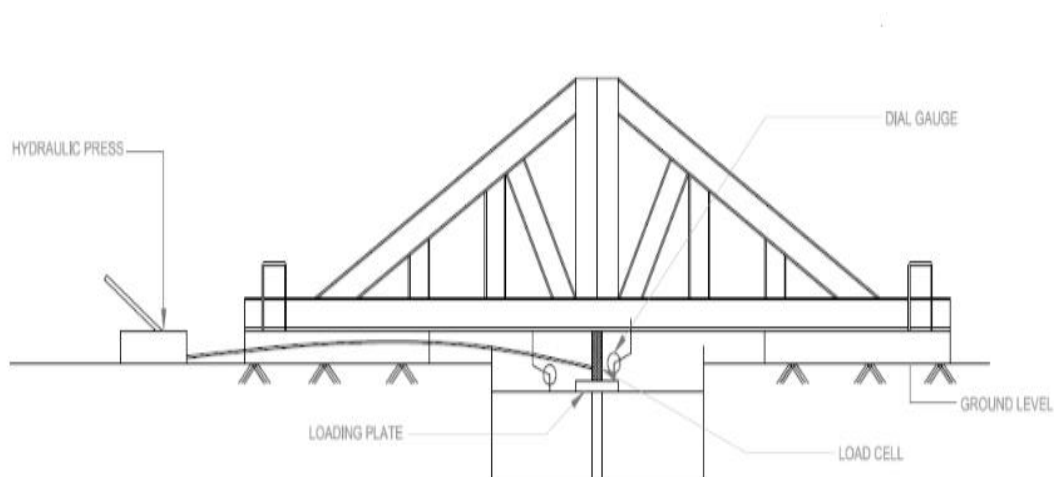


Figure 3.4. Line sketch of the loading frame

3.3.2 Loading and Measurement System

The tank includes a strong loading frame and one loading system that allows soft soil and the stone column materials to be loaded (Figure 3.3). The loading system for this test was stress controlled, where the loading rate was established by a hydraulic jack (Figure 3.5) with a capability of 20 kN. The test steps entail implementing a vertical monotonic load to the clay treated with a stone column and calculating the load-displacement behaviour of the softer clay. The settlement was recorded by using 3 dial gauges placed at an angle of 120°. The final settlement was considered as the average of the three dial gauges.

3.3.3 Iron Plate for Testing

Iron plate having diameter 200mm and thickness of 25mm was utilised for loading at the surface of the soil. The picture of steel plate is shown in Figure 3.5.



Figure 3.5. Test setup showing various components

3.3.4. Pipes for construction of Stone Column

Steel pipes having internal diameter equal to the diameter of the stone column were utilised for constructing the stone column by the help of replacement method. The sizes of the pipes have been selected to keep the suggested area replacement ratio within the range of 5 to 35%. These hollow pipes have been employed to create the soft soil bed's hollow. Three different pipes having diameter 50, 75 and 100cm were used. All the pipes measure 2 mm in thickness and 600 mm in length, respectively. The pipe has one bevelled end to minimise disturbance when inserting it into a soft soil bed. Pipe used in this study is shown in Figure 3.6.



Figure 3.6. Pipes used for making stone column

3.3.5 Compaction Tools

A customised tamper unit of 200×200 mm in plan was used to compact clay by lowering the tamper from a distance of 250 mm high. A steel rod with a mass of 1.5 kg, a diameter of 20 mm, and a length of 100 mm was employed to compact the stone fill.

3.4 MODELLING CONSIDERATIONS

The boundary effects, L/D ratio, and geometric similitude ratio were considered while modelling the stone column and test tank characteristics (length (L) and diameter (D)). As per Wood et al. (2000), the diameter of a prototype type stone column varied between 0.6 m and 1 m. Furthermore, the minimal diameter of the column, which can be erected entirely intact, was around 13 mm (Shahu and Reddy, 2011). Moreover, the L/D ratio of the prototype varied between 5 and 20 (Shahu and Reddy, 2011). Thus, the diameters of the columns employed in the current study were 50, 75, and 100 mm.

3.5 CLAY BED PREPARATION

The process of preparing clay beds was performed in a model tank with a size of 1200 mm \times 900 mm and 600 mm in height. The soil was poured using the rainfall process, with every layer being 50 mm deep. The uniformity of the unit weight was maintained for each layer having a bulk density of 18 kN/m^3 and was verified continually during filling with a mould having a specific volume at three separate points inside the layer. In total, ten layers of sample were applied to reach a final height of 50 cm attained. In water content inside the clay bed exhibited a marginal deviation of less than 1.5%.

3.6 STONE COLUMNS CONSTRUCTION FOR UNREINFORCED COLUMNS

Different aspects, such as the boundary effects and geometric similitude ratio (L/D), were considered when determining the stone column specifications (length (L) and diameter (D)). As a result, in our investigation, we employed a diameter of 50, 75, and 100 mm and a L/D ratio ranging between 5-10. Pipes having an internal diameter of 50, 75, and 100 mm and an external thickness of around 2 mm were utilised to build the stone columns. To avoid a substantial disturbance of the underlying soil, a thin coating of oil was applied to the inner and outer surfaces of the pipes in every sample.

3.6.1 Single Stone Column

The tank's centre was appropriately marked and the pipe of desired diameter was positioned into the clay bed. Enough precaution was taken to keep the pipe vertical. Soil replacement technique is employed to complete the casting of stone columns. This approach has been utilised for a small-scale stone column making as opposed to force penetration and soil displacement methods used in the field. A steel casing measuring 50, 75, and 100 mm internally and 2 mm thick was used to cast the stone columns, which were then buried in the soil under investigation. The primary goal of employing top-down techniques was to prevent soil cave-ins when drilling boreholes. A screw augur with a 38 mm diameter was employed to extract the clay from the casing.

Figure 3.7. Single column to be made up with stones having $d = 75\text{mm}$

3.6.2 Group of Stone Columns

The initial phase is comparable to the single column without reinforcement. Selecting the stone column spacing and arrangement pattern is crucial before hollow pipe is created. Stone columns were created in triangular as well as square pattern with three different

spacing(S)/diameter(D) ratio. The s/d ratio used were 2, 3 and 4. The group of three and four stone columns' casting is completed using the soil replacement technique for triangular and square pattern respectively. Same auger as discussed earlier was used for the soil removal from the pipes. Figure 3.8 represents the triangular and square pattern arrangement of stone column in groups for a typical diameter of 50mm having a S/D ratio of 3. Similarly, the arrangements were done for other S/D ratio and also for various diameter of column as per the testing requirements.

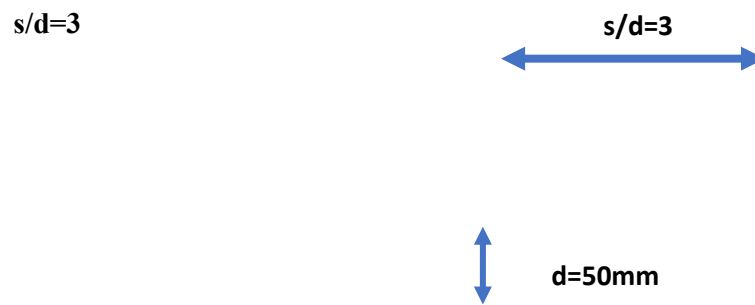


Figure 3.8. Typical arrangement of triangular and square pattern of stone column in groups for $D=50mm$ and $S/D=3$

3.7 STONE COLUMNS CONSTRUCTION FOR VERTICALLY ENCASED STONE COLUMNS

Geotextile was shaped into the necessary diameter tube and inserted with the casing for the encased stone columns. The casing pipe's diameter was marginally less than the stone column's formation diameter to guarantee that the ultimate diameter of the encased stone column is equal to the stone column's diameter. Vertical encasement was provided for four different lengths of reinforcement. At first, length of geotextile reinforcement was provided throughout the length of the column ($L_r=L$) for which geotextile was wrapped for the whole length of the pipe. For $L_r=0.75L$, the geotextile was wrapped up to $3/4^{\text{th}}$ the length of the pipe. For $L_r=0.5L$ the geotextile was wrapped for half the length of the pipe and for $L_r=0.25L$ the wrapping was done for $1/4^{\text{th}}$ length of the pipe. The pipe was completely encased by the geotextile and was lowered into the desired position. The stones were put into the geotextile-wrapped tube and compacted similarly to that done during ordinary stone column case.

For stone column in groups, again triangular and square pattern of columns were arranged for s/d ratio of 2, 3 and 4. The required pipes as per the desired pattern (only for

L_r=L was analysed for group case) were encased around it and lowered into the soil as the designated position. The pipes are subsequently filled with the amount of aggregate calculated and compacted as it was done in the previous case.

3.8 STONE COLUMNS CONSTRUCTION FOR HORIZONTALLY REINFORCED STONE COLUMNS

In order to schedule the installation of spherical horizontal discs, pipes are labelled and sized according to the intended testing interval at each necessary interval. The geotextile material was cut into 50, 75, and 100mm diameter circular discs. The three different arrangement of horizontal disc was studied for the analysis. First, the discs were placed at 100mm spacing(s) throughout the length of the column. The pipe was inserted and aggregate were placed and compacted up to 100mm after which first layer of horizontal disk was placed. The process was repeated till 4 discs were provided for the total length of the column (500mm) at 100mm spacing. Second arrangement was done by providing two layers of horizontal disc placed at 100mm spacing from head of the column till the centre of the column and the last arrangement was provided with two discs at 100mm spacing from centre of the column to the end of the column.

For stone columns in group, similar approach was adopted for providing the horizontal disc. All the columns in group were provided with the horizontal reinforcement at the desired depth. For group arrangement, analysis was done only when the reinforcement was provided throughout the length of the column at 100mm spacing.

3.9 TEST PROCEDURE

As described in the scholarly literature, the area replacement ratio (A_r) refers to the proportion of the area in the cross-section occupied by columns concerning the overall area of the foundations. In practice, stone columns are loaded for an area replacement ratio ranging between 5 and 35%. Utilising a loading plate having 200 mm of diameter, individual stone column tests on columns were carried out having diameters of 50, 75, and 100 mm. The observed percentages of A_r in the present investigations were 6.25, 14.06, and 25% for columns having diameters of 50, 75, and 100 mm, respectively. The loading plate thickness was determined through an iterative process involving repeated experimentation and analysis. This approach aimed to minimise any observable deformation of the plate under loading conditions. Ultimately, a loading plate with a thickness of 25 mm was selected as it exhibited negligible distortion.

3.10 DETAILS OF EXPERIMENTAL PROGRAM

To accomplish the required goals, the laboratory research is basically separated into various test series. The test series were divided into two portions. First series was done for single stone column for unreinforced and reinforced case. The reinforcement was provided as vertical reinforcement (i.e., vertical reinforced stone column, VESC) as well as horizontal reinforcement (i.e., horizontally reinforced stone column, HRSC) in the form of circular disc. In the case of vertical reinforcement, four variation was employed for the length of the reinforcement (L_r).

The second series was conducted for the stone columns in the group arranged in a triangular and square pattern for varying S/D ratio of 2, 3 and 4. The group analysis was also conducted for three different diameters of the column i.e., 50, 75 and 100mm. Both vertical encasement and horizontal reinforcement by a disc were used to study the encasement effect similar to that done in the analysis of a single stone column. The length of encasement (L_r) was used as $L_r=L$ for VESC and when horizontal discs were employed at 100mm spacing throughout the length of the column for HRSC tests. Also, only G1 type geotextile was used as an encasement material for both VESC and HRSC group analysis. Figure 3.9 represents the variation of both vertical and horizontal reinforcement used for the single stone column analysis. Table 3.4 and 3.5 shows the outline of the various experiments performed for single stone column and stone column in groups respectively.

Figure 3.9. Schematic of (a) OSC (b) VESCs with various Lr (c)HRSCs with various geosynthetic arrangement

Table 3.4. Outline of the various tests performed on single stone column

Table 3.5. Outline of the various tests performed on stone columns in group

A total of 46 tests were performed on a single stone column, and 54 tests were performed on a group of stone columns arranged in triangular and square patterns with different s/d ratios.

3.11 NUMERICAL MODELLING

3.11.1 General

A combination of compatibility, equilibrium, material efficiency, and boundary standards of forces and displacement must all be satisfied for a geotechnical problem to have an exact solution. It has been discovered in recent years that numerical techniques of analysis fully satisfy these requirements. Since then, there have been enormous strides achieved in numerical methods due to the broad applications of this cutting-edge technology and software that can complete difficult computations in a reasonable amount of time. Among the most widely utilised numerical techniques are the discrete element method (DE), boundary element method (BE), finite element method (FE), and finite difference method (FD).

The finite element model (FEM), which analyses the behaviour of the infinite number and reduces it to a finite amount in the form of ordinary or partial differential equations, is the method utilised for this analysis. Any arrangement of the components allows for the modelling of any shape. The approach eliminates the need for various types of analytical solutions in order to solve problems involving problematical non-linear equations and complicated geometry. The continuum behaviour, composite equations, and non-finite periphery conditions are all well handled by the FEM approach. The method's strength is its ability to easily accept variations in material stiffness, even at the elemental level. In order to provide an approximated answer for a physical problem that is universally acceptable, it also allows the use of several boundary criteria.

3.11.2. PLAXIS 3D

Because of its theory, which necessitates the utilisation of simulated work to predict the extent of stress and pressure throughout a continuum, the approximate Finite Element Method (FEM) has shown itself to be an important instrument for the investigation of complicated engineering issues. PLAXIS 3D is a three-dimensional (3-D) finite element programme specifically created for geotechnical applications. This programme is quite good at simulating its complex functioning of a small group of granular columns, and it was used for the subsequent finite elemental analysis. This programme uses sophisticated constitutive models, which are explained in the chapter, to mimic the characteristics of both soil and stone. To obtain accurate numerical assessments, a number of preliminary tests must also be performed, including mesh sensitivity and distance from the boundary.

The numerical analysis was performed by comparing the load-settlement of the experimental inquiry and the model test using PLAXIS 3D software (finite element approach). The Mohr-coulomb model was utilised to implement the boundary condition for the soil and stone column. Regarding the clay and column, a drained behaviour was predicted. In order to mesh, fifteen nodding triangles were employed. The performance of the stone column surrounded by soil, typical deformation, and stone column mesh were all represented by the boundary conditions that limited medium deformation. Aggregates, the surrounding soil medium, and the geotextile have all been modelled utilising the several Plaxis code models.

3.11.3 Material Properties

One popular and basic model for linear elastic completely plastic soil behaviour that can be utilised as an initial approximation is the Mohr-Coulomb model. Hooke's law of the isotropic elasticity serves as the foundation for the Mohr-Coulomb model's linear elastic component. According to the Mohr-Coulomb failure requirement, which was developed within a non-associated plasticity framework, is the totally plastic portion. A constitutive model having the same yield surface that is, a yield surface completely determined by model specification and unaffected by (plastic) straining is known as a perfectly-plastic model. All strains are reversible and its behaviour is completely elastic for stress states expressed by points inside the yield surface. Figure 3.10 represents the nonlinear behaviour of soil by two bilinear lines.

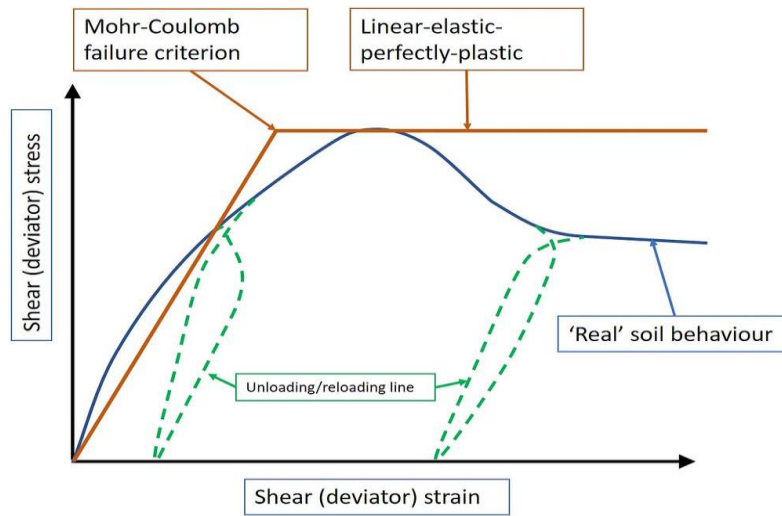


Figure 3.10. Real soil behaviour by Mohr - Coulomb model

This Mohr-Coulomb model was employed to model the soft clay and aggregate used in the current study. Five parameters in total are needed for the linear elastic perfectly-plastic Mohr-Coulomb model; these can be derived from simple tests on soil samples and are typically known to most geotechnical engineers. These specifications with their standard units are shown below:

E : Young's modulus [kN/m^2]

ϕ : Friction angle [$^\circ$]

ν : Poisson's ratio [-]

ψ : Dilatancy angle [$^\circ$]

c : Cohesion [kN/m^2]

In elastic model and the Mohr-Coulomb model, PLAXIS employs the Young's modulus as the fundamental stiffness modulus; however, some other stiffness moduli are also shown. Stress is a dimension of a stiffness modulus. Particular consideration must be given to the stiffness parameter values used in a computation because many geomaterials exhibit non-linear characteristics right from the start of the loading. Typically, during the triaxial testing of soil samples, the secant modulus at 50% strength is written as E_{50} , and the beginning slope of a stress-strain curve, or tangent modulus, is written as E_0 . It is practical to use E_0 for materials having a wide linear elastic range, although E_{50} is typically used for soil loading.

Instead of using E_{50} , one should use an unload-reload modulus (E_{ur}) in light of unloading issues.

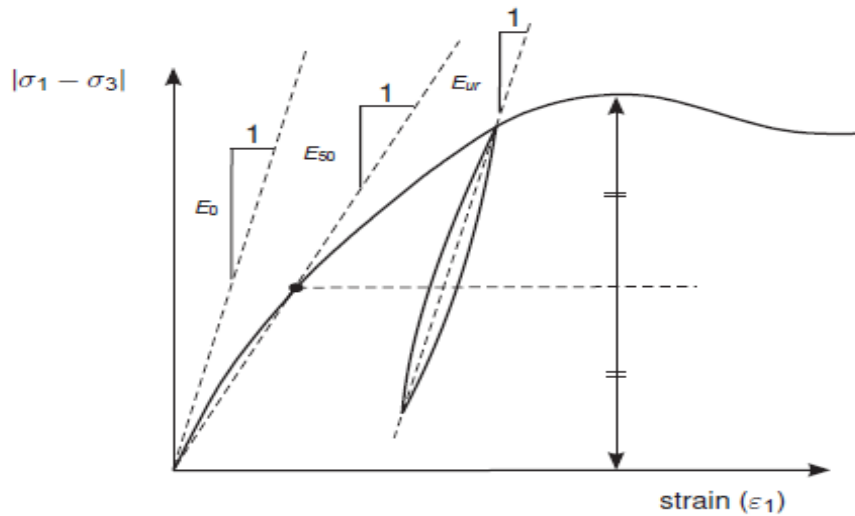


Figure 3.11. E_0 , E_{50} and E_{ur} of a soil sample from triaxial test results

The Mohr-Coulomb model is employed in the context of one-dimensional compression for gravity loads. Realistic ratios of $K_0 = \sigma_h' / \sigma_v'$ should be provided by PLAXIS for this kind of loading. It is simple to choose a Poisson's ratio that provides a reasonable value of K_0 because the model will yield the well-known ratio of $\{\sigma_h' / \sigma_v'\} = \{v / (1 - v)\}$ for one-dimensional compression. v is therefore assessed by matching K_0 . One will frequently receive v readings in the 0.3–0.4 range. Generally speaking, loading circumstances other than one-dimensional compression can also make use of such variables.

Stress is one of the dimensions of cohesive strength. The effective cohesion c' of the soil in the Mohr-Coulomb type model can be modelled using the cohesive parameter in conjunction with a reasonable effective friction angle ϕ' . High friction angles, which are occasionally observed in dense sands, significantly escalate the computational effort for plastics. Furthermore, high friction can exhibit strain-softening behaviour, meaning that under significant deformation, extremely high friction angles cannot be sustained. The dilatancy angle is expressed in degrees and is called ψ . Clay soils, aside from severely over-consolidated strata, often exhibit minimal dilatancy ($\psi \sim 0$).

The inability to determine aggregate sizes is the only drawback to simulating aggregates with PLAXIS. As shown in Table 3.6, shear strength parameters and the unit weight of the modelled aggregates and soil are taken from the lab testing.

Table 3.6. Properties of soil and aggregate used for PLAXIS modelling

Geogrids are elastic, flexible elements that mimic a grid or sheet of fabric; they are not able to withstand compressive forces. A geogrid data set typically corresponds to a particular kind of geogrid material and can be linked to the relevant geogrid element or group in the geometry model. In the case of elastoplastic behaviour, the parameters needed for geogrids can be divided into stiffness properties and strength properties. The axial stiffness EA should be provided for elastic behaviour. The following characteristics of orthotropic and anisotropic material behaviour in geogrids are supported by PLAXIS 3D:

EA1 - The normal elastic stiffness in 1-direction (in-plane).

EA2 - The normal elastic stiffness in 2-direction.

GA - In-plane shear stiffness (anisotropic behaviour).

The axial stiffness EA is typically supplied by the geogrid supplier and can be found using diagrams that show the longitudinal elongation of the geogrid plotted vs the applied force. The ratio of axial force (F) per unit width to the axial strain ($\Delta l/l$, where Δl is the elongation and l is the original length) is called as axial stiffness and represented as:

$$EA = \frac{F}{\Delta l/l}$$

For isotropic behaviour only EA1 input is required and $EA2 = EA1$ and $GA = EA1/2$.

In the case of elastoplasticity, two strength parameters are required:

Np,1 - The maximum force in 1-direction.

Np,2 - The maximum force in 2-direction.

The force per unit width, or Np, is the highest axial tension force that may be measured. In the event that Np is surpassed, stresses are reallocated in accordance with the plasticity

theory to ensure that the maxima are met. Deformations that are irreversible will follow from this. The nodes provide the output of axial forces, which necessitates extrapolating the values at the stress points. The nodal value for the axial force may marginally exceed N_p because of the location of the points of stress in a geogrid element. The input is restricted to $N_{p,1}$ if the Isotropic selection is selected, when $N_{p,2} = N_{p,1}$.

3.11.4 Model Generation/ Geometry Modelling Process

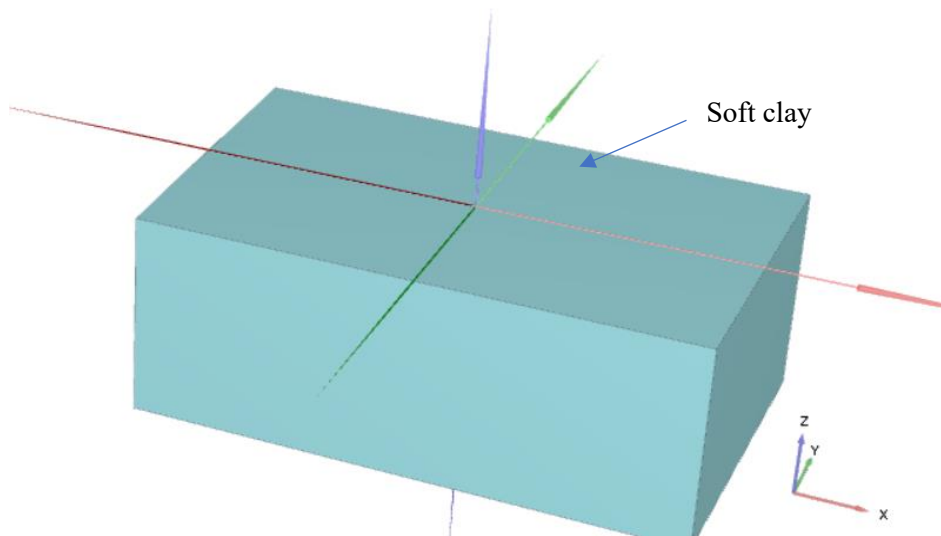


Figure 3.12. Model setup of soft clay

Figure 3.13. Model setup of an ordinary stone column for a reference case of $D=50\text{mm}$

Figure 3.14. Model setup of VESC with $L_r=L$ for a reference case of $D=50\text{mm}$

Figure 3.15. Model setup of VESC with $L_r=0.75L$ for a reference case of $D=50\text{mm}$

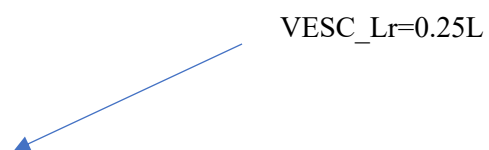


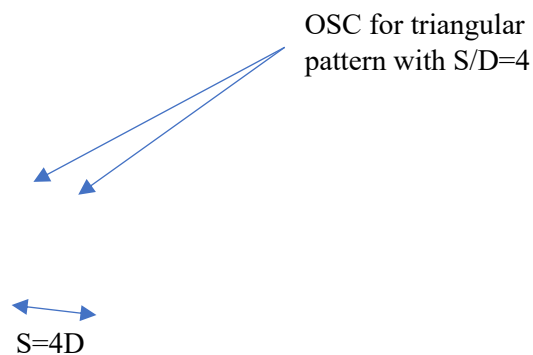
Figure 3.18. Model setup of HRSC with $L_r=L$ for a reference case of $D=50\text{mm}$

Figure 3.19. Model setup of HRSC with $L_r=0.5L$ from column's head to its centre for a reference case of $D=50\text{mm}$

For group analysis, Figure 3.21, 3.22 and 3.23 represents ordinary stone column arranged in triangular pattern with $S/D=2$, 3 and 4, respectively. Figure 3.24, 3.25 and 3.26 represents ordinary stone column arranged in square pattern with $S/D=2$, 3 and 4, respectively. Figure 3.27, 3.28, and 3.29 represents VESC ($L_r=L$) arranged in triangular pattern with $S/D=2$, 3 and 4, respectively. Figure 3.30, 3.31 and 3.32 represents VESC ($L_r=L$) arranged in square pattern with $S/D=2$, 3 and 4, respectively.



Figure 3.21. Model setup of ordinary stone column arranged in a triangular pattern for $S/D=2$ for a reference case of $D=50\text{mm}$



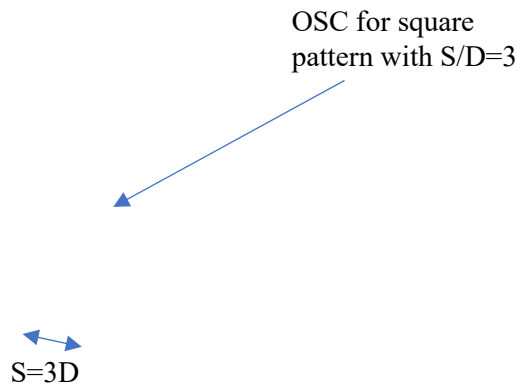
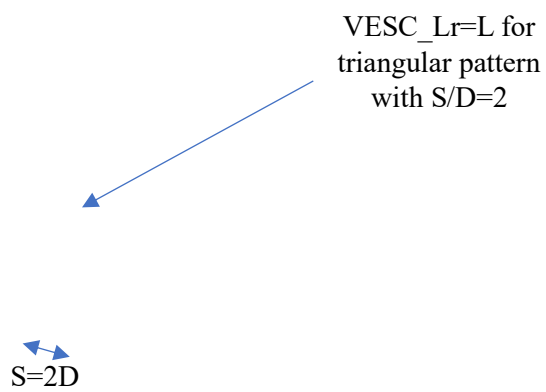
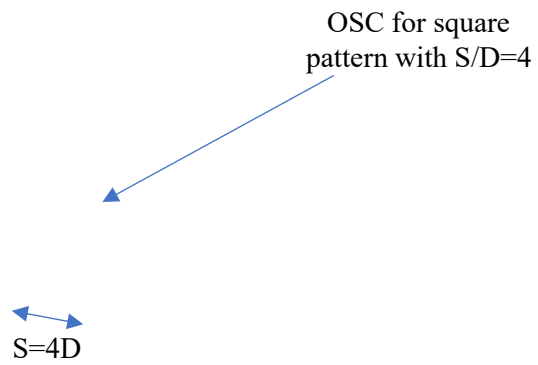


Figure 3.25. Model setup of ordinary stone column arranged in a square pattern for $S/D=3$ for a reference case of $D=50\text{mm}$



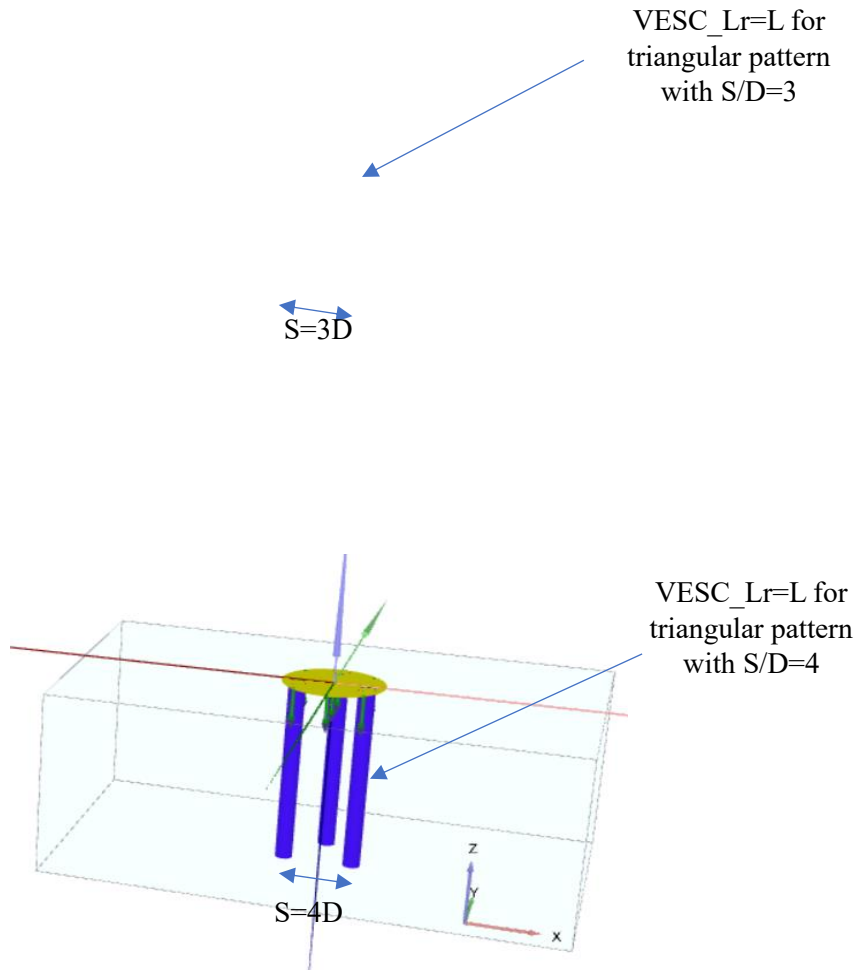


Figure 3.29. Model setup of VESC with $L_r=L$ arranged in a triangular pattern with $S/D=4$ for a reference case of $D=50\text{mm}$

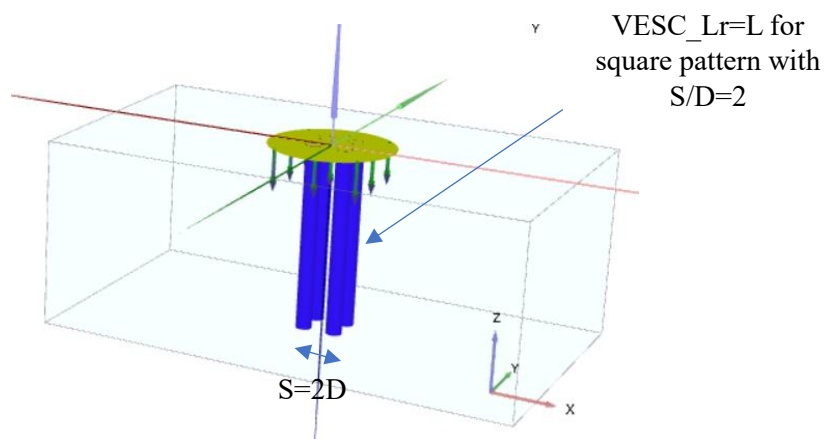


Figure 3.30. Model setup of VESC with $L_r=L$ arranged in a square pattern with $S/D=2$ for a reference case of $D=50\text{mm}$

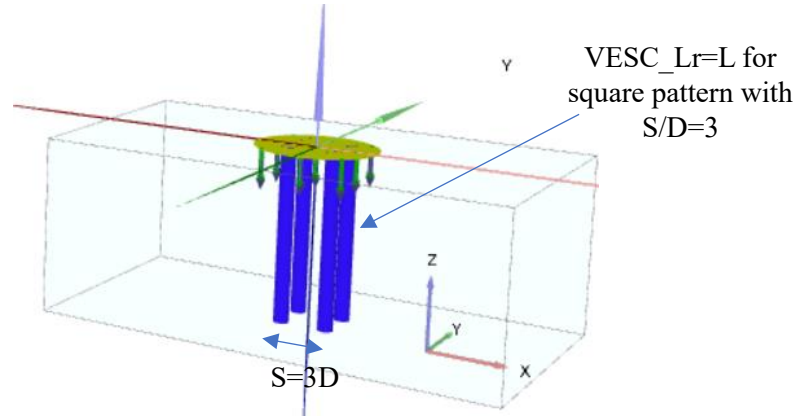


Figure 3.31. Model setup of VESC with $L_r=L$ arranged in a square pattern with $S/D=3$ for a reference case of $D=50\text{mm}$

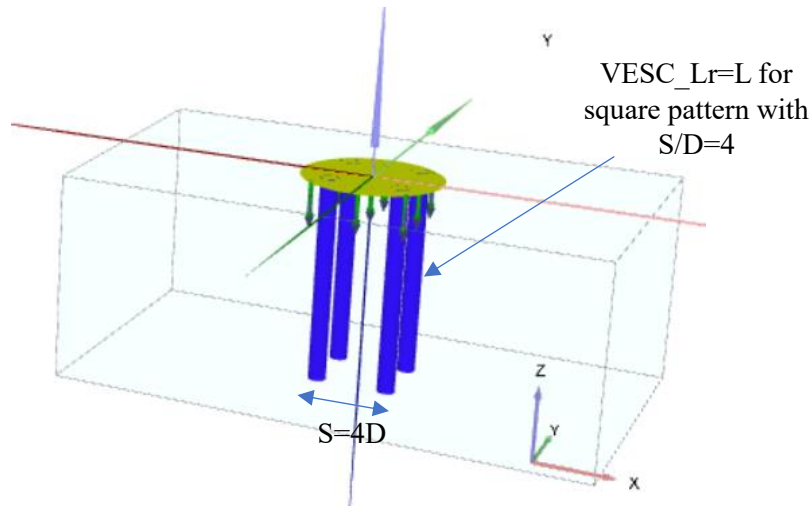


Figure 3.32. Model setup of VESC with $L_r=L$ arranged in a square pattern with $S/D=4$ for a reference case of $D=50\text{mm}$

3.11.5 Mesh Generation

The creation of a suitable Finite Element mesh is a crucial transitional phase that occurs between the phases of geometry specification and staged construction. To execute finite element computations, the geometry must be partitioned into finite elements once the geometry framework has been fully defined. A mesh is an arrangement of finite elements. A number of requirements must be met by the finite element mesh in order for the computation to proceed smoothly and accurately. The mesh needs to be of good quality, meaning that the components shouldn't be overly lengthy or thin in order for the calculation to be numerically stable. The elements must be small enough for the calculation to be accurate, particularly in the places where major changes in stress or strain are anticipated during the investigation. However, this does not imply that one should just create a mesh made up of minuscule

pieces, as this will result in a very long calculation time. Therefore, in monitoring the mesh quality, care should be given to strike the ideal balance among accuracy and computation time. Finite element meshes are generated entirely automatically by the PLAXIS 3D software. The process of creating the mesh considers all structural elements, loads, boundary conditions, and the soil stratigraphy. Tetrahedral elements with 10 nodes are the fundamental elements of soil in a 3D finite element mesh (figure 3.33).

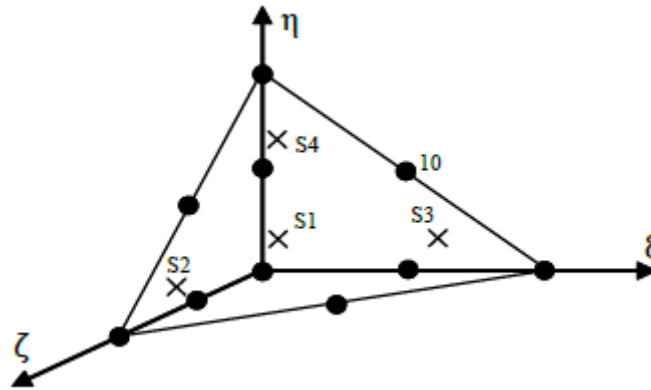


Figure 3.33. 10 - noded tetrahedral 3D soil element

The desired element dimension, represented by the global meshing parameter l_e , is required by the mesh generator. The outside geometry dimensions (x_{\min} , x_{\max} , y_{\min} , y_{\max} , z_{\min} , z_{\max}) are used to determine this parameter. The target element dimension is calculated using the equation below.

$$l_e = r_e \times 0.05 \times \sqrt{(x_{\max} - x_{\min})^2 + (y_{\max} - y_{\min})^2 + (z_{\max} - z_{\min})^2} \quad (3.1)$$

where r_e = relative element size factor; which is being determined from the element distribution. Element distribution has five global levels as represented in table 3.7.

Table 3.7. Predefined value of r_e (element distribution)

Element distribution	r_e
Very coarse	2.0
Coarse	1.5
Medium	1.0
Fine	0.7
Very Fine	0.5

The geometry's shape and local refinement settings that are chosen will determine the precise number of elements. A more precise (finer) finite element mesh is preferred in regions

where significant stress concentrations or deformation gradients are anticipated, but a fine mesh may not be necessary in other portions of the geometry. This kind of scenario frequently arises when a geometry model has corners, edges, or structural elements. Each geometric object can have a local coarseness factor set, which serves as the foundation for local refinement. This factor indicates how big an element is in relation to the target element size, which is established by the element distribution parameter. For most geometric entities, the coarseness factor value is set to 1.0 by default; for structural objects and loads, the value is set to 0.5. The element size is cut in half when the coarseness factor value is set to 0.5. Acceptable values fall between 0.0625 and 8.0. The mesh is locally coarsened when a value greater than 1.0 is used. PLAXIS 3D will perform automatic mesh refinements to provide a high-quality mesh for each geometry, accounting for the required mesh refinement around structural elements, loads, and prescribed displacements.

For current analysis, in order to accurately assess deformations and stresses, fine mesh creation is achieved in the vicinity of the soil-stone column contact. Additionally, this makes it possible to record bulging failures that happen when stone columns are loaded. The meshing has been produced with increasingly coarser meshing towards the lateral borders and finer meshing near the interface.

3.11.6 Staged Construction and Calculations

Following the discretization of the composite ground, the starting ground water level and equilibrium stresses are described. Usually, this is accomplished by placing the phreatic line at the designated spot. Since Plaxis primarily functions on the effective stress state, this parameter becomes crucial in scenarios involving undrained soil conditions. In geotechnical engineering, specifying a set of beginning stresses is necessary for many analysis issues. The total weight of the soil and the formation's history both affect a soil body's early stresses. Typically, this stress condition is marked by a initial vertical effective stress ($\sigma'_{v,0}$). The coefficient of lateral earth pressure connects the initial vertical effective stress to the initial horizontal effective stress, $\sigma'_{h,0}$.

$$\sigma'_{h,0} = K_0 \times \sigma'_{v,0} \quad (3.2)$$

Initial stresses in PLAXIS 3D can be produced via the Field stress option, the Gravity loading technique, or the K_0 procedure. In the current analysis, the initial stresses were developed by the K_0 procedure which account for the loading history of the soil. In actuality, it is frequently believed that the friction angle and the value of K_0 for a typically consolidated soil are connected by Jaky's empirical expression:

$$K_0 = 1 - \sin\phi \quad (3.3)$$

The default value of K_0 which Plaxis uses is based on the Jackey's formula mentioned above. In the K_0 method, either extremely low or extremely high K_0 -values could result in stresses that breach the Mohr-Coulomb failure condition. In this instance, the lateral strains are automatically decreased using PLAXIS 3D so that the failure condition is met. As a result, these stress spots are designated as plastic points since they are in a plastic state. When the K_0 technique is used, PLAXIS 3D produces the vertical stress that balance the soil's self-weight. On the other hand, horizontal stresses are computed using the given value of K_0 . Since the K_0 process does not produce shear stresses, it cannot guarantee that the entire stress domain is in equilibrium, even if the value of K_0 is selected to ensure that plasticity is avoided. A horizontal soil surface, any soil stratum parallel to the surface, and a parallel phreatic level are the only conditions that allow for full equilibrium. Because shear stresses are necessary to produce an equilibrium stress field for non-horizontal surfaces, the K_0 technique is not advised in these situations.

After the initial phase were created implying the initial stress using K_0 procedure, another phase was added where all the model constituents i.e., soil, stone columns and geogrid were activated. In the next phase, the prescribed displacement and corresponding boundaries were activated for the analysis and the calculation was started. Both unreinforced and reinforced stone columns' deformation and failure are assessed in the current study using plastic computation. The primary justification for employing plastic analysis stems from the fact that the stiffness matrix is developed utilising the original, undeformed state of the stone column reinforced ground condition as a starting point. Furthermore, the plastic computation is thought to be best suited for elastic-plastic deformation without taking into account the gradual depreciation of surplus pore water pressure. For a group of stone columns, the same modelling and analytical process is used.

3.12. SUMMARY

The soft clay bed was reinforced with ordinary stone column (OSC), vertically encased stone column (VESC) and horizontally reinforced stone column (HRSC) for varying length of reinforcement to enhance the load carrying efficiency of the soft clay bed. ults and discussion has been presented in the next chapter i.e., chapter 4.

CHAPTER 4

RESULTS AND DISCUSSIONS OF EXPERIMENTAL AND NUMERICAL INVESTIGATIONS

4.1 GENERAL

The primary emphasis in this chapter is on comparing the behaviour of the encased stone column with that of the conventional stone column, which is also known as the ordinary stone column. Both columns are put in weak cohesive soil beds that have identical features. To compare their respective performances, individual stone columns and groups of stone columns (organised in triangular and square patterns) were created separately on cohesive soil beds, both with and without encasement, and then tested. For load settlement, unreinforced, vertically enclosed geosynthetics as well as horizontally reinforced geosynthetics installed in single stone columns have been investigated. When the tests were done for the group of stone columns, only vertically encased stone column were analysed for the reinforced case. The analysis was done on the experimental results to determine the relative variation in the bearing capacity of the soil. Numerical analyses were also conducted to validate the experimental results.

4.2 EXPERIMENTAL RESULTS: FINDINGS FROM MODEL TESTS FOR SINGLE STONE COLUMN

4.2.1 Analysis of the load-settlement behaviour of a clay bed

Initially, a load test on pure clay without any reinforcement was performed to determine the load–settlement behaviour. The load was applied through a hydraulic jack, and load carrying capacity at an ultimate settlement of 50mm was determined.

4.2.2 Clay bed reinforced with ordinary stone column- Single Stone Column

Three different diameters of the stone column were used to understand the effect of the area replacement ratio (A_r). Area replacement ratio is defined as the area of the stone column with respect to that of the surrounding soil. In the current study, $D=50, 75$ and 100mm were used. A loading plate of 200mm diameter was used.

4.2.3 Clay bed reinforced with encased stone column- Single Stone Column

In very soft soil conditions, ordinary stone columns can provide only vertical load bearing support but cannot provide significant lateral support, which can cause concern. In such situations, lateral confinement is provided by encasing the stone column with a geosynthetic material. This study used two encasements: vertically encased stone columns (VESC) and horizontally reinforced stone columns (HRSC).

4.2.3.1 Vertically Encased Stone Column (VESC)

Figure 4.3 depicts the load-settlement behaviour of vertically encased stone columns with various reinforcement lengths for $D=50\text{mm}$. Similarly, Figures 4.4 and 4.5 show the load-settlement behaviour of VESC with various reinforcement lengths for $D=75$ and 100mm , respectively.

To understand the effect of varying stiffness of the encasement material, another geosynthetic material (G2) of higher stiffness than that of the G1 type was used.. The same trend was observed as it was seen with G1 type geotextile where the load carrying capacity increases with an increase in reinforcement lengths.

Figure 4.9, 4.10 and 4.11 shows a comparison between unreinforced, reinforced with ordinary stone column and reinforced with encased stone column having various length of reinforcement for $D=50$, 75 and 100mm , respectively. For all three cases, maximum load carrying capacity was observed when G2 type geotextile was used for $L_r=L$.

The load ratio (LR) parameter can be used to analyse and estimate the efficiency of stone columns in terms of ultimate bearing capacity. It is the ratio of the ultimate load sustained by a stone column reinforced soil (ordinary and encased) to the ultimate load carried by soft soil without a stone column (unreinforced).

4.2.3.2 Horizontally Reinforced Stone Columns (HRSC)

Figure 4.15 depicts the load-settlement behaviour of vertically encased stone columns with various reinforcement lengths for $D=50\text{mm}$. Similarly, Figures 4.16 and 4.17 show the load-settlement behaviour of VESC with various reinforcement lengths for $D=75$ and 100mm , respectively.

the G1 type was used to understand the effect of varying stiffness of encasement material. Figures 4.18, 4.19, and 4.20 represent the load-settlement behaviour of the HRSC with various lengths of reinforcement for the G2 type of geotextile for $D=50$, 75 , and 100mm ,

respectively. For $D=50\text{mm}$, the load carrying capacity for different reinforcement lengths of $L_r=L$, $L_r=0.5L$ from the column head to the column .

Similar to VESC analyses, load ratio (LR) parameter was be used to analyse and estimate the efficiency of stone columns in terms of ultimate bearing capacity. Also, for $D=100\text{mm}$, LR value was 1.41 for OSC, 1.18 for $L_r=L$ for G1 type geotextile, 1.22 for $L_r=L$ for G2 type geotextile, 1.26 for $L_r=0.5L$ from column head to centre for G1 type geotextile, 1.30 for $L_r=0.5L$ from column head to centre for G2 type geotextile, 1.34 for $L_r=0.5L$ from column centre to end for G1 type geotextile, 1.37 for $L_r=0.5L$ from column centre to end for G2 type geotextile.

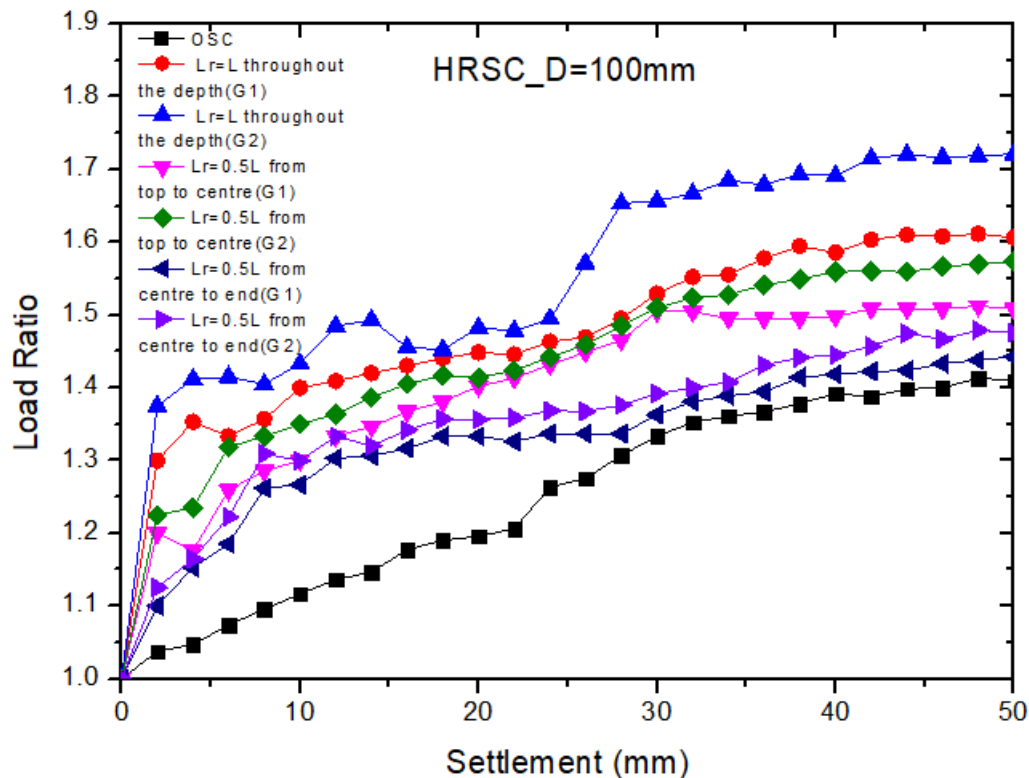


Figure 4.26. Load ratio- Settlement variation of HRSC for various L_r on single stone column for $D=100\text{mm}$

4.2.4 Comparison between VESC and HRSC

For the comparison between VESC and HRSC, a full-length encasement in the case of VESC and horizontal reinforcement at equal intervals throughout the depth of the column was studied for both types of geotextiles taken for the study.

Vertical encasing reinforcement, in contrast to horizontal reinforcement sheets, necessitates using specialised equipment. In comparison to VESCs, HRSCs do not require

improvement initiatives. In this study, the amount of geosynthetic used in HRSCs is much lesser than that used in VRSCs. As a result, compared to VESCs, HRSCs save more than half of the reinforcing material. HRSCs may be one of the cost-effective alternatives, particularly in big projects, due to the ease of constructing horizontal sheets as a reinforcing element in HRSCs. They are also a good approach for reinforcing stone columns, enhancing the ultimate capacity

At a displacement of 50 mm, the failure of all the columns was considered. The surrounding clay from the loading setup was removed, and the stone columns were excavated. Uncased stone columns with distorted shapes were studied. The cause of the failure was determined to be the deformation of the stone columns, resulting in bulging.

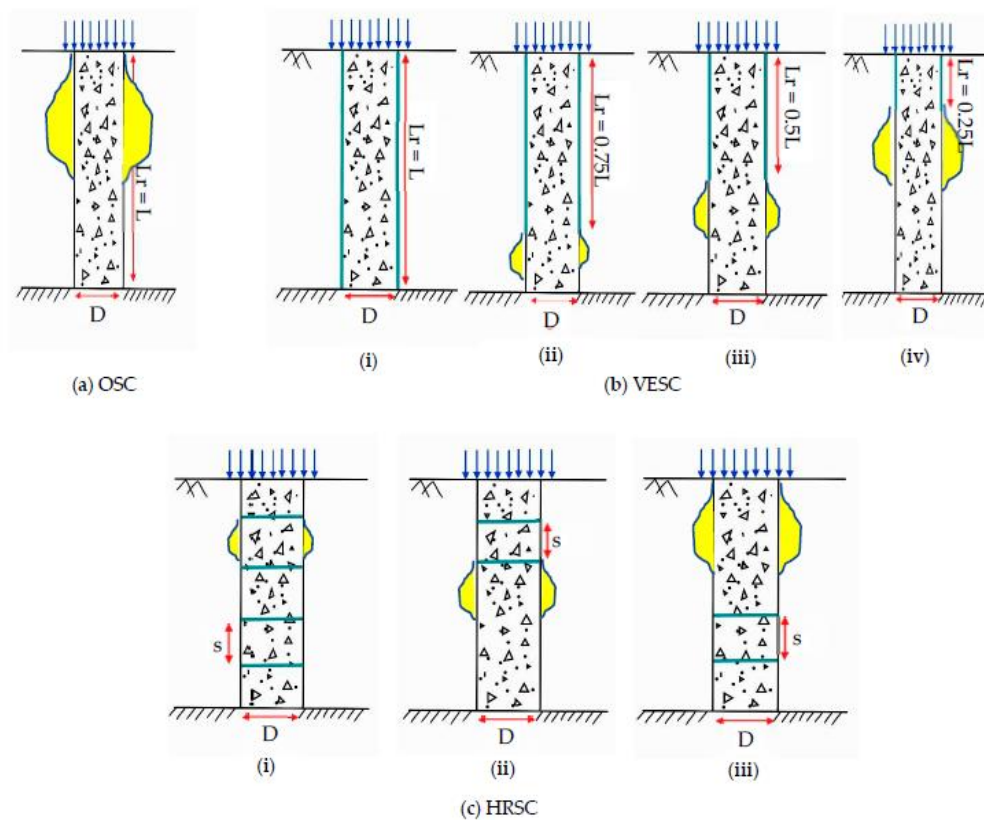


Figure 4.33. Multiple failure mechanisms for a column with a 100 mm diameter: **(a)** OSC, **(b)** VESC (i) $L_r = L$ (ii) $L_r = 0.75 L$ (iii) $L_r = 0.5 L$ (iv) $L_r = 0.25 L$, **(c)** HRSC (i) Equal interval throughout the depth (ii) Top half—0.5 L from head (iii) Bottom half—from centre to bottom

4.3 NUMERICAL RESULTS: SINGLE STONE COLUMN

4.3.1 Validation

The validation of the numerical models involved the simulation of the load settling behaviour observed in the model tests conducted by Murtaza and Samadhiya [35]. The

researchers conducted laboratory experiments utilizing the unit cell approach to assess individual stone columns embedded in soft clays. The experiments were conducted on stone columns with two diameters, 75 and 90 mm. The columns were subjected to two loading circumstances: (a) loading the column solely and (b) loading the entire area of the unit cell. These loading conditions were applied in both end-bearing and floating conditions. The present study focused on validating the scenario of a column area loading only for an end-bearing column. The study considered a single column of 75 mm in diameter and the length of the column was 525 mm. A geotextile was chosen as the encasement material, with a tensile strength of 4.4 kN/m. The details of the material properties for the chosen material model can be found in the referred study of Murtaza and Samadhiya [35]. Figure 4.34 shows the vertical load intensity settlement behaviour of the end-bearing granular piles of the present study and the experimental result of Murtaza and Samadhiya [35]. According to the current study's findings, the settlement varied by less than 3% for most of the values. Additionally, at a settlement of roughly 20–30 mm, a maximum difference of 15% was noted. The findings of this study indicate that the current model aligns well with the experimental observations mentioned and that the chosen modelling approach is appropriate for the simulation of the behaviour of clayey soil reinforced with vertically and horizontally encased stone columns.

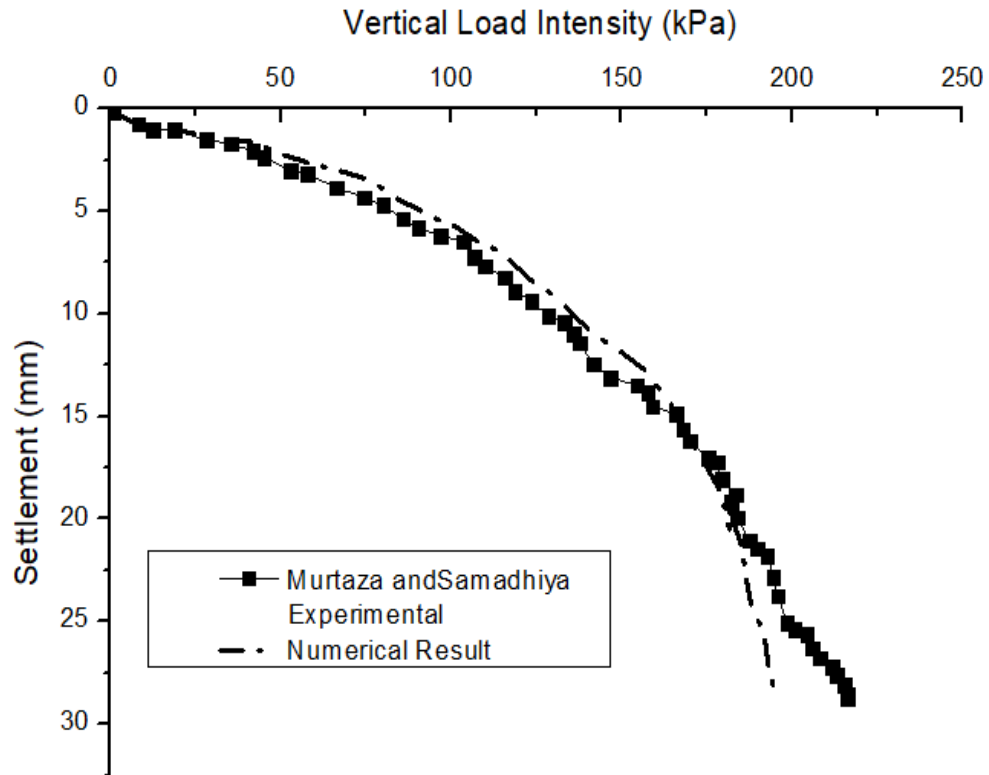


Figure 4.34. Comparison of vertical load intensity settlement behaviour of end bearing column

4.3.2 Analysis of the load-settlement behaviour of a clay bed

A numerical analysis was done to understand the load-settlement behaviour of unreinforced clay bed. Figure 4.35 shows a load-settlement response of an untreated/unreinforced soft clay bed. For an ultimate settlement of 50mm, load carrying capacity was 5.4kN.

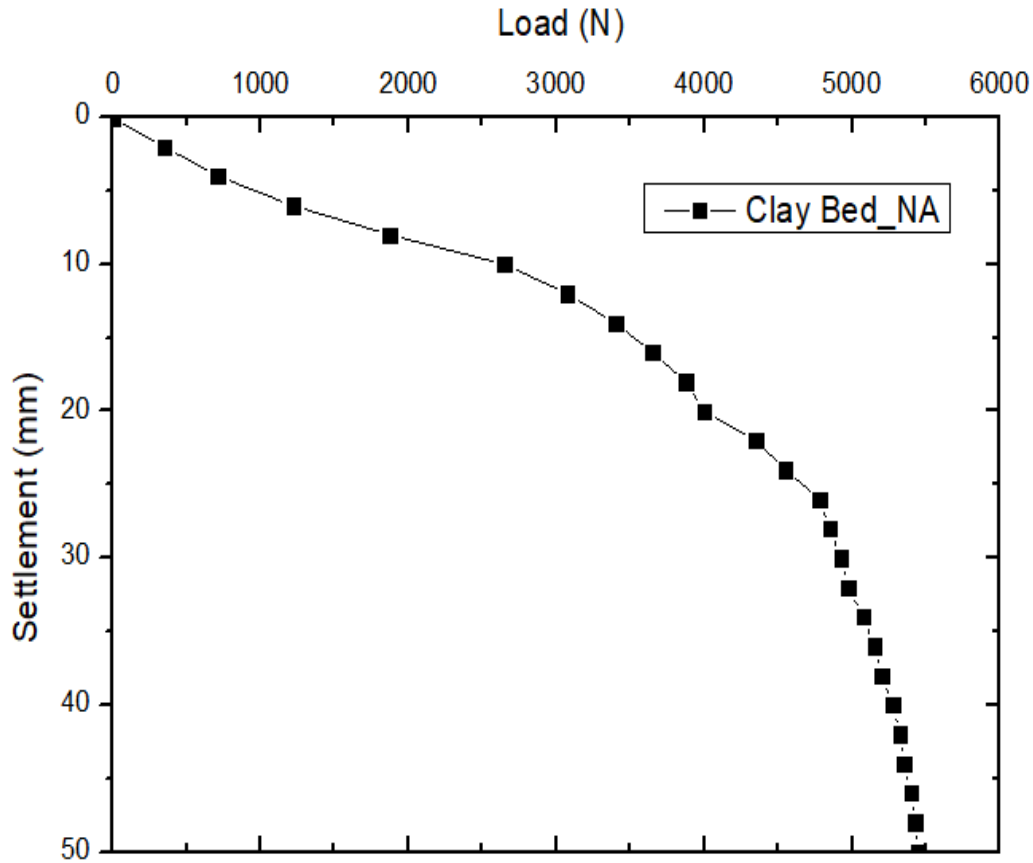


Figure 4.35. Load-Settlement variation of clay bed without any reinforcement

4.3.3 Clay bed reinforced with ordinary stone column- Single Stone Column

Similar to the experimental investigation, three different diameters of stone columns ($D=50, 75$ and 100mm) were used for numerical analysis. A loading plate of 200mm diameter was used. The observed percentages of A_r in the present investigations were 6.25, 14.06, and 25% for columns having diameters of 50, 75, and 100 mm, respectively.

4.3.4 Clay bed reinforced with encased stone column- Single Stone Column

To comprehend the behaviour of the encased stone column, unlike experimental analysis where two varieties of geotextiles were used, in the numerical analysis, only G1 type geotextile was used to determine the behaviour of composite soil bed. The analysis was carried out for both vertically encased stone column (VESC) and horizontally reinforced stone column (HRSC).

4.3.4.1 Vertically Encased Stone Column (VESC)

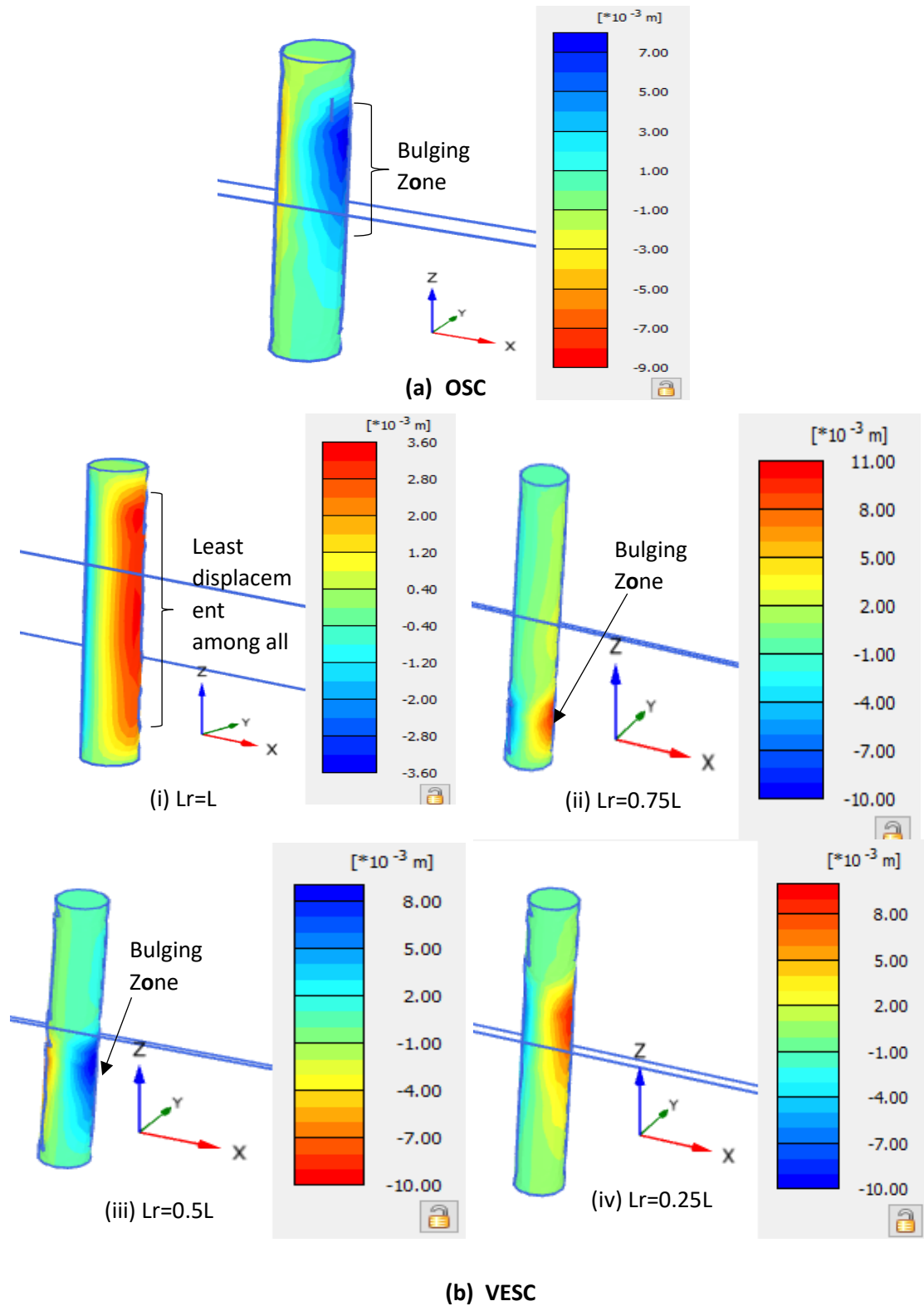
Figure 4.37, 4.38 and 4.39 depicts the load-settlement behaviour of vertically encased stone columns with various reinforcement lengths for $D=50$, 75 and 100mm, respectively.

4.3.4.2 Horizontally Reinforced Stone Column (HRSC)

Figure 4.40, 4.41 and 4.42 depicts the load-settlement behaviour of horizontally reinforced stone columns with various reinforcement lengths for $D=50$, 75 and 100mm, respectively. For $D=50$ mm, the load carrying capacity for different reinforcement lengths of $L_r=L$, $L_r=0.5L$ from the column head to the column centre

Failure mechanisms in numerical results were also studied as done in experimental analysis. Figure 4.41 illustrates the pattern of column bulging at varying depths for two conditions: uncased (OSC) and encased (VESC and HRSC) columns.

For HRSCs, when the spacing between reinforcements was 100 mm throughout the column length, local bulging was noted (similar to that of OSCs), indicating large spacing between the reinforcements .



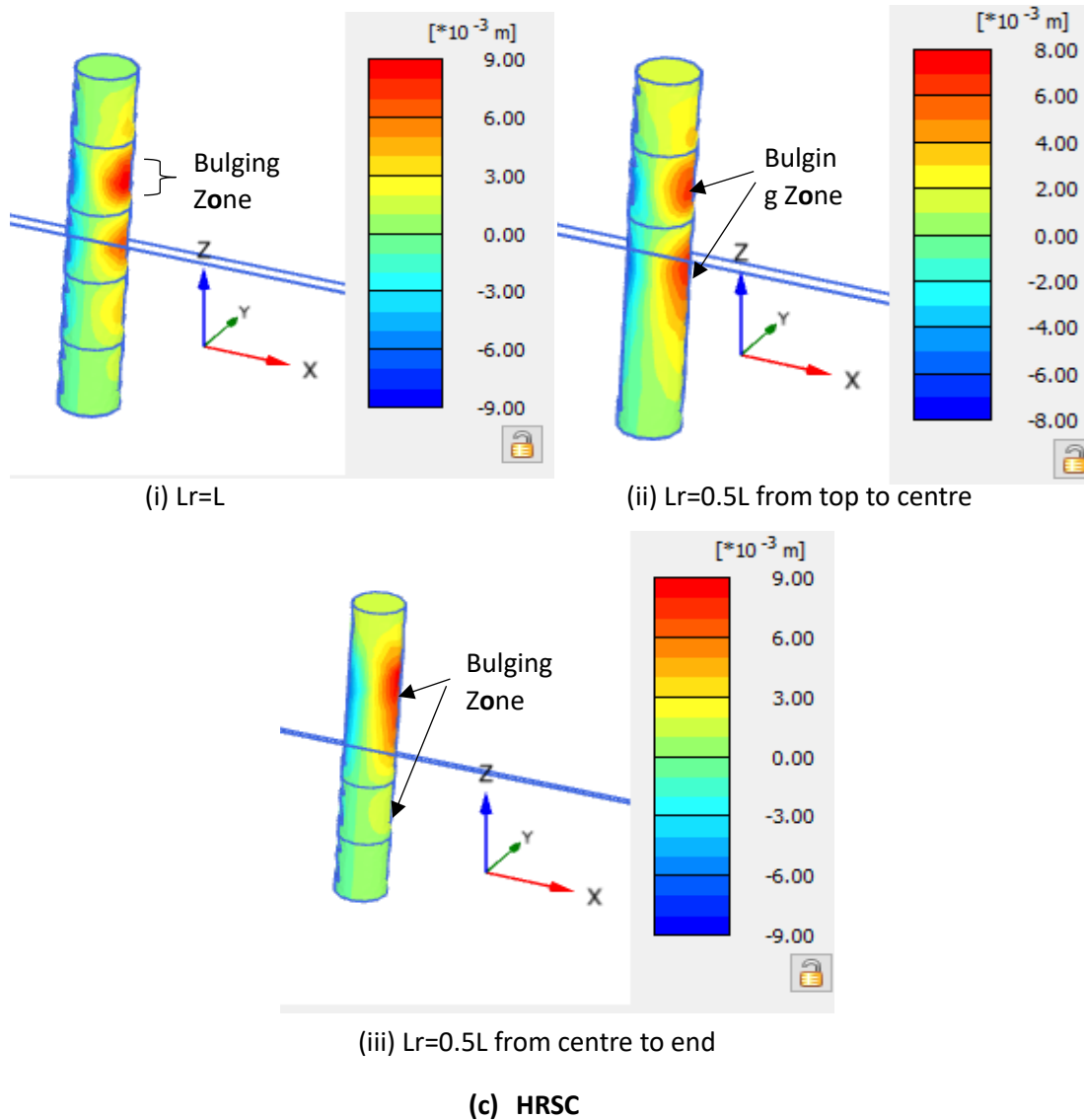


Figure 4.43. Various failure modes by numerical analysis for 100 mm diameter column (a) OSC (b) VESC (c) HRSC

4.4 COMPARATIVE ANALYSIS OF EXPERIMENTAL AND NUMERICAL OUTCOMES OF TESTS PERFORMED ON SINGLE STONE COLUMN

A comparison with the numerical data obtained by Plaxis 3D was also conducted to validate the experimental results. The failure mechanism was similar in both cases, which can be very well observed from Figures 4.33 and 4.41. The deformation was higher in unreinforced soil than reinforced soil (OSC). However, the failure of the OSC was due to bulging, which was controlled by providing an encasement around the OSC. The encasement provided was both vertical and horizontal layering of a geotextile. Both the experimental and numerical analyses exhibited the same trend regarding failure mechanisms.

CHAPTER 6

CONCLUSIONS

6.1 GENERAL

Important findings from testing and finite element analysis are presented in this chapter, which also gives a brief summary of the investigation's contents. Suggestions for more studies are also included in the chapter.

6.2 CONCLUSIONS

Within the context of soft clay systems, this study performed a set of model experiments on both reinforced and unreinforced single and group of stone columns. Ordinary stone column (OSC), vertically encased stone column (VESC), and horizontally reinforced stone column were used for reinforcing the soil bed. The current study used three different diameters of stone columns, namely 50, 75, and 100mm, to investigate the effect of area replacement ratio. To investigate the impact of encasement length (L_r), four distinct L_r values were employed in the VESC case, where L is the column length, we have $L_r=0.25L$, $L_r=0.5L$, $L_r=0.75L$, and $L_r=L$. For HRSC case, three different lengths of reinforcement were studied where $L_r=L$ throughout the length of the column, $L_r=0.5L$ from the column's head to the centre of the column and $L_r=0.5L$ beginning at the middle of the column and ending at the very end of the column. For all the above analyses, two varieties of geotextiles (G1 and G2) were used to investigate the impact of the stiffness of the encasement. For the group analysis, triangular and square patterns of OSC, VESC and HRSC were studied for spacing(S)/diameter(D) ratios of 2, 3 and 4. The usage of steel slag as a filler for columns subjected to embankment loading and reinforced with encased stone columns was the subject of an additional investigation. The following conclusions were made from the experimental and numerical results:

1. The predominant failure mechanism observed in all the ordinary stone column experiments was bulging. It was observed that bulging failure occurred between D and $2D$ below the stone column head. This bulging failure reduces by using vertical encasement and horizontal disc at the required depth.
2. The load-carrying capability was found to be higher in both the experimental and numerical analyses when the area replacement ratio was increased for an eventual settlement of 50 mm.

3. In single stone column analysis, for VESCs, the full-length encasement resulted in a higher load capacity of 23.52, 23.95, and 18.86% for $D = 50, 75,$ and 100 mm , respectively, in the experimental results as compared to their OSC results. A similar trend was observed in the numerical results.
4. In single stone column analysis, for HRSCs, when reinforcement was provided for the entire column length at equal intervals, the load capability increased by 17.72, 19.78, and 12.24% for $D = 50, 75,$ and 100 mm , respectively, when compared to their OSC values. Similar results were observed for the numerical analysis.
5. The ultimate load capacity of HRSC and VESC grows as the reinforcing geotextiles' stiffness increases. In VESCs when $L_r=L$ the load ratio for G1 type geotextile was 1.39 and for G2 type geotextile it was 1.41. Similar trends were observed for other lengths of reinforcement. For HRSCs when $L_r=L$ the load ratio for G1 type geotextile was 1.30 and for G2 type geotextile it was found to be 1.33. Similar trend was observed for other lengths of reinforcement.
6. For the present study, the most effective HRSCs reinforcement was found when the reinforcement sheets were provided at equally spaced interval throughout the length compared to partial reinforcements. In the case of VESCs, the total length of encasement ($L_r = L$) was found to be most effective as compared to partial reinforcement.
1. A novel study on various arrangement of horizontally reinforced stone column. Using the horizontal layer of the geosynthetic at the top half ($0.5L$ from column head) and the bottom half of the length of the column ($0.5L$ from the centre of column to the base) at the same and equal spacing as used for the layering of geosynthetic throughout the length of the column.
2. An extensive comparison was made between horizontally layered and vertically encased stone columns, improving soft clay's performance. This comparison was made for the varying diameters of stone columns (i.e., 50m , 75mm and 100mm) and also in terms of load ratio for various cases.
3. Use of sustainable material i.e., steel slag as a column filler for improving the soft soil's characteristics. The displacement analysis, stress investigation and stress concentration ratio were analysed and compares with the unreinforced soil.

6.3 AREA OF FUTURE RESEARCH

The current level of advancement in this field has certain noticeable deficiencies that are of considerable significance for gaining a more comprehensive expertise of the behaviour of ground reinforced with columns of stone and accurately predicting its reaction to applied loads. Additional investigation can be conducted on the subsequent subjects:

1. Research into the effectiveness of reinforced stone columns in multi-layer soil structures can be undertaken in the future. Considering the existing characteristics of the site, it is common to find a sand layer sandwiched between clay layers, or vice versa. In such cases, stone columns have been seen to function well. Nevertheless, the utilisation of reinforced stone columns in such circumstances has received limited attention and lacks comprehensive analysis.
2. As the current study assess the utilisation of both vertical as well as horizontal reinforcement individually, stone columns that are both horizontally reinforced and vertically enclosed have an equivalent load-bearing capacity. In addition, there is a scarcity of field experiments that investigate the combination of vertical and horizontal reinforcement. Therefore, stone columns supported in both vertical and horizontal orientations can be studied in future experiments using either small-scale or field-scale testing.
3. Only the utilisation of geotextile has been employed in the current investigation. The geotextile can be substituted with a geogrid or any other type of geosynthetic material.
4. End-bearing ordinary and encased columns were investigated in this study; floating columns may be the subject of future investigations.
5. The utilisation of pressure cells allows for a more in-depth investigation into the stress concentration on both the column and the soil. Consequently, it is possible to ascertain the manner in which the load is distributed between the columns and the soil that is surrounding them.
6. The use of steel slag as a column filler was analysed numerically. More detailed experimental investigation is necessary. Also, the effect of leaching of steel needed to be studied.
7. Another field of research on stone columns involves evaluating the practicality of utilising modified aggregates as infill material. Potential stone column material can be assessed by considering materials like crumbed rubber infused stone columns, aggregates from C&D wastes, or other waste material utilised for backfilling.

REFERENCES

- Aboshi, H., Ichimoto, E., Enoki, M., and Harada, K. (1979). The composer-A method to improve characteristics of soft clays by inclusion of large diameter sand columns. *Proceedings of the International Conference on Soil Reinforcement*, Paris, 1, 211-216.
- Abusharar, S. W., and Han, J. (2011). Two-dimensional deep-seated slope stability analysis of embankments over stone column-improved soft clay. *Engineering Geology*, 120(1-4), 103-110. <https://doi.org/10.1016/j.enggeo.2011.04.002>
- Alexiew, D., Daniel B., and Steve L. (2005). Geotextile encased columns (GEC): load capacity, geotextile selection, and pre-design graphs. *Contemporary Issues in Foundation Engineering*. 1-14
- Alexiew, D., and Thomson, G. (2013). Foundations on geotextile encased granular columns: Overview, experience, and perspectives. *Proceedings of International Symposium on Advances in Foundation Engineering (ISAFE 2013)*.
- Ali, K., Shahu, J. T., and Sharma, K. G., (2012). Model tests on geosynthetic-reinforced stone columns: a comparative study. *Geosynthetics International*, 19(4), 292-305.
- Ambily, A. P., and Gandhi, S. R. (2007). Behavior of stone columns based on experimental and FEM analysis. *Journal of Geotechnical and Geoenvironmental Engineering*, 133(4), 405-415.
- Balaam, N. P., Poulos, H. G., and Brown, P. T. (1978). Settlement analysis of soft clays reinforced with granular piles. *Proc., 5th Asian Conf. on Soil Engineering*, Bangkok, Thailand, 81-92.
- Barksdale, R. D. (1987). Applications of the state of the art of stone columns-liquefaction, local bearing failure, and example calculations, Technical Report. REMR-GT-7, The Georgia Institute of Technology, Atlanta, USA.
- Barksdale, R. D., and Bachus, R. C. (1983). Design and construction of stone columns: Volume 1. Rep. No.FHWA/RD-83/026, Federal Highway Administration, Washington DC, US.

Basarkar, S. S., Panse, V., and Wankhade, R. R. (2009). Ground Strengthening by Vibro-Stone Columns—A Case Study. Proc. Indian Geotechnical Conference (IGC-2009). Guntur, India. 2009.

Basack, S., Indraratna, B., Rujikiatkamjorn, C., and Siahaan, F. (2017). Modeling the Stone Column Behavior in Soft Ground with Special Emphasis on Lateral Deformation. *Journal of Geotechnical and Geoenvironmental Engineering*, 143(6). [https://doi.org/10.1061/\(asce\)gt.1943-5606.0001652](https://doi.org/10.1061/(asce)gt.1943-5606.0001652)

Bauer, G.E., and Joulani, N (1996), Laboratory and Analytical Investigation of Sleeve Reinforced Stone Columns. *Geosynthetics: application, design and construction*, pp. 463-466.

Black, J. A., Sivakumar, V., and Bell, A. (2011). The settlement performance of stone column foundations. *Geotechnique*, 61(11), 909–922. <https://doi.org/10.1680/geot.9.P.01>.

Bouassida, M., De Buhan, P., and Dormieux, L. (1995). Bearing capacity of a foundation resting on a soil reinforced by a group of columns. *Geotechnique*, 45(1), 25–34. <https://doi.org/10.1680/geot.1995.45.1.25>.

Bowels, J. E. (1996). *Foundation analysis and design*. 5th ed. Mc Graw Hill Book Company, p 1175, ISBN 0-07-118844-4. <http://doi.org/10.1061/9780784408650>.

Brauns, J. (1978). Reinforcing soft cohesive soil with granular piles. *Geotechnique*, ol. 55, 263-271.

Castro, J., and Sagaseta, C. (2009). Consolidation around stone columns: Influence of column deformation. *International Journal for Numerical and Analytical Methods in Geomechanics*, 33, 851-877.

Castro, J., Cimentada, A., daCosta, A. D., Cañizal, J., and Sagaseta, C. (2013). Consolidation and deformation around stone columns: Comparison of theoretical and laboratory results. *Computers and Geotechnics*, 49, 326-337.

Castro, J., Karstunen, M., and Sivasithamparam, N., (2014). Influence of stone column installation on settlement reduction. *Computers and Geotechnics*, 59, 87-97.

Chandrawanshi, S. (2018). Settlement Behaviour of Very Soft Soil Reinforced with Stone Columns: An Experimental Study. Ph.D. Thesis, Maulana Azad National Institute of Technology, India.

- Charles, J. A., and Watts, K. A. (1983). Compressibility of soft clay reinforced with stone columns. *Proc. 8th European Conference Soil Mechanics and Foundation Engineering*, Helsinki, 347-352.
- Chen, J. F., Wang, X. T., Xue, J. F., Zeng, Y. and Feng, S. Z. (2018). Uniaxial compression behavior of geotextile encased stone columns. *Geotextiles and Geomembranes*, 46(3), 277–283. <https://doi.org/10.1016/j.geotexmem.2018.01.003>
- Choobbasti, A. J., Zahmatkesh, A. and Noorzad, R. (2011). Performance of Stone Columns in Soft Clay: Numerical Evaluation. *Geotechnical and Geological Engineering*, 29(5), 675–684.
- Cimentada, A., da Costa, A., Cañizal, J. and Sagaseta, C. (2011). Laboratory study on radial consolidation and deformation in clay reinforced with stone columns. *Canadian Geotechnical Journal*, 48(1), 36–52. <https://doi.org/10.1139/T10-043>.
- Das, B.M. (2010). *Principle of Foundation Engineering*. CL-engineering, Amata Nakron industrial Estate, 7th Edition, March 2010.
- Das, A. K., and Deb, K. (2018). Experimental and 3D Numerical Study on Time-Dependent Behavior of Stone Column–Supported Embankments. *International Journal of Geomechanics*, 18(4), 04018011
- Datye, K. R., and Nagaraju, S. S. (1981). Design approach and field control for stone columns. *Proc., 10th Int. conf. on Soil Mech. and Found. Eng., Stockholm*, Vol. 3, 637-640.
- Dayte, K. R., and Madhav, M. R. (1988). Case Histories of Foundations with Stone Columns. *International Conference on Case Histories in Geotechnical Engineering*. 5.
- Deb, K., Samadhiya, N. K., and Namdeo, J. B. (2011). Laboratory model studies on unreinforced and geogrid-reinforced sand bed over stone column-improved soft clay. *Geotextiles and Geomembranes*, 29(2), 190-196
- Deb, K., and Behera, A. (2017). Rate of Consolidation of Stone Column–Improved Ground Considering Variable Permeability and Compressibility in Smear Zone. *International Journal of Geomechanics*, 17(6). [https://doi.org/10.1061/\(asce\)gm.1943-5622.0000830](https://doi.org/10.1061/(asce)gm.1943-5622.0000830).
- Deb, K., and Shiyamalaa, S. (2015). Effect of Clogging on Rate of Consolidation of Stone Column–Improved Ground by Considering Particle Migration. *International Journal of Geomechanics*, 16(1), 1-10.

- Debnath, P., Dey, A. K., (2017). Bearing capacity of geogrid reinforced sand over encased stone columns in soft clay. *Geotextiles and Geomembranes*, 45(6), 653-664.
- Deshpande P.M. and Vyas A.V. (1996), Interactive Encased Stone Column Foundation. Sixth Intl. Conf. and Exhibition on Piling and Deep Foundation, DFI'96, ISSMFE, pp. 1-19.
- Dutta, S., Nadaf, M. B., Lal Birali, R. R., and Mandal, J. N. (2016). Encased stone columns for soft ground improvement. In *Geo-Chicago 2016* (pp. 746-755)
- Elsawy, M. B. D. (2013). Behaviour of soft ground improved by conventional and geogrid-encased stone columns, based on FEM study. *Geosynthetics International*, 20(4), 276–285. <https://doi.org/10.1680/gein.13.00017>.
- Etse, G., and Willam, K. (1999). Failure Analysis of Elastoviscoplastic Material Models. *Journal of Engineering Mechanics*, 125(1), 60–69. [https://doi.org/10.1061/\(asce\)0733-9399\(1999\)125:1\(60\)](https://doi.org/10.1061/(asce)0733-9399(1999)125:1(60))
- Fattah, M. Y., and Majeed, Q. G. (2012). Finite Element Analysis of Geogrid Encased Stone Columns. *Geotechnical and Geological Engineering*, 30(4), 713–726. <https://doi.org/10.1007/s10706-011-9488-8>
- Fattah, Mohammed Y., Bushra Zabar S., and Hanan Hassan A. (2014). An experimental analysis of embankment on stone columns. *Journal of Engineering* 20(7), 62-84.
- Gniel, J., and Bouazza, A. (2009). Improvement of soft soils using geogrid encased stone columns. *Geotextiles and Geomembranes*, 27(3), 167-175
- Han, J. (2015). *Principles and Practices of Ground Improvement*, John Wiley & Sons, New Jersey.
- Han, J., and Ye, S.L. (2001). Simplified Method for Consolidation Rate of Stone Column Reinforced Foundations. *Journal of Geotechnical and Geoenvironmental Engineering*, 127(7), 597–603.
- Han, J., and Ye, S. L. (2002). A Theoretical Solution for Consolidation Rates of Stone Column-Reinforced Foundations Accounting for Smear and Well Resistance Effects. *International Journal of Geomechanics*, 2(2), 135–151. [https://doi.org/10.1061/\(asce\)1532-3641\(2002\)2:2\(135\)](https://doi.org/10.1061/(asce)1532-3641(2002)2:2(135)).
- Hanna, A. M., Etezzad, M., Ayadat, T., (2013). Mode of Failure of a Group of Stone Columns in Soft Soil. *International Journal of Geomechanics*, ASCE, 13(1), 87-96.

Hasan, M., Samadhiya, N. K., (2016). Experimental and numerical analysis of geosynthetic-reinforced floating granular piles in soft clays. *International Journal of Geosynthetics and Ground Engineering*, 2(3), 22.

Hasan, M., and Samadhiya, N. K. (2017). Performance of geosynthetic-reinforced granular piles in soft clays: Model tests and numerical analysis. *Computers and Geotechnics* 87: 178-187.

Huasmann, M.R. (1990). *Engineering Principles of Ground Modification*, McGraw-Hill, New York.

Hughes, J. M. O., and Withers, N. J. (1974). Reinforcing of soft cohesive soils with stone columns. *Ground Engineering* 7(3), 42-49.

Hughes, J. M. O., Withers, N. J., and Greenwood, D. A. (1975). A field trial of the reinforcing effect of a stone column in soil. *Geotechnique*, 25(1), 31-44.

Indraratna, B., Basack, S. and Rujikiatkamjorn, C. (2013). Numerical solution to stone column reinforced soft ground considering arching, clogging and smear effects. *Journal of Geotechnical and Geoenvironmental Engineering* 139(3): 377-394.

IS 15284 (Part 1)-2003. Indian standard code of practice for design and construction for ground improvement guidelines. Part 1: Stone columns. Bureau of Indian Standards, New Delhi, India.

IS 2720 -1983. Indian standard methods of test for soils. Bureau of Indian Standards, New Delhi, India.

Jadid, M. N. (2013). A Practical Approach for Computing Soil Bearing Capacity Under Shallow Foundations Using Vibro-Replacement Method. *International Refereed Journal of Engineering and Science*, 2(5), 54–62.

Kolekar, Y. A., and Dasaka, S. M. (2014). Ariability in the soil properties of the consolidated clay beds. *International Journal of Geotechnical Engineering*, 8(4), 365-371.

Kumar, S. G., Robinson, R. G., Rajagopal, K. (2014). Improvement of soft clays by combined vacuum consolidation and geosynthetic encased stone columns. *Indian Geotechnical Journal*, 44(1), 59-67.

- Kumar, R., and Jain, P. K. (2013). Expansive Soft Soil Improvement by Geogrid Encased Granular Pile. *International Journal on Emerging Technologies*, 4(1), 55-61.
- Madhav, M. R., and Miura, N. (1994). Stone Columns. Panel Rep., 13th Int. Conference on Soil Mechanics and Foundation Engineering, New Delhi, Jan., pp. 163-64.
- Madun, A., Meghzili, S. A., Tajudin, S. A. A., Yusof, M. F., Zainalabidin, M. H., Al-Gheethi, A. A., Dan, M. F. M., and Ismail, M. A. M. (2018). Mathematical solution of the stone column effect on the load bearing capacity and settlement using numerical analysis. *Journal of Physics: Conference Series*, 995(1). <https://doi.org/10.1088/1742-6596/995/1/012036>.
- Malarvizhi, S. N., and Ilamparuthi, K. (2004). Load versus settlement of clay bed stabilized with stone and reinforced stone columns. *The Asian Regional Conf. on Geosynthetics*, Seoul, 322-329.
- Malarvizhi, S. N., and Ilamparuthi, K. (2007). Comparative study on the behavior of encased stone column and conventional stone column. *Soils and Foundations*, 47(5), 873- 885.
- McCabe, B. A., Nimmons, G. J., and Egan, D. (2009). A review of field performance of stone columns in soft soils. *Proceedings of the Institution of Civil Engineers-Geotechnical Engineering*, 162(6), 323-334.
- McKelvey, D., and Sivakumar V. (2000). A review of the performance vibro stone column foundations. *Proc. of 3rd International Conference on Ground Improvement Techniques*. Singapore: CI-Premier Ltd, Singapore.
- McKelvey, D., Sivakumar V., and Bell, A. (2004). Modelling vibrated stone columns in soft clay. *Proceedings of the Institution of Civil Engineers-Geotechnical Engineering* 157(3): 137-149
- Mehrannia, N., Farzin, K., and Navid, G.(2018). Experimental study on soil improvement with stone columns and granular blankets. *Journal of Central South University* 25.4: 866-878.
- Miranda, M., and Da Costa, A. (2016). Laboratory analysis of encased stone columns. *Geotextiles and Geomembranes*, 44(3), 269–277. <https://doi.org/10.1016/j.geotexmem.2015.12.001>.

- Miranda, M., Da Costa, A., Castro, J., & Sagaseta, C., (2017). Influence of geotextile encasement on the behaviour of stone columns: Laboratory study. *Geotextiles and Geomembranes*, 45(1), 14-22.
- Mohanty, P., and Samanta, M. (2015). Experimental and numerical studies on response of the stone column in layered soil. *International Journal of Geosynthetics and Ground Engineering* 1.3: 27.
- Murugesan, S., and Rajagopal, K. (2006). Geosynthetic-encased stone columns: numerical evaluation. *Geotextiles and Geomembranes*, 24(6), 349–358.
- Murugesan, S., and K. Rajagopal (2009). Experimental and numerical investigations on the behaviour of geosynthetic encased stone columns. *Indian Geotechnical Conference*.
- Murugesan, S., and Rajagopal, K. (2010). Studies on the behavior of single and group of geosynthetic encased stone columns. *Journal of Geotechnical and Geoenvironmental Engineering*, 136(1), 129-139
- Muir Wood, D., Wenzheng Hu, and David FT Nash. (2000). Group effects in stone column foundations: model tests. *Geotechnique* 50.6: 689-698.
- Najjar, S. S., (2013). A state-of-the-art review of stone/sand-column reinforced clay systems. *Geotechnical and Geological Engineering*, 31(2), 355-386
- Nazaruddin, A. T., Shakri, M. S., and Hafez, M. A. (2013). A laboratory study on bearing capacity of treated stone column. *Electronic Journal of Geotechnical Engineering*, 18 Y, 5871–5880
- Needleman, A. (1988). Material rate dependence and mesh sensitivity in localization problems. *Computer Methods in Applied Mechanics and Engineering*, 67(1), 69–85. [https://doi.org/10.1016/0045-7825\(88\)90069-2](https://doi.org/10.1016/0045-7825(88)90069-2)
- Ng, K. S., and Tan, S. A. (2014). Design and analyses of floating stone columns. *Soils and Foundations*, 54(3), 478–487.
- Priebe, H.J. (1976). To estimate the usage behavior of a building site improved by plugging. *Civil engineering*, (53), 160-162.
- Priebe, H. J. (1995). The design of vibro replacement. *Ground Engineering* 28 (10): 31.

Priebe, H. J. (2005). Design of vibro replacement: The application of Priebe's method to extremely soft soils, 'floating' foundations and proof against slope or embankment failure. *Ground Engineering* January (2005), 25-27

Rajesh, S. (2017). Time-dependent behaviour of fully and partially penetrated geosynthetic encased stone columns. *Geosynthetics International*, 24(1), 60–71. <https://doi.org/10.1680/jgein.16.00015>.

Rajesh, S., and Jain, P. (2015). Influence of permeability of soft clay on the efficiency of stone columns and geosynthetic-encased stone columns - A numerical study. *International Journal of Geotechnical Engineering*, 9(5), 483–493. <https://doi.org/10.1179/1939787914Y.00000000088>.

Raithel, M., and Kempfert, H. G. (2000). Calculation models for dam foundations with geosynthetic coated sand columns. *Proceedings of International Conference on Geotechnical and Geological Engineering, GeoEng 2000, Melbourne, Australia*, 347–352.

Raithel M., Kirchner A., Schade C. and Leusink E. (2005), Foundation of Constructions on Very Soft Soils with Geotextile Encased Columns - State of the Art. *Geofrontiers 2005, GSP 131 Innovations in grouting and soil improvement*, pp. 1-11.

Rangear, D., Phan, P. T., Martinez, J., and Lambert, S. (2016). Mechanical behavior of fine-grained soil reinforced by sand columns: An experimental laboratory study. *Geotechnical Testing Journal*, 39(4), 648-657

Ranjan, G., and Rao, B. G. (1983). Skirted granular piles for ground improvement. *Proc., VIII European Conf. on Soil Mech. and Found. Eng., Helsinki*

Ranjan, G., and Rao, A.S.R. (2000). *Basic and applied soil mechanics*. Second edition, New Age International (P) Ltd. Publisher, Daryahang, New Delhi.

Rao, B. G. (1982). Behavior of skirted granular pile foundation. PhD thesis, University of Roorkee, Roorkee, India.

Rao, N., Madhiyan, S. M., and Prasad, Y. (1992). Influence of bearing area on the behavior of stone columns. *Indian Geotechnical Conf*, 235–237.

Richard D.S. and Yogesh P. (2005), Repairing Railway Spur Roadbed Failure Using Geotextile-Encased Columns. 05-0881, Kleinfelder, Inc. Annual TRB Meeting 2005.

- Schreyer, H. L., and Neilsen, M. K. (1996). Analytical and numerical tests for loss of material stability. *International Journal for Numerical Methods in Engineering*, 39(10), 1721–1736.
- Serridge, C. (2005). Achieving sustainability in vibro stone column techniques. *Proceedings of the Institution of Civil Engineers -Engineering Sustainability*, 158(4), 211-222.
- Shahu, J. T., and Reddy, Y. R. (2011). Clayey Soil Reinforced with Stone Column Group: Model Tests and Analyses. *Journal of Geotechnical and Geoenvironmental Engineering*, 137(12), 1265–1274.
- Shenkman, R., and Ponomaryov, A. (2016). Experimental and Numerical Studies of Geotextile Encased Stone Columns in Geological Conditions of Perm Region of Russia. *Procedia Engineering*, 143, 530–538. <https://doi.org/10.1016/j.proeng.2016.06.067>.
- Singh, R., Das, A., and Sathiyamoorthy, R. (2019). Efficacy of Coupled Solid–Fluid Formulation in Regularizing an Ill-Posed Finite Element Model. *Indian Geotechnical Journal*, 49(4), 409–420.
- Sivakumar V., Mckelvey D., Graham J. and Hughes D. (2004), Triaxial Tests on Model Sand Columns in Clay. *Canadian Geotechnical Journal*, Vol. 41, pp. 299-312.
- Stacho, J., and Sulovska, M. (2017). Determination of the density of stone columns using in-situ testing. *International Multidisciplinary Scientific GeoConference Surveying Geology and Mining Ecology Management, SGEM*, 17(12), 223–230. <https://doi.org/10.5593/sgem2017/12/S02.029>
- Waltham, T. (2009). *Foundations of engineering geology*, CRC Press, London.
- Wang, W. M., Sluys, L. J., and De Borst, R. (1997). Viscoplasticity for instabilities due to strain softening and strain-rate softening. *International Journal for Numerical Methods in Engineering*, 40(20), 3839–3864.
- Wehr, J.(2006). The undrained cohesion of the soil as a criterion for the column installation with a depth vibrator. *Transvib 2006*. Genin, Holeyman & Rocher-Lacoste. (ed) LCPC. Paris: France.
- Weber, T., Laue, J., and Springman, S. (2006). Centrifuge modelling of sand compaction piles in soft clay under embankment load. *Proc. of the 6th International Conference on Physical Modelling in Geotechnics*, Kowloon, Hong Kong.

Wood, D. M., Hu, W., Nash, D. F. T., (2000). Group effects in stone column foundations: model tests. *Geotechnique*, 50(6), 689-698.

Yoo, C. and Kim, S. B. (2009). Numerical modeling of geosynthetic encased stone column-reinforced ground. *Geosynthetics International*, 16(3), 116–126.

LIST OF PUBLICATIONS

SCIE Publications

1. Srijan and Gupta, A.K. (2023). Horizontally Layered and Vertically Encased Geosynthetic Reinforced Stone Column: An Experimental Analysis. Appl. Sci., 13, 8660. <https://doi.org/10.3390/app13158660>.
2. Srijan and Gupta, A.K. (2023). Vertically and Horizontally Reinforced End-Bearing Stone Column: An Experimental and Numerical Investigation. Appl. Sci., 13, 11016. <https://doi.org/10.3390/app131911016>.

Conference Publications

1. Srijan and Gupta, A.K. (2020). Effectiveness of Triangular and Square Pattern of Stone Column with Varying S/D Ratio on Consolidation Behaviour of Soil. Second ASCE India Conference, Kolkata, March-2020- AIC 2020-318- 862.
2. Srijan and Gupta, A.K. (2021). A Review article on Construction, Parametric Study and Settlement Behaviour of Stone Colum. IOP Conference Series: Earth and Environmental Science 796, 012021, <https://doi:10.1088/1755-1315/796/1/012021>.
3. Srijan and Gupta, A.K. (2022). Numerical Investigation of Behaviour of Geosynthetic Encased Stone Column in Soft Clay Bed Proceedings of the Indian Geotechnical Conference 2022 Volume 3. IGC 2022. Lecture Notes in Civil Engineering, vol 478. Springer, Singapore. https://doi.org/10.1007/978-981-97-1745-3_14.
4. Srijan and Gupta, A.K. (2022). A Basic Study on Ground Improvement Techniques and its Applications. 9th Civil Engineering Conference in the Asian Region (CECAR9) 2022, Goa, India.
5. Srijan, Narula, G., Sharma, A. and Dogra, V.K (2023). Effect of Fly Ash on Geotechnical Properties of Soft Soil: A Critical Review, Eng. Proc., 56, 269. <https://doi.org/10.3390/ASEC2023-16619>.